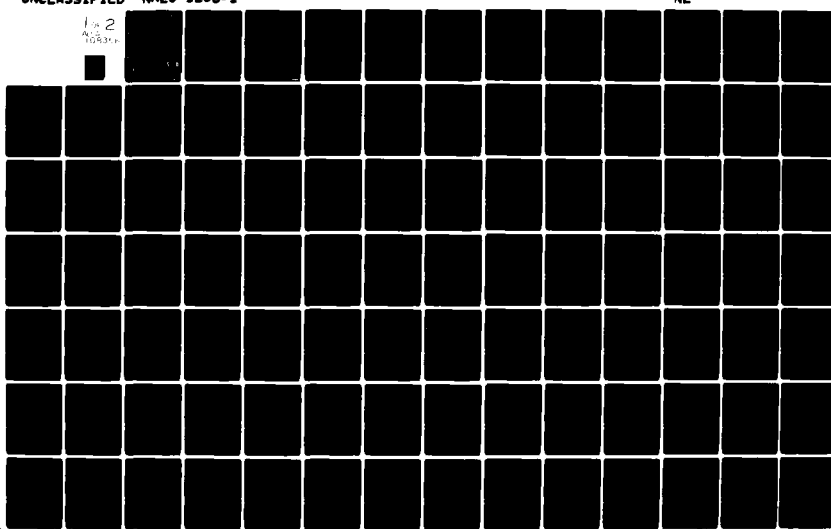
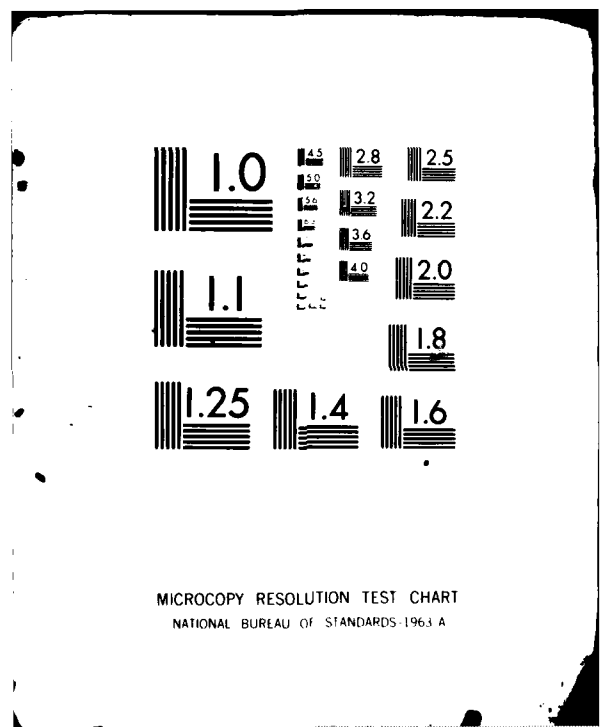


AD-A108 356 NORTHERN RESEARCH AND ENGINEERING CORP WOBURN MA F/G 13/7
ANALYTICAL INVESTIGATION OF AIR DYNAMOMETER CONCEPTS FOR FUTURE--ETC(U)
MAR 76 S N THIRUMALAI SAMY N68335-75-C-2098
UNCLASSIFIED NL
NRCC-1253-1

1 in 2
AUG 2 1976
104344





LEVEL

(1)
NREC 1253-1

AD A108356

**ANALYTICAL INVESTIGATION OF
AIR DYNAMOMETER CONCEPTS FOR
FUTURE TURBOSHAFT ENGINES**

Final Report

March 1976

By

S.N.Thirumalaisamy

Prepared Under Contract No. N68335-75-C-2098

for

PROPELLION DIVISION, NAVAL AIR ENGINEERING CENTER

Lakehurst, New Jersey

DTIC FILE COPY

DTIC
ELECTED
DEC 10 1981
S D

By

NORTHERN RESEARCH AND ENGINEERING CORPORATION

Cambridge, Massachusetts

DISTRIBUTION STATEMENT A
Approved for public release
Distribution Unlimited

81 11 06 015

NREC-1253-1

ANALYTICAL INVESTIGATION OF AIR DYNAMOMETER CONCEPTS
FOR FUTURE TURBOSHAFT ENGINES

Final Report

(February 1975 to March 1976)

March 1976

By

S. N. Thirumalaisamy

Prepared Under Contract No. N68335-75-C-2098

for

Propulsion Division, Naval Air Engineering Center
Lakehurst, New Jersey

| | |
|------------------------------|-------------------------------------|
| Accession For | |
| NTIS GRA&I | <input checked="" type="checkbox"/> |
| DTIC TAB | <input type="checkbox"/> |
| Unannounced | <input type="checkbox"/> |
| Justification | |
| By <i>Per LK on file</i> | |
| Distribution/ | |
| Availability Codes | |
| Avail and/or Dist Special | |
| A | |

By

Northern Research and Engineering Corporation
Cambridge, Massachusetts

66-5611

DISTRIBUTION STATEMENT A

Approved for public release;
Distribution Unlimited

FOREWORD

This report presents the results of an investigation of air dynamometer concepts for future turbojet engines. The investigation was carried out for the Propulsion Division, Naval Engineering Center, Lakehurst, New Jersey, under Navy Contract No. N68335-75-C-2098, with Mr. Wayne Sule of the Advanced Technology Section, Propulsion Division, Naval Air Engineering Center, acting as the project coordinator.

The work was carried out at Northern Research and Engineering Corporation under the technical direction of Dr. W. Jansen with Mr. A. F. Carter assuming the project responsibility. Other major participants in the program were Messrs. J. W. Beckenbach, T. A. Blatt, D. B. Chouinard, N. Guletsky, A. M. Heitmann, R. E. Penfield, W. H. Robinson, R. S. Scharlack, M. Shaw, and S. N. Thirumalaisamy. Among the participants, special mention should be made of Mr. A. M. Heitmann, who was very helpful in the evaluation of different compressor concepts for the dynamometer.

ABSTRACT

This report is concerned with the analytical phase of the Navy's effort to develop the technology necessary for the design of dynamometers to meet the Navy's future needs. In the analytical phase, several compressor concepts were analyzed for feasibility. The analyses indicated that only the dynamic rotary compressors (centrifugal, radial-outflow, and axial) would be feasible for the dynamometers of specified requirements and general constraints. Therefore, several dynamic rotary compressor systems were selected and investigated for range extension with inlet and exit valves as well as with other possible range extension methods: bleed valve control, recirculation, water injection, and variable geometry. The results of the investigation were then employed for the evaluation and rating of the compressor systems based on several different factors relating to the dynamometer application. Based on the evaluation, a double-entry radial-outflow compressor with variable shroud for power modulation was selected as the optimum system. Also, an outline of an experimental program for the demonstration of the selected concept is given.

TABLE OF CONTENTS

| | |
|---|----|
| SUMMARY | 1 |
| INTRODUCTION | 2 |
| Background | 2 |
| Objective | 2 |
| Required Ranges and Constraints | 2 |
| Report Contents | 3 |
| FEASIBILITY ANALYSIS OF SEVERAL COMPRESSOR CONCEPTS | 4 |
| Introduction | 4 |
| Selection of Operating Points for Analysis | 4 |
| Centrifugal Compressors | 4 |
| Axial Compressors | 7 |
| Drag Compressor | 8 |
| Positive Displacement Rotary Compressors | 10 |
| PRELIMINARY ANALYSIS OF FEASIBLE COMPRESSOR SYSTEMS | 12 |
| Introduction | 12 |
| Centrifugal Compressors | 12 |
| Radial Outflow Compressor | 16 |
| Axial Compressor | 16 |
| RANGE AND REQUIRED NUMBER OF DYNAMOMETERS WITH INLET AND EXIT VALVES | 22 |
| Introduction | 22 |
| Frame 1 Size Compressors | 22 |
| Range with Inlet and Exit Valves | 24 |
| Number of Frame Sizes and Dynamometers | 25 |
| ANALYSIS OF RANGE EXTENSION WITH OTHER POSSIBLE METHODS | 27 |
| Introduction | 27 |
| Bleed Control | 27 |
| Recirculation | 29 |
| Water Injection | 30 |
| Variable Geometry | 31 |

| | |
|---|-----|
| SELECTION AND DETAILED ANALYSIS OF THREE COMPRESSOR SYSTEMS | 36 |
| Introduction | 36 |
| Selection of Compressor Systems for Further Analysis | 36 |
| Number of Frame Sizes and Dynamometers for the Selected Compressor Systems | 37 |
| Control System and Torque Measurement | 39 |
| Preliminary Mechanical Design and Analysis | 41 |
| DYNAMOMETER SYSTEM EVALUATION | 44 |
| Introduction | 44 |
| Applicability | 44 |
| Controllability | 46 |
| Cost Effectiveness | 49 |
| Configuration | 51 |
| Safety | 51 |
| Environmental | 53 |
| Rating | 54 |
| Analysis of Two Alternate Compressor Systems | 56 |
| Selection of the Optimum System | 57 |
| ANALYSIS OF EXPERIMENTAL PROGRAM REQUIREMENTS | 60 |
| Introduction | 60 |
| Low Power Operation | 60 |
| Shroud Seal | 61 |
| Thrust Balance | 61 |
| Controls | 61 |
| Dynamometer Development | 62 |
| EXPERIMENTAL PROGRAM FOR CONCEPT DEMONSTRATION | 64 |
| Introduction | 64 |
| Outline of Experimental Program | 64 |
| REFERENCES | 66 |
| TABLES | 67 |
| FIGURES | 102 |

LIST OF TABLES

| | | |
|--------------|---|----|
| Table I: | Over-all Details of Centrifugal Compressor Stages for Point A | 67 |
| Table II: | Over-all Details of Centrifugal Compressor Stages for Point B | 68 |
| Table III: | Over-all Details of Double-Entry Radial Outflow Compressors for Points A and B | 69 |
| Table IV: | Over-all Details of a Constant-Tip Three-Stage Axial Compressor for Point A | 70 |
| Table V: | Over-all Details of a Constant-Tip Five-Stage Axial Compressor for Point B | 71 |
| Table VI: | Over-all Details of Drag Compressors for Point B | 72 |
| Table VII: | Over-all Details of Various Positive Displacement Compressors for Point B | 73 |
| Table VIII: | Preliminary Geometric Data and Stage Characteristics of Centrifugal Compressors | 74 |
| Table IX: | Results of the Scaling Analysis - Centrifugal Compressor | 75 |
| Table X: | Comparison of Over-all Dimensions of Scaled Unit with Those of Preliminary Design - Centrifugal Compressor . . | 76 |
| Table XI: | Results of the Scaling Analysis - Axial Compressor . . . | 77 |
| Table XII: | Preliminary Blading Details for the Axial Compressor Configuration B-AC51 | 78 |
| Table XIII: | Preliminary Design Details of Drag Compressors | 79 |
| Table XIV: | Preliminary Design Details of Helical Screw Compressors | 80 |
| Table XV: | Over-all Geometry and Performance Characteristics Frame 1 Size Centrifugal Compressors | 81 |
| Table XVI: | Over-all Geometry and Performance Characteristics Frame 1 Size Radial Outflow Compressors | 82 |
| Table XVII: | Over-all Geometry and Performance Characteristics Frame 1 Size 5-Stage Axial Compressor -- F1-AC5-H . . . | 83 |
| Table XVIII: | Over-all Details of Dynamometers with Inlet and Exit Valves -- Single-Stage Centrifugal Compressor (CC-S) . . | 84 |
| Table XIX: | Over-all Details of Dynamometers with Inlet and Exit Valves -- Double-Entry Centrifugal Compressor (CC-D) . . | 85 |

| | | |
|---------------|---|-----|
| Table XX: | Over-all Details of Dynamometers with Inlet and Exit Valves -- 2-Stage (Tandem) Centrifugal Compressor (CC-T) | 86 |
| Table XXI: | Over-all Details of Dynamometers with Inlet and Exit Valves -- Single-Stage Radial Outflow Compressor (ROC-S) | 87 |
| Table XXII: | Over-all Details of Dynamometers with Inlet and Exit Valves -- Double-Entry Radial Outflow Compressor (ROC-D) | 88 |
| Table XXIII: | Over-all Details of Dynamometers with Inlet and Exit Valves -- 5-Stage Constant Hub Axial Compressor (AC5-H) | 89 |
| Table XXIV: | Physical Details and Design Operational Characteristics of Compressor Systems - Frame 1 Size | 90 |
| Table XXV: | Achievable Range with Inlet and Exit Valves and Variable Geometry | 91 |
| Table XXVI: | Over-all Details of Tandem Centrifugal Dynamometers with VIGV-Throttle and Exit Valve | 92 |
| Table XXVII: | Over-all Details of Radial Outflow Dynamometers with Variable Shroud | 93 |
| Table XXVIII: | Weight of Control Systems with Inlet and Exit Valves | 94 |
| Table XXIX: | Results of Mechanical Design and Analysis of Three Selected Compressor Systems | 95 |
| Table XXX: | Rating of Three Selected Compressor Systems | 96 |
| Table XXXI: | Comparison of Cost and Mechanical Design Details of Single-Stage and Double-Entry ROC Configurations | 97 |
| Table XXXII: | Over-all Details of Dynamometers with Inlet and Exit Valves -- 10-Stage Constant-Hub Axial Compressor (AC10-H) | 98 |
| Table XXXIII: | Comparison of Cost and Mechanical Design Details of 5-Stage and 10-Stage Axial Compressors | 99 |
| Table XXXIV: | Final Rating of Five Compressor Systems | 100 |
| Table XXXV: | Over-all Dimensions, Stress Levels, and Estimated Weight of Dynamometers -- Single-Stage Radial Outflow Compressor with Variable Shroud | 101 |

LIST OF FIGURES

| | |
|--|-----|
| Figure 1: Envelope of Operation | 102 |
| Figure 2: Effect of Specific Speed on Flow Rate, Pressure Ratio and Efficiency for a Single Stage Centrifugal Compressor | 103 |
| Figure 3: Effect of Specific Speed on Exit Temperature, Tip Speed, and Maximum-to-Impeller Exit Diameter Ratio for a Single Stage Centrifugal Compressor | 104 |
| Figure 4: Effect of Specific Speed on Over-all Pressure Ratio, Over-all Dimensions, and Exit Mach Number - Single Stage Radial Outflow Compressor | 105 |
| Figure 5: Effect of Specific Speed on Over-all Pressure Ratio, Over-all Dimensions, and Exit Mach Number - Double Entry Radial Outflow Compressor | 106 |
| Figure 6: Effect of Number of Stages on Various Mean Stage-Design Quantities - Axial Compressor for Point A | 107 |
| Figure 7: Effect of Number of Stages on Various Mean Stage-Design Quantities - Axial Compressor for Point A | 108 |
| Figure 8: Illustration of Shroud-Cuts | 109 |
| Figure 9: Flow Path of Tandem Centrifugal Compressor for Point A - Configuration A-CCT2 | 110 |
| Figure 10: Power-Speed Characteristics of Various Scaled Units | 111 |
| Figure 11: Flow Path of 5-Stage Axial Compressor for Point B - Configuration B-AC51 | 112 |
| Figure 12: A Drag Compressor Unit Sized for Point A - Configuration A-DC2 | 113 |
| Figure 13: A Helical Screw Compressor Sized for Point A - Configuration A-HS2 | 114 |
| Figure 14: Radial Variation of Blade Angles for Frame 1 Size Axial Compressor -- F1-AC5-H | 115 |
| Figure 15: Performance Characteristics of Single-Stage Centrifugal Compressor -- F1-CC-S | 116 |
| Figure 16: Performance Characteristics of Double-Entry Centrifugal Compressor -- F1-CC-D | 117 |
| Figure 17: Performance Characteristics of Tandem Centrifugal Compressor -- F1-CC-T | 118 |
| Figure 18: Performance Characteristics of Single-Stage Radial Outflow Compressor -- F1-ROC-S | 119 |

| | | |
|------------|--|-----|
| Figure 19: | Performance Characteristics of Double-Entry Radial Outflow Compressor -- F1-ROC-D | 120 |
| Figure 20: | Performance Characteristics of 5-Stage Axial Compressor -- F1-AC5-H | 121 |
| Figure 21: | Effect of RPM, and Inlet and Exit Valves on Power - Single Stage Centrifugal Compressor (F1-CC-S) | 122 |
| Figure 22: | Effect of RPM, and Inlet and Exit Valves on Power - Double Entry Centrifugal Compressor (F1-CC-D) | 123 |
| Figure 23: | Effect of RPM, and Inlet and Exit Valves on Power - Tandem Centrifugal Compressor (F1-CC-T) | 124 |
| Figure 24: | Effect of RPM and Inlet and Exit Valves on Power - Single Stage Radial Outflow Compressor (F1-ROC-S) | 125 |
| Figure 25: | Effect of RPM and Inlet and Exit Valves on Power - Double Entry Radial Outflow Compressor (F1-ROC-D) | 126 |
| Figure 26: | Effect of RPM and Inlet and Exit Valves on Power - Constant Hub 5-Stage Axial Compressor (F1-AC5-H) | 127 |
| Figure 27: | Performance Envelopes of Dynamometers with Inlet and Exit Valves - Single-Stage Centrifugal Compressor (CC-S) | 128 |
| Figure 28: | Performance Envelopes of Dynamometers with Inlet and Exit Valves - Double-Entry Centrifugal Compressor (CC-D) | 129 |
| Figure 29: | Performance Envelopes of Dynamometers with Inlet and Exit Valves - Tandem Centrifugal Compressor (CC-T) | 130 |
| Figure 30: | Performance Envelopes of Dynamometers with Inlet and Exit Valves - Single-Stage Radial-Outflow Compressor (ROC-S) | 131 |
| Figure 31: | Performance Envelopes of Dynamometers with Inlet and Exit Valves - Double-Entry Radial Outflow Compressor (ROC-D) | 132 |
| Figure 32: | Performance Envelopes of Dynamometers with Inlet and Exit Valves - 5-Stage Constant Hub Axial Compressor (AC5-H) | 133 |
| Figure 33: | Effect of Interstage Bleed on Power Absorption - Tandem Centrifugal Compressor | 134 |
| Figure 34: | Effect of Recirculation on Power and Exit Temperature for Radial Outflow Compressors | 135 |
| Figure 35: | Effect of Variable Inlet Guide Vanes on Flow and Power - Double Entry Centrifugal Compressor (F1-CC-D) | 136 |
| Figure 36: | Effect on Range of Variable Inlet Guide Vanes with Inlet Throttling and Exit Valve - 2-Stage Tandem Centrifugal Compressor (F1-CC-T) | 137 |
| Figure 37: | Effect of Passage-Recirculation on Power and Exit Temperature for Radial Outflow Compressors | 138 |

| | | |
|------------|---|-----|
| Figure 38: | Potential Range and Probable Exit Temperature for Variable-Shroud Radial-Outflow Compressors | 139 |
| Figure 39: | Effect of RPM on Maximum Range for Various Compressor Systems with Inlet and Exit Valves | 140 |
| Figure 40: | Performance Envelopes of Tandem Centrifugal Dynamometers with VIGV-Throttle and Exit Valve | 141 |
| Figure 41: | Performance Envelopes of Radial Outflow Dynamometers with Variable Shroud | 142 |
| Figure 42: | Effect of Initial Operating Point on Effective Range with Inlet Valve for 5-Stage Axial Compressor | 143 |
| Figure 43: | Schematic of Control Configuration for Dynamometers | 144 |
| Figure 44: | Preliminary Design Layout of Tandem Centrifugal Dynamometer with VIGV and Exit Valve-- F1-CC-T | 145 |
| Figure 45: | Preliminary Design Layout of Single-Stage Radial-Outflow Dynamometer with Variable Shroud-- F1-ROC-S | 146 |
| Figure 46: | Preliminary Design Layout of 5-Stage Axial Dynamometer with Inlet Valve-- F1-AC5-H | 147 |
| Figure 47: | Preliminary Design Layout of an Optimum Configuration for Double-Entry Radial-Outflow Dynamometer with Variable Shroud-- F1-ROC-D | 148 |
| Figure 48: | Performance Envelopes of Dynamometers with Inlet and Exit Valves - 10-Stage Constant Hub Axial Compressor (AC10-H) . . | 149 |

LIST OF SYMBOLS

| <u>Symbol</u> | <u>Description</u> | <u>Units</u> |
|-----------------|---|-----------------------------|
| C _p | Specific heat | Btu/lbm deg R |
| D | Diameter | ft, in |
| g | Gravitational constant | 1bm/1bf ft/sec ² |
| HP | Horsepower | hp |
| J | Mechanical equivalent of heat | ft lbf/Btu |
| \dot{m} | Mass flow rate | 1bm/sec |
| N | Rotational Speed | rpm |
| N _s | Specific speed, $\frac{N\sqrt{C_1}}{\bar{P}^{1/4}(g\pi)^{1/4}}$ | -- |
| P | Pressure | psf, psi |
| P _R | Pressure ratio | -- |
| Q | Volume flow rate | ft ³ /sec |
| r | Radius | in |
| S _L | Linear scale factor | -- |
| T | Temperature | deg R |
| T _R | Temperature ratio | -- |
| U | Blade speed | ft/sec |
| V | Velocity | ft/sec |
| Z | Axial distance | in |
| ΔH | Adiabatic head | ft |
| ΔP _s | Static pressure rise | psi |
| ΔT | Temperature rise | deg F or R |
| β | P/P _{STD} ($P_{STD} = 14.7$ psia) | -- |
| σ | Solidity, blade chord/spacing | -- |
| Φ _f | Flow coefficient, $\frac{V_a}{U}$ | -- |
| Ψ _t | Temperature rise coefficient, $\frac{2gTC_P\Delta T}{U^2}$ | -- |
| ε | T/T _{STD} ($T_{STD} = 518.7$ deg R) | |

| <u>Subscripts</u> | <u>Description</u> |
|-------------------|--|
| a | Axial |
| b | Basic |
| d | Design |
| e | Exit |
| is | Isentropic |
| s | Scaled |
| STD | Standard conditions ($T_{STD} = 518.7$ deg R, $P_{STD} = 14.7$ psia) |
| R | Ratio |
| S | Static conditions |
| T | Total or stagnation conditions |
| U | Tangential |
| 0 | Stage inlet |
| 1 | Rotor inlet |
| 2 | Rotor exit |
| 3 | Diffuser exit |
| 4 | Stage exit |

SUMMARY

This report presents the analytical investigation of air dynamometer concepts for future turbojet engines. For the dynamometers, several compressor concepts were analyzed for feasibility. The concepts can be classified into three broad categories: dynamic rotary compressors, regenerative compressors, and positive-displacement rotary compressors. The analyses of the above compressor concepts indicated that only the dynamic rotary compressors (centrifugal, radial-outflow, and axial compressors) would be feasible for the dynamometers of specified requirements and general constraints.

Therefore, seven different dynamic rotary compressor systems (three centrifugals, two radial-outflow types, and two axials) were selected and were analyzed for range extension with inlet and exit valves. Also, selected and applicable compressor systems were analyzed for range extension with bleed valve control, recirculation, water injection, and variable geometry. In addition, preliminary mechanical design and analyses were performed on selected compressor systems.

For the final evaluation and selection of the optimum system, five compressor systems were identified. These compressor systems were then evaluated and rated employing several different factors relating to the dynamometer application. The evaluation and the subsequent rating established that the variable-shroud radial-outflow compressor systems are far superior to the other compressor systems. Among the two versions of the radial-outflow compressors, the double-entry version is found to be better than the single-stage version from considerations of stress and temperature levels, thrust balance, and growth potential. Therefore, a double-entry radial-outflow compressor with variable shroud for power modulation was selected and recommended as the optimum system for the dynamometers of the Navy's future engines.

This report also contains a brief summary of the problem areas to be solved in the development of the future dynamometers with this concept as well as an outline of an experimental program for the demonstration of this concept with the potential for a very wide power range.

INTRODUCTION

Background

The Navy has a continuing requirement for both pre-and post-maintenance testing of a variety of turboshaft engines at Fleet Activities. At these activities, testing is conducted on portable test trailers. Current Navy philosophy is to use air dynamometers as the load absorption devices for these systems due to their simplicity of operation. Current development programs at the Naval Air Engineering Center should provide the necessary air dynos for at least the next 4 or 5 years based on the projected growth of existing engines. However, beyond this, the Navy will be introducing engines into service that will generate shaft horsepowers greater than the capability of the dynos now under development. Since the technology does not presently exist to design and fabricate the necessary advanced dynamometers, it will have to be developed. The Navy would like to develop this technology in a two-phase effort-- analytical and experimental phases. The program completed by NREC is concerned with the analytical phase of this effort.

Objective

The objective of the program is to perform an analytical study to advance air dyno technology and generate design data on possible dyno systems to be used in trade-off studies for the development of future systems. The studies will consider systems that fall within the general requirements and constraints outlined in the following section. Resulting systems should represent the optimum performance within financial and operational constraints.

Required Ranges and Constraints

The general areas of shaft horsepower and rotational speed for which dynamometers will be required are listed below along with the operational and physical constraints that will be placed on any future system. These requirements are to be used as a guide throughout the analysis so that more emphasis can be placed on the optimum systems. The engine ratings (shaft horsepower and rotational speed) are not to be considered specific design points but rather as the center of a possible range of design points. It is known that future engines will fall within the given ranges but the specific ratings have not yet been determined.

Required Dynamometer Ranges

| <u>Shaft Horsepower</u> | <u>Rotational Speed (rpm)</u> |
|-------------------------|-------------------------------|
| 2,500 | 6,600 |
| 4,000 | 6,600 |
| 6,000 - 10,000 | 7,000 |
| 6,000 - 10,000 | 12,000 |
| 2,500 | 20,000 |

In the above five horsepower-speed combinations, the first four were part of the original specifications; the last one, which corresponds to

the anticipated growth version of the T58 engine, was added by the Navy to the original requirements in the earlier part of the program.

Constraints

1. Dyno system must not exceed 48 inches in over-all diameter.
2. Dyno system should weigh about 1,000 pounds so that it can be removed with the existing crane.
3. Dyno system must be direct drive from engine (no gearbox).
4. For dynos with extended range that can test future as well as existing engines, consideration must be given to the fact that the output shafts on different engines may rotate in different directions.
5. Dyno power absorption during engine testing must be adjustable using a single control that is not overly sensitive.
6. Dyno system must have a high degree of reliability so that maintenance requirements are minimal.

From preliminary sizing and weight calculation in the earlier part of the program, it was found that the first two constraints, especially the second one on weight, could not be satisfied by dynamometers for the high horsepower, low speed engine requirements. A discussion of this with the Navy personnel resulted in their recommendation that these restrictions, which have to be satisfied by the dynamometers of the present engines, should be used only as guidelines and not as absolute restrictions for the dynamometers of future engines. Also, the Navy later specified that the minimum power range should be at least 2:1 for the testing of engines at design speed.

Report Contents

The main results of the program are documented in this report in eight sections. The first section contains the general sizing and feasibility analysis of various concepts for the future dynamometer application. Further analysis of the feasible compressor concepts with respect to sizing and preliminary weight calculation are reported in the second section. The third section contains the range and required number of dynamometers for the six selected compressor systems with inlet and exit valves. Selected compressor systems were analyzed for achievable range extension by various other methods. The results of this analysis are included in the fourth section. The fifth section contains the analysis for range and the preliminary mechanical design and analysis of three selected compressor systems. The sixth section discusses the good and bad points of the selected compressor concepts. It also includes a rating evaluation of the different compressor concepts. The seventh section contains the analysis of experimental program requirements. In the final section, an outline of the proposed experimental program for the demonstration of the optimum concept is presented.

FEASIBILITY ANALYSIS OF SEVERAL COMPRESSOR CONCEPTS

Introduction

For the dynamometers, several compressor concepts were studied for feasibility in terms of size and number of units or stages necessary to satisfy the given requirements. The concepts can be classified into three broad categories: dynamic rotary compressors, regenerative compressors, and positive displacement rotary compressors. Centrifugal, axial and radial outflow compressors comprise the first category while the second category consists of only the drag (peripheral) compressor. The last category includes helical screw, spiral axial, straight lobe, slide vane and liquid liner compressors. The important results of the analysis are given and discussed in this section.

Selection of Operating Points for Analysis

Shown in Figure 1 is the envelope of operation for the specified requirements. In the figure, the original engine design points are shown connected by continuous lines. Of the six original design points, the most important or critical points for the design of dynamometers would be Points A and B. Point A (high power - low speed combination) would require the maximum physical size for any system. Point B (high power-high speed combination) would limit the physical size of a system due to limitations on tip speed. A smaller size could make the required number of units or stages prohibitively high because of the high power requirement. Also, a higher number of units or stages would make the weight and the length of the system excessively high. Hence, points A and B were selected for the feasibility analysis of the various compressor concepts.

Centrifugal Compressors

The analysis was conducted on three different centrifugal compressor systems: single stage units, double-entry units (or two stages operating in parallel), and two-stage tandem (series operation) units. Even though Points A and B were selected for the feasibility analysis, the analysis of the single stage units involved three other operating points: Points C, D and E. For the analysis, the relationship between specific speed and normalized efficiency given in Reference 1 was utilized. Various simplifying assumptions were also employed for the analysis. They are:

1. The optimum impeller efficiency is 0.92 and its variation with specific speed follows that of a stage.
2. The impeller is radial at the exit.
3. The slip factor is 0.88.
4. The absolute velocity at the impeller exit is equal to the blade tip speed resulting in an absolute flow angle of 61.6 degrees.
5. The stage consists of a vaneless diffuser and a simple collector or ducting downstream of the impeller.
6. The static pressure rise downstream of the impeller corresponds to that of a constant width vaneless diffuser of outer diameter 48 inches and effectiveness ($\Delta P_s / \Delta P_{sis}$) of 0.75.

7. For the tandem units, the specific speeds of the two stages are equal.

With the above assumptions, the centrifugal compressor systems were analyzed.

The effect of specific speed on various single stage design parameters for the five operating points are shown in Figures 2 and 3. An analysis of the figures reveal the following:

1. The flow rate increases with specific speed (Fig 2).
2. The pressure ratio decreases with specific speed (Fig 2).
3. The over-all efficiency (based on vaneless diffuser exit static pressure) attains its maximum value between specific speed values of 0.11 and 0.13 before decreasing at an increasingly faster rate with increasing specific speed (Fig 2).
4. The exit temperature and tip speed decrease with increase in specific speed (Fig 3).
5. The maximum-to-impeller exit diameter ratio increases with specific speed. However, the rate of increase decreases with specific speed (Fig 3).
6. The maximum-to-impeller diameter ratio is less than 1.2 for operating point A (Fig 3).

Since item 6 would be critical from space available for collector or duct assembly, the single stage design for operating Point A was analyzed for the feasibility of designing a collector geometry within the initially specified maximum diameter of 48 inches. The particular design for this analysis was selected at a specific speed value of 0.13 since it represents an optimum configuration from range (pressure ratio) considerations. Also, the small increase in available space for ducting when the specific speed is increased from 0.13 to 0.15 is partially offset by the increase in flow rate.

A simple collector with circular cross-section and near sonic exit velocity would require a radial height of around 13.5 in compared to an available radial height of 3.5 in at the diameter ratio (D_{max}/D_1) of 1.17. The required radial height, however, could be substantially reduced by designing a collector configuration which is wrapped around the impeller. Such a system would not only have high turning losses but would also have no static pressure rise beyond the impeller exit and, as a result, the available pressure ratio would be considerably reduced. A reduced pressure ratio would reduce the range that can be achieved by inlet throttling. For instance, a turning loss coefficient of around 0.5 with no pressure recovery in the collector would reduce the pressure ratio from 1.89 (Fig 2) to 1.32. An annular exit with the possible use of axial straightening vanes for torque measurement purposes would further reduce the available pressure ratio. Therefore, a single-stage centrifugal compressor configuration is not a feasible concept if the over-all maximum diameter, D_{max} , is restricted to 48 in.

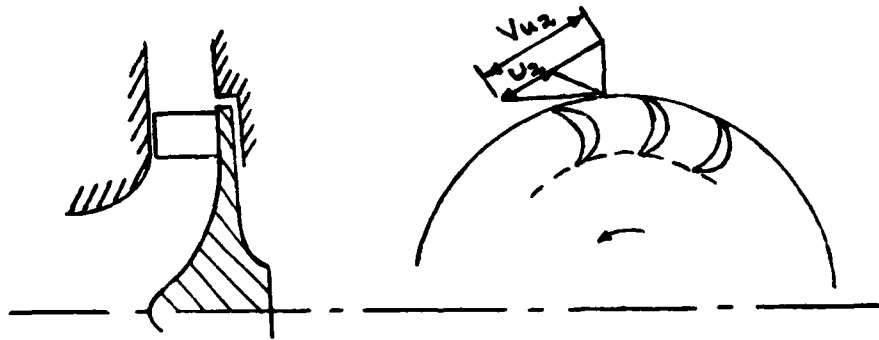
Assuming a specific speed of 0.13 for the stages, both double-entry and tandem configurations were sized for operation at Points A and B. The important design quantities are listed in Table I and Table II along with those of the single-stage configuration. It can be seen from Table I that the available space for ducting has more than doubled and the flow rate is reduced by about one third when the single-stage configuration is replaced by

either the double-entry or the tandem configuration for Point A.

The operating characteristics of one side of the double-entry unit are similar to those of the first stage of the tandem unit which has a slightly higher flow, pressure ratio and diameter. For a constant specific speed of 0.13, the first stage of the tandem unit is larger than the second stage resulting in a 55:45 power split for Point A and a 60:40 power split for Point B. The use of common basic impeller shape (with shroud and tip cuts) could alter the relationship between the two stages of the tandem units to some extent. The main advantage of the tandem configuration over the double entry configuration is in its higher pressure ratio which would facilitate higher range by inlet throttling.

Radial Outflow Compressor

This compressor is essentially a centrifugal one. It differs from the conventional type in certain respects: blades resembling those of impulse turbines and situated in the radial part of the rotor only, high forward slopes for the blades resulting in more than twice the work absorption per pound ($U_2 V_{u2}$) of conventional type for a given blade speed, and usually a constant passage width across the rotor blades as shown in the sketch below.



Since it is essentially a centrifugal compressor, the specific speed-efficiency relationship employed for the conventional centrifugal compressors was adopted for the preliminary analysis of the radial-outflow compressors. Apart from this relationship, various other simplifying assumptions were used for the analysis. They are:

1. The rotor is of impulse (turbine) type with 60-degree blade angles.
2. At the rotor blade exit, the absolute tangential velocity is twice the blade speed ($V_{u2}=2U_2$).
3. The stage utilizes a rotating vaneless diffuser downstream of the rotor.
4. The pressure recovery effectiveness of the diffuser is 0.75.

5. The radial height required for ducting downstream of the diffuser is 1.5 times the rotor exit passage width.
6. The casing thickness is 0.5 in.
7. There is no static pressure recovery downstream of the vaneless diffuser.

With the above assumptions, both single-entry and double-entry configurations were analyzed for Points A and B. The effect of specific speed on over-all pressure ratio, over-all dimensions, and absolute Mach number at diffuser exit for single-entry configurations, is shown in Figure 4. It can be seen from the figure that a single-entry configuration is not feasible for Point A within the over-all diameter restriction of 48 inches since there is no pressure rise across the stage as indicated by the variation of over-all pressure ratio with specific speed. This results from, one, the assumed absence of static pressure rise across the rotor and, two, the insufficient length available for diffusion downstream of the rotor.

Similar to Figure 4, the effects of specific speed for double-entry configurations are shown in Figure 5. For Point A, the over-all pressure ratio is maximum at $N_s = 0.09$. At this specific speed, the diffuser length, $(D_3 - D_2)/s$, is maximum and the absolute exit Mach number is near minimum. For Point B, the pressure ratio is maximum at $N_s = 0.07$. However, a design with N_s of 0.09 would be optimum from considerations of diffuser length and exit Mach number. Hence, the over-all stage quantities and dimensions were obtained at $N_s = 0.09$ for Points A and B and given in Table III.

Axial Compressors

As for the centrifugal compressor, the analysis of axial compressor utilized the specific speed-efficiency relationship. This relationship for axial compressors was based on that of Reference 2 with some reduction in the given peak efficiency value. Based on previous designs and an initial analysis, the following simplifying assumptions were made for the analysis:

1. The optimum stage efficiency is 0.85.
2. The axial velocity across a stage is constant.
3. The velocity at the stage exit is axial.
4. The specific speed of the first stage is 0.5.
5. The average hub-to-tip diameter ratio is 0.6.
6. Power absorption is equally divided between stages.
7. The dynamic head at the exit of a compressor is lost.

With the above assumptions, the effect of number of stages on various stage design parameters was analyzed for Point A. The results of the analysis are shown in Figures 6 and 7. It can be seen from Figure 6 that a minimum of three stages is required to bring down the tip Mach number to an acceptable level from considerations of stable operation. A reduced tip Mach number would be accompanied by a lower tip speed which would reduce the stress level and increase mechanical reliability. Also, the increase in over-all pressure ratio with higher number of stages would increase the range.

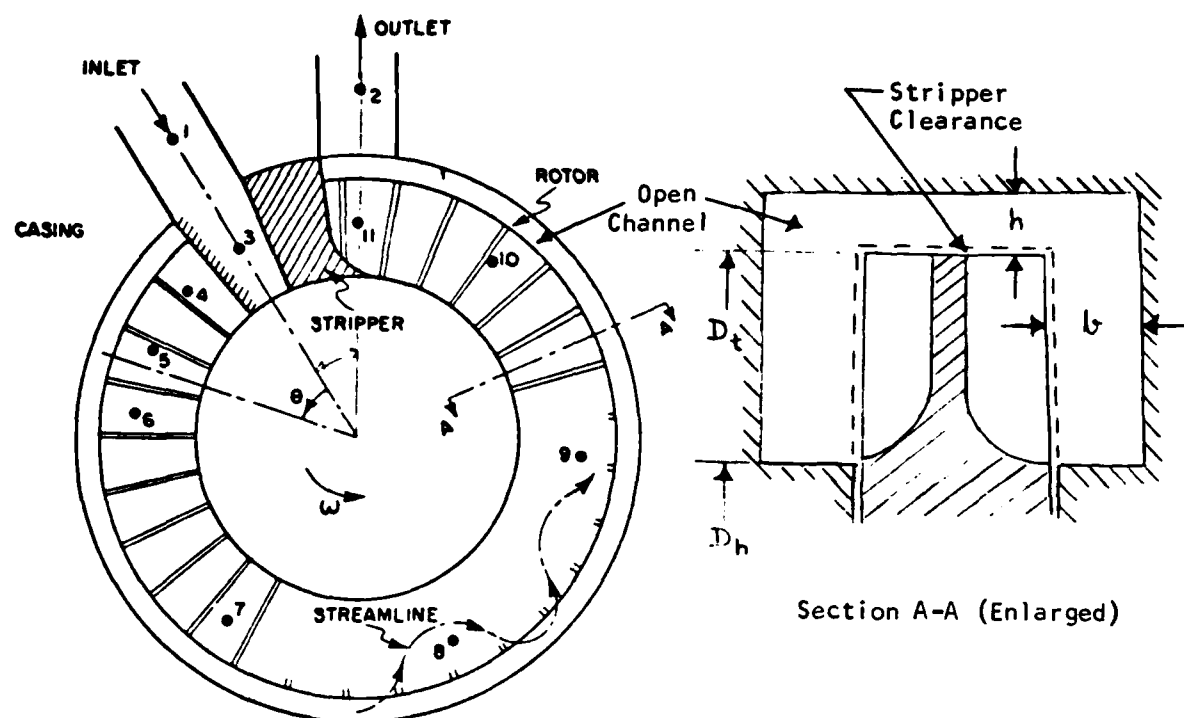
For the above analysis, the tip diameter of the stages was allowed to vary. Assuming the tip diameter to be constant, a three-stage design was arrived at for Point A and its design quantities are listed in Table IV. The tip relative Mach number is transonic for all three stages. Of the three stages, the first stage is critical since it has comparatively high tip Mach number as well as high temperature rise coefficient with high flow coefficient. An analysis of a four-stage configuration indicated that a reduction of about 10 per cent can be realized in tip relative Mach number. However, this decrease in tip Mach number was followed by an increase in both flow coefficient and temperature rise coefficient of the first stage.

An analysis of a four-stage configuration for Point B indicated a very high tip Mach number for the first stage. Hence, a five-stage configuration was analyzed and its design quantities are listed in Table V. It can be seen from the table that the inlet tip relative Mach number is relatively high even with five stages. An analysis of the five-stage configuration, with redistribution of work between the stages, did not materially change the individual stage designs when the specific speed of the last stage was not allowed to decrease below 0.29. Also, a sizing of a five-stage configuration with a constant hub diameter resulted in temperature rise coefficient of as high as 1.5 for the last stage indicating the need for additional stages.

The analysis of axial compressors so far has revealed that axial compressors could be designed within the limitation of 48 inches outer diameter. However, the weight could be a limiting factor especially for constant hub diameter designs which offer some advantages in terms of common blading between stages.

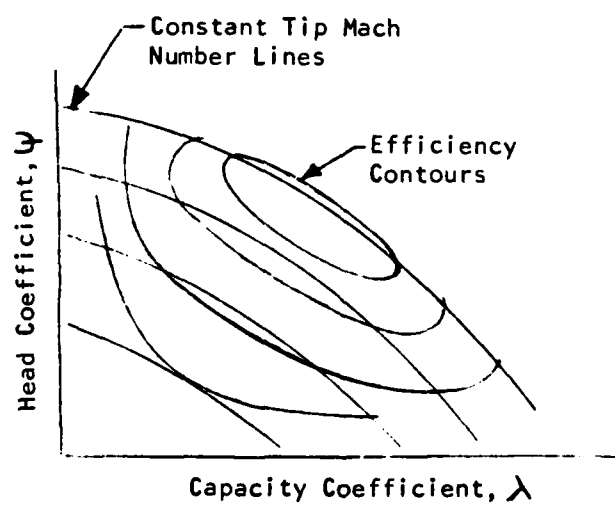
Drag Compressor

The drag compressor is a low specific speed machine and its main advantage is the absence of surge even at zero flow. It is also known under various names: peripheral, regenerative, friction, traction, turbine or tangential compressor. It usually consists of a wheel with small vanes that "drags" the flow along the periphery and finally discharges as is shown in the sketch on the next page. As indicated by a streamline, the fluid passes through the vanes from the open channel many times between the inlet and exit. This repeated path through the rotor vanes or regenerative flow pattern, which can be thought of as internal multistaging, absorbs many times the work per pound of dynamic rotary compressors. The inlet and exit is separated by the stripper which, except for the leakage through the stripper clearance, allows only the fluid within the impeller vanes to pass through to the low pressure inlet.



Section A-A (Enlarged)

The nondimensional performance characteristics of a drag compressor can be represented as shown in the sketch below. The head coefficient is



defined by

$$\psi = g H / U_t^2 \quad (1)$$

where H is the adiabatic head (ft) and U_t is the impeller tip speed (ft/sec). The capacity coefficient is defined by

$$\lambda = Q_s / U_t A_c \quad (2)$$

where Q_s is the inlet volume flow (cfs) and A_c is the cross-sectional area of open channel (ft^2). The impeller tip Mach number is defined as the ratio of U_t and the inlet stagnation speed of sound. Other details of interest can be found in Reference 3.

The sizing of drag compressors was mainly based on the performance characteristics of a compressor (ORGDP-1 compressor) and its modifications given in Reference 3. The channel height, h , width, b , and the hub diameter, D_h , were normalized with respect to the impeller tip diameter, D_t (see sketch on page 9 for the details of the channel). An initial analysis indicated that the operating point B would require the larger number of units. Hence, only the results of the analysis for Point B configurations are given in Table VI.

Of the six configurations listed in the table, configurations DC1, DC2 and DC3 were obtained from the given characteristics of Reference 3. Configuration DC4 utilizes an extrapolated impeller tip Mach number assuming that there is no undue aerodynamic and mechanical penalty associated with a higher than normal tip Mach number. Configuration DC5 reflects the maximum enlargement of the channel that was incorporated in the basic design of Reference 3. Configuration DC6 was sized on the assumption that an equal additional enlargement of the channel would be equally beneficial.

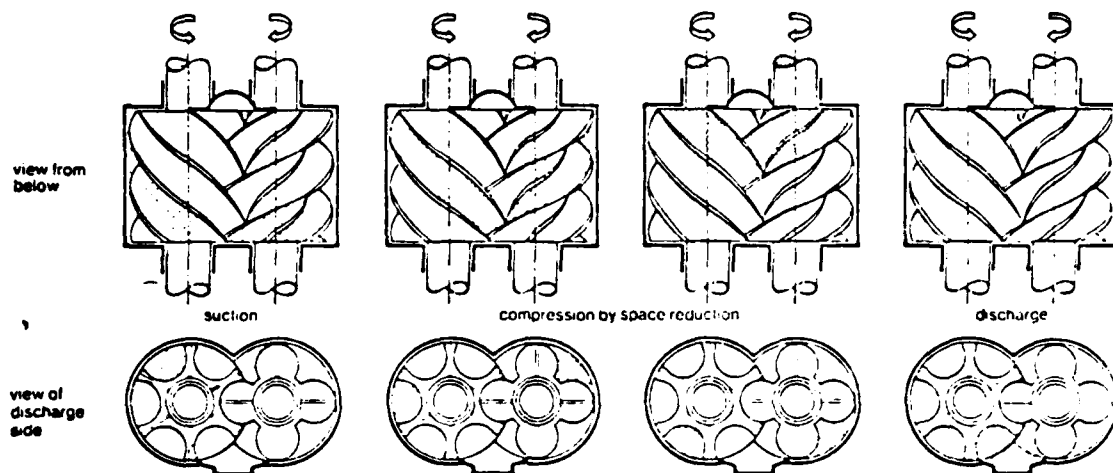
It can be seen from the table that a modest advancement of the present state-of-the-art technology would not reduce the required number of units to a reasonable level. If further high tip Mach number levels and enlargement of the channel could be used, the number of units could be reduced to a lower level. However, the total weight in that case may exceed the limit since each unit would be bigger in size.

Positive Displacement Rotary Compressors

Similar to the drag compressor, the rotary compressors are low specific speed machines. Like the reciprocating compressors, they are positive-displacement machines with internal compression; the compression is accomplished by reduction in the volume of space occupied by the gas when it is carried from the inlet to the discharge port. These compressors are limited by low tip Mach numbers (tip speed/inlet stagnation speed of sound).

In the past, various new versions of rotary compressors have been introduced. Of these various types, the helical screw compressor is the most versatile. A detailed description of the operation and performance evaluation

of this type of compressor is given in Reference 4. It is a two-shaft rotary piston machine and its operation is illustrated in the sketch below.



The analysis of the helical screw compressor and four other types of positive displacement rotary compressors was based on the method and information given in Reference 5. From the analysis, the number of units required for Point B (critical from number of units) was calculated for all five types: helical screw, spiral axial, straight lobe, sliding vane and liquid liner compressor. For each type, two configurations were sized with the first configuration using the maximum value of the pressure ratio range and the length-to-diameter ratio normally employed, the limiting tip Mach number, and the characteristic displacement constant. The second one incorporates an arbitrary increase of 50 per cent in the above quantities.

Table VII lists the various parameters and the required number of units for the compressor configurations. It can be seen from the table that the required number of units would be prohibitively high for all types in the first category. An increase of 50 per cent in the operating or geometric characteristics would make only the helical screw compressor a possible candidate system. The pressure ratio of the helical screw compressors could be increased to 6 or more but the characteristic displacement constant may not be changed very much. If this constant alone is kept unchanged, the number of required units would increase to 10 or 11. While an increase in length-to-diameter ratio would decrease the number of units, it would add weight to the system. Further, an increase in pressure ratio may not go hand in hand with an increase in length-to-diameter ratio.

PRELIMINARY ANALYSIS OF FEASIBLE COMPRESSOR SYSTEMS

Introduction

In the feasibility analysis, several compressor concepts were analyzed for the Navy's future dynamometer application. The analysis indicated the following:

1. For Point A, a single stage configuration is not feasible for both centrifugal and radial outflow type compressor within the initially specified maximum over-all diameter of 48 inches for the compressor systems.
2. In axial compressors, a minimum of three stages for Point A and a minimum of five stages for Point B is required.
3. The drag compressor and the helical screw compressor are marginally feasible and require further analysis to establish their feasibility.

In the feasibility analysis, the compressor concepts were studied only in terms of over-all diameter and number of units or stages. In the preliminary analysis reported in this section, the feasible compressor systems were further analyzed to determine the major dimensions. These were then used to obtain the flow paths of the systems and, hence, their weight. In addition, an analysis was conducted to determine whether it would be possible to design a basic configuration from which the different dynamometer units could be obtained by simple geometric scaling to cover the range of possible design points.

Centrifugal Compressors

Stage Design Analysis

As in the previous feasibility analysis, the stage design analysis employed the relationship between specific speed and normalized efficiency. In addition, the analysis employed various simplifying assumptions and considerations some of which were based on the results of the feasibility analysis. They are:

1. The optimum impeller efficiency is 0.92 and its variation with specific speed follows that of a stage.
2. The impeller is radial at the exit.
3. The slip factor is 0.88.
4. The stage consists of a vaneless diffuser and a simple collector or ducting downstream of the impeller.
5. The static pressure rise downstream of the impeller corresponds to that of a constant width vaneless diffuser of outer diameter 48 inches and effectiveness ($\Delta P/\Delta P_{is}$) of 0.75.

6. Where possible, use of common impeller blading with simple shroud-cuts.

With the above assumptions, both double entry (or double unit) and tandem units were sized for operating Points A and B. Also, single stage configuration was sized for operating Point D. The stage characteristics and geometric data are listed in Table VIII for the various stages.

It can be seen from the table that the second stages of the tandem units employ the same impeller as that of the first stages with simple shroud-cuts. This results in slightly reduced values for inducer tip radius and impeller exit passage width. Also, the impeller of the single stage unit for Point D is obtained by this way from the impeller for Point A. The shroud-cut is illustrated in Figure 8.

The flow angle at inducer tip for the configurations was kept around 60 degrees; a value found optimum from NREC design practice. The slight variation in this value from one to the other design results from shroud-cut. Similarly, the variation in specific speed results from reduction in flow capacity caused by shroud-cut. The absolute exit flow angle was kept relatively low from flow range consideration. The relatively high inducer tip relative Mach number for Configuration B-CCD2 (or B-CCT2-1) results from the combination of high volume flow and high rotational speed.

Estimation of Weight

Using the over-all dimensions of stages A-CCT2-1 and A-CCT2-2 given in Table VIII, the flow path of the tandem unit for operating Point A (configuration A-CCT2) was obtained. The flow path thus obtained is shown in Figure 9 which incorporates a row of IGV at the inlet and deswirl vanes at the exit of the stages. The incorporation of a row of variable IGV would serve two purposes: variation of power absorption per lbm of flow rate and variation of flow rate by throttling effect. The deswirl vanes ahead of the second stage would provide axial flow at the second stage inlet and those at the exit would eliminate any exit swirl to avoid possible reaction upon the torque measuring system based on the stator casing reaction.

From the flow path of Figure 9, a preliminary layout was made. From the layout, the weight of the tandem unit (A-CCT2) was estimated to be 2,020 lbs. This weight is based on using aluminum for all parts except for the shaft and the second stage rotor which were assumed to be made of titanium. The above weight estimation is based on first-cut preliminary analysis with the consideration to obtain a lighter unit. For instance, the casing was assumed to be relatively thin at 0.5 in thickness. Also, the weight of any required inlet and exhaust ductings extraneous to the flow path of Figure 9 was not included in the weight estimation.

The weight of double-entry unit (A-CCD2) is expected to be close to that of A-CCT2; a weight reduction of around 150 lbm is possible in double-entry units since aluminum would be used for both rotors. In any event, it is not possible to design a centrifugal compressor configuration for Point A as one unit weighing around 1000 lbm. The only way to get around the problem is to design two units, lift them separately and couple them. A double unit in parallel would involve simple coupling of the shafts whereas the double unit for series (multistaging) operation would require additional complication with respect to interstage ducting.

Basic Design Configuration

The exact number of dynamometer units required to cover the specified range of design points depends on the range of each dynamometer unit and, therefore, can only be calculated based on the results of the range analysis. However, a minimum of three dynamometer units would be required: one for the high speed point (Point G), another for the medium speed range (Points B and C), and a third one for the low speed range (Points A, F, E and D). At the low speed range, a single dynamometer unit would be required to have power range of about 8:1 at constant speed for the Navy's requirement of at least 2:1 power range at design speed of each engine. Hence, it is likely that two dynamometer units would be required for the design points of low speed range.

In the absence of an exact knowledge of the number of units required for the dyno system, it would be desirable to arrive at a basic design configuration which would provide scaled versions to cover the range not covered by the basic dyno unit. In this way, repetitive calculations could be avoided and any additional requirement could be included in the analysis without significant additional effort. Also, this would simplify the design and development of dynamometers resulting in reduction of over-all cost and effort. Therefore, an analysis of the centrifugal compressors was conducted for scaling with the following assumptions:

1. At constant blade speed, the power absorption is proportional to the square of the linear scale factor.
2. For a given unit, the power absorption is proportional to the cube of the rotational speed.
3. The weight of a unit is proportional to the cube of its linear dimensions.

Assumption 1 can be expressed as:

$$\frac{P_s}{P_b} = S_L^2 \quad (3)$$

where S_L is the linear scale factor
 P is the total power absorption
 U is the blade speed
and b and s are the subscripts which refer, respectively, to the basic design configuration and the scaled unit.

From assumption 2, the power absorption, P_s , at any rotational speed, N_s , for the scaled unit is given by,

$$\frac{P}{P_{s,d}} = \left(\frac{N}{N_{s,d}}\right)^3 \quad (4)$$

where $P_{s,d}$ is the power absorption of the scaled unit at the design rotational speed, $N_{s,d}$, which is related to the design rotational speed of the basic unit by

$$N_{s,d} = N_{b,d} / S_L \quad (5)$$

Combining Equations 3, 4, and 5, the scale factor, S_L , can be expressed as

$$S_L = \left(\frac{P_s}{P_{b,d}}\right)^{1/5} \left(\frac{N_{b,d}/N_s}{N_{s,d}}\right)^{3/5} \quad (6)$$

where P_s is the power absorption required of the scaled unit at rotational speed, N_s , and $P_{b,d}$ is the design power absorption of the basic unit. From assumption 3 the weight, W_s , of the scaled unit can be related to the weight, W_d , of the basic unit by

$$\frac{W_s}{W_d} = S_L^3 \quad (7)$$

With the above relationships and the tandem configuration for Point A (A-CCT2) as the basic configuration, an analysis was conducted to determine the features of scaled units for each of the other six operating points (Table IX). It can be seen from the table that the minimum scale factor is 0.41 and the blade speed ratio varies from a minimum of 0.74 for Point D to a maximum of 1.24 for Point B. Also, all but Point D of the low speed operating points would need dynamometers weighing greater than 1000 lbm. The range of variation in the scaling factors and the operating point blade speed ratios can be easily incorporated into a good basic design configuration. Therefore, it is sufficient to design a basic configuration and to produce the other required dynamometers by direct scaling. The required number of dynamometers would, of course, depend on the power range of the dynamometers. A 2:1 power range within the range of blade speed ratios would dictate a dynamometer for each operating point.

With the tandem configuration A-CCT2 as the basic unit, the simple scaling relationships (Equations 3 to 7) were employed to obtain Figure 10. Each of the positive-sloped lines ($S_L = \text{constant}$) represents the power-speed relationship of a scaled dynamometer for a particular scaling factor, S_L . The dotted line ($S_L = 0.791$) corresponds to the dynamometer unit with a weight of 1000 lbm. Any operating point to the left of this line would require a dynamometer unit weighing greater than 1000 lbm. This is readily seen from the weights of scaled units shown in Table IX for Points A, E, and F. Any change in the weight of the basic unit would, of course, shift this dividing line for 1000 lbm to the right or left, depending upon whether the weight of the basic unit is heavier or lighter than 2020 lbm. Also, any deviation in cubic rule for the variation of weight with scale factor would shift this dividing line. For instance, a likely value of 2.8 instead of 3 would shift this dividing line for 1000 lbm to the right, and the dotted line on the figure would then correspond to a scaled unit of around 1050 lbm.

The negative-sloped lines shown in the figure (Fig 10) correspond to the operation of the scaled units at constant blade speed ratios, $U_b/U_{b,d}$. The scaled unit for Point B ($S_L = 0.714$) could be applied to Point C if the range of power absorption is greater than 3.3:1 at 12000 rpm. The range of power absorption, however, has to be at least 6.7:1 at 6600 rpm for the basic unit to cover all four low speed operating points. Any range less than 6.7:1 but greater than 3.3:1 would require two dynamometers to cover the low speed operating points. The second low speed unit could also be obtained as a shroud-cut version instead of a scaled unit. In the shroud-cut version the weight of the unit for the low power points (Points E and D) would be practically the same as that of the basic unit and it would also operate at a higher blade speed than that of the scaled unit.

In Table X, the over-all dimensions given in Table I for B-CCD2 (or B-CCT2-1) are compared with those of the unit scaled from the configuration A-CCD2 (or A-CCT2-1). Except for the exit passage width, the other dimensions are practically the same for the two. The increase in exit passage width for the scaled version would result in less than 3 degrees increase in the absolute flow angle at the impeller exit. The above comparison, therefore, also points to the adequacy of the dyno analysis with a basic configuration. The basic configuration would, of course, have to be analyzed at different rotational speeds as the scaled units would have to operate at blade speeds different from that of the basic unit designed for a particular operating point.

Radial Outflow Compressor

As explained earlier in connection with the feasibility analysis, the radial outflow compressors form a particular type of centrifugal compressors. Therefore, the conclusions of the scaling analysis for the centrifugal compressors would be equally valid for the radial outflow compressors. Also, the results of the feasibility analysis included the over-all dimensions necessary for a preliminary weight calculation. Hence, the weight of the double entry unit for Point A (A-ROCD2) was estimated.

The estimated weight of the double entry unit (A-ROCD2) is 1970 lbm. This weight is based on using aluminum for the casing and titanium for the shaft and rotor. As for the centrifugal compressor unit, the casing was assumed to be relatively thin (0.5 in thickness). Also, the weights of any required inlet and exhaust ductings for non-axial flow inlet and non-radial exhaust were not included in the preliminary weight calculations.

Axial Compressor

Estimation of Weight

The flow path of the 5-stage axial compressor for Point B (B-AC51) is shown in Figure 11. This was obtained using the geometric information generated during the feasibility analysis (Table V) and various other assumptions: the average axial chord of rotor blades is 2.2 in with an average axial aspect ratio (blade height/axial chord) of 2, the axial chord of stator blades is 2.5 in with an average axial aspect ratio of 1.6, and the

axial spacing between the blade rows is approximately equal to one half of the average axial chord length of the blade rows. In addition, it was assumed that the stage incorporates a row of IGV of 3 in axial chord.

From the flow path of Figure 11, a preliminary layout was made. From the layout, the weight of configuration B-AC51 was estimated to be 636 lbm. (The weight of a comparable centrifugal compressor unit scaled for Point B is 767 lbm, Table IX.) The weight of B-AC51 is based on using aluminum for all parts except for the shaft and the last two rotors, which were assumed to be made of titanium. As in the case of the centrifugal compressor unit, the aim was to obtain a lighter unit. Therefore, the casing was assumed to be relatively thin (0.5 in thickness), and the weight of any required inlet and exhaust ductings was assumed to be negligible.

Scaling Analysis

The assumptions employed for the scaling analysis of the axial compressors are similar to those employed for the centrifugal compressors except for the additional assumption associated with the variation in number of stages. The various simplifying assumptions are:

1. The power absorption is equally distributed between stages.
2. At constant blade speed, the power absorption is proportional to the square of the linear scale factor.
3. For a given unit, the power absorption is proportional to the cube of the rotational speed.
4. The length of a unit is proportional to the number of blade rows and the scale factor.
5. The weight of a unit is proportional to the length of the unit and the square of its diameter.

From assumptions 1 and 2,

$$\frac{n_b P_s}{n_s P_b} = S_L^2 \quad \text{when} \quad U_s = U_b \quad (8)$$

where S_L is the linear scale factor for a stage
 P is the total power absorption
 N is the number of stages
 U is the blade speed
and b and s are the subscripts which refer, respectively, to the basic design configuration and the scaled unit.

From assumption 3, the power absorption, P_s , at any rotational speed, N_s , for the scaled unit is given by

$$\frac{P_s}{P_{s,d}} = \left(\frac{N_s}{N_{s,d}} \right)^3 \quad (9)$$

where $P_{s,d}$ is the power absorption of the scaled unit at the design rotational speed, $N_{s,d}$ which is related to the design rotational speed of the basic unit by

$$N_{s,d} = N_{b,d} / S_L \quad (10)$$

Combining Equations 8, 9 and 10, the linear scale factor, S_L , can be expressed as

$$S_L = \left(\frac{n_b/n_s \times P_s/P_{b,d}}{n_s} \right)^{1/5} \left(\frac{N_{b,d}/N_s}{n_b} \right)^{3/5} \quad (11)$$

where P_s is the total power absorption of the scaled unit of n_s stages at rotational speed, N_s , and $P_{b,d}$ is the design power of the basic unit of n_b stages. From assumption 5 and Equation 11, the weight, W_s , of the scaled unit can be expressed as

$$\frac{W_s}{W_b} = \left(\frac{2n_s+1}{2n_b+1} \right) S_L^3 \quad (12)$$

With the above relationships, an analysis was conducted for the effect of scaling. For the analysis, the five-stage configuration for point B (B-AC51) was taken to be the basic design configuration. The analysis included 5, 4 and 3 stage configurations for Points A and G. A review of the results given in Table XI reveals the following:

1. A decrease in the number of stages would result in a unit with a shorter axial length and a larger tip diameter.
2. For a given operating point, the weight of the unit is not significantly affected by the number of stages. A decrease in the number of stages from 5 to 3 would result in only about 14 per cent reduction in weight.
3. The number of stages could be reduced to 3 for points A and G.
4. The 3 stage scaled unit for Point A has a tip diameter of 32.9 in compared to 35 in for the unit (configuration A-AC31, Table IV) independently sized for this point. This difference mainly results from the use of different hub-to-tip diameter ratios for the stages in the scaled unit.

The results of the scaling analysis definitely indicate that it is sufficient to design a basic configuration and analyze it at different non-dimensional speeds to cover the entire range of requirements.

Basic Design Configuration Details

The configuration for Point B (B-AC51) has the maximum number of stages and, therefore, it could be used to arrive at scaled configurations with equal or reduced number of stages for other operating points. The definition given in Table V for this configuration is mainly concerned with the over-all stage performance, important design parameters, and annulus geometry definition in terms of hub-to-tip diameter ratio and tip diameter. For further definition as well as to judge the feasibility of the five-stage configuration B-AC51 in terms of blading, the blading details were obtained. For this, the following simplifying assumptions and considerations were employed:

1. The stages are of 50 per cent reaction, i.e., the static pressure rise is equally distributed between rotor and stator blade rows.
2. The axial velocity is constant across the stages and from hub to tip.

3. The temperature rise is uniform from hub to tip across the rotor.
4. The incidence, i , to the blade rows is 4 degrees.
5. The deviation angle, δ , can be expressed as

$$\delta = 0.405 \phi / (\sigma - \frac{1}{2} \sin \xi) \quad (13)$$

where ϕ is the blade camber angle
 ξ is the blade stagger angle
and σ is the blade solidity

6. The mean solidity, σ_m , is 1.2 and the chord length is constant from hub to tip.

From assumptions 1 and 2, the flow angles at the inlet (α_1) and exit (α_2) of both rotor and stator blade rows can be expressed as

$$\alpha_1 = \tan^{-1} \{ (2 + 4t) / 4 \phi_f \} \quad (14)$$

$$\alpha_2 = \tan^{-1} \{ (2 - 4t) / 4 \phi_f \} \quad (15)$$

where t is the temperature rise coefficient and ϕ_f is the flow coefficient. The inlet and exit blade angles (α_1 and α_2) are related to the flow angles and blade camber and stagger angles by the following relationships:

$$\beta_1 = \alpha_1 - i \quad (16)$$

$$\beta_2 = \alpha_2 - \delta \quad (17)$$

$$\phi = (\beta_1 - \beta_2) \quad (18)$$

$$\xi = (\beta_1 + \beta_2) / 2 \quad (19)$$

With the above relationships and the previously defined mean stage design quantities (Table V), an iterative procedure was employed to arrive at the blading details listed in Table XIII. The blading details indicate that a five-stage design is feasible but it would involve high camber at the hub. As a result, the number of stages cannot be reduced below five without introducing excessively high camber at the hub. The high hub camber angle obtained for the five-stage design could be reduced by increasing the diameter ratio. This, however, would be accompanied by an increase in relative Mach number at the tip of the rotor blades. It should be noted that the continuous variation in annulus area (or diameter ratio) from inlet to exit would introduce some difference between the rotor and stator blading.

Drag Compressor

During the feasibility analysis, it was found that the number of units required for Point B would be excessive. The number of units could, however, be reasonable for Point A. Therefore, drag compressors were further analyzed including the sizing of two configurations for Point A. The details of these two configurations are listed in Table XIII along with those of corresponding configurations sized earlier for Point B. Of the four configurations in the table, configurations A-DC1 and B-DC1 are based on stage characteristics and parameters normally employed in drag compressor designs. The alternate configurations (A-DC2 and B-DC2) are based on characteristics and parameters which are

judged to be achievable by further development in the present state-of-the-art technology. As shown in the table, the number of units could be reduced to a reasonable value (6) for Point A with advanced designs.

A compressor unit of the configuration A-DC2 is shown in Figure 12. As shown in the figure, the over-all diameter of the compressor system is 50.6 in. Since the minimum length for each unit would be at least 16 in (Fig 12), the total length of the compressor system would exceed 96 in. In addition, the total weight of the 6-unit system was determined to be 6200 lbm based on some conservative assumptions: the casing is made of aluminum with 0.5 in thickness, and the shaft and rotor are made of titanium.

The analysis of the drag compressor for the Navy dynamometer application has resulted in two important findings: one, the number of units required for high power-high speed engine design (Point B) would be excessively high; two, even though the number of units for high power-low speed engine design (Point A) would be reasonable, the total weight of the compressor system would exceed several times the desired weight. Hence, the drag compressor is not a suitable concept for the dynamometer of specified requirements and desired constraints.

Helical Screw Compressor

During the feasibility analysis, five different compressor types were analyzed under positive displacement rotary compressors and the results of the analyses are given in Table VII. Of the five compressor types, only the helical screw compressor was found to be a possible candidate system if an increase of about 50 per cent is achievable in the presently employed values for the operating and geometric characteristics of this compressor. Hence, this type of compressor was further analyzed including the sizing of two configurations for each of the two important operating points (points A and B). The main stage characteristics and parameters for these four configurations are shown in Table XIV.

The important design parameters which characterize the helical screw are four: pressure ratio, tip Mach number, characteristic displacement constant, and length-to-diameter ratio. Design configurations A-HS1 and B-HS1 were sized by employing typical values for the pressure ratio, displacement constant and length-to-diameter ratio. For the tip Mach number, the present maximum value of 0.35 was used instead of a typical value of 0.24. Configurations A-HS2 and B-HS2 were sized by using design parameters judged to be achievable by further development. The pressure ratio could be increased still further. However, an increase in pressure ratio may not be possible with simultaneous increases in displacement constant and length-to-diameter ratio.

It can be seen from the table that the required number of units could be considerably reduced by further advancement in the design technology. Still, the required number of units for operating Point B is excessively high at 15. Assuming a 4-lobe male rotor and a 6-lobe female rotor system,

configuration A-HS2 was sized in detail (Fig 13) for the estimation of over-all length, diameter and weight. As shown in the figure, the over-all diameter of the compressor system is relatively low at 40.5 in but the length of a single unit is 61 in which would dictate an excessively long 5-unit system required for Point A. Also, the total weight of the 5-unit compressor system was found to be 5900 lbm based on the use of titanium for shaft and rotors, and aluminum for stationary parts.

The above analysis of the helical screw compressor indicates that this type of compressor has drawbacks similar to that of the drag compressor: the required number of units for point B is excessively high and the total weight of the system (5-unit) for point A is considerably higher than the desired weight of 1000 lbm. In addition, the total length would be a limiting factor. Also, the helical screw compressors require an oil supply system for cooling, lubrication and sealing purposes. Hence, this type of compressor is not a viable concept for the dynamometers of specified requirements and desired constraints.

RANGE AND REQUIRED NUMBER OF DYNAMOMETERS WITH INLET AND EXIT VALVES

Introduction

The analysis concerning the feasibility of the various compressor concepts and the subsequent preliminary analysis of the feasible compressor concepts have established that only the dynamic rotary compressors (centrifugal, radial outflow and axial compressors) would be suitable for the future Navy dynamometers. As a result, only the dynamic rotary compressors were considered for further analysis.

Based on preliminary analysis and further detailed analysis by NREC design-analysis computer programs, a total of six compressor systems were selected for the analysis of range achievable with inlet and exit valves. The selected compressor systems are:

1. Single-Stage Centrifugal
2. Double-Entry Centrifugal
3. Tandem (2-Stage) Centrifugal
4. Single-Stage Radial Outflow
5. Double-Entry Radial Outflow
6. 5-Stage Constant-Hub Axial

The scaling analysis discussed in the previous section has indicated that, for range analysis, it is sufficient to design one basic compressor for each of the compressor systems. Therefore, the basic compressor was sized for each of the above six compressor systems, and, for valid comparison, the basic compressors were sized for a common operating point (Point A). The basic compressors were then analyzed for the achievable range with inlet and exit valves at various rotational speeds. From the range thus obtained, the six compressor systems were further analyzed for the number of dynamometers required to meet all engine specifications.

Included in this section are the results of these various analyses: sizing of basic (Frame 1 size) compressor systems, range analysis, and the analysis for the required number of dynamometers with inlet and exit valves.

Frame 1 Size Compressors

As explained earlier, the basic compressor systems were sized for a common operating point so that a valid comparison can be made of the different compressor systems. The common operating point was taken to be Point A, which requires the largest physical size. The basic compressors are designated as Frame 1 size compressors and are sized to absorb an average horsepower of 10,000 hp at 7,000 rpm. The average horsepower is taken to be the average of horsepowers at surge and choke operating points with standard inlet conditions.

Since the original restriction on the maximum allowable diameter was later relaxed to be considered only as a guideline on the maximum physical size,

the single stage centrifugal compressor was included as one of the three centrifugal compressor systems for further analysis. The over-all geometry and performance characteristics of these three compressor systems for Frame 1 size are listed in Table XV. The geometries listed in the table were finalized based on performance analysis by NREC design-analysis program (PREDM) at 7,000 rpm. For the tandem and double-entry units, the preliminary design values of these units for Point A (Table VIII) were used as the initial values for the analysis. As such, the design geometries of these units for Frame 1 sizes (F1-CC-T and F1-CC-D) differ very little from those of the preliminary configurations for Point A (A-CCT2 and A-CCD2). As for the preliminary configurations, the geometries of these two designs have certain common features: the first stage of the tandem unit is identical to that of one side of the double-entry unit and the second stage of the tandem unit is a shroud-cut version of the first stage. Also, the single-stage unit was obtained by scaling up the stage geometry (one side) of the double-entry unit. The exit tip diameter was increased by about 10 per cent and the exit passage width was increased by about 33 per cent to match the Frame 1 size power absorption. The relatively high increase in flow width resulted in about 4 per cent reduction in the value of rotor tip diameter compared to that resulting from direct scaling.

In the case of the radial outflow compressors, an analysis of the preliminary double-entry configuration for Point A (A-ROCD2, Table III) by Program PREDM of Reference 6 indicated the following:

1. With variable width across the rotor blades, the range extension potential of this type of compressor with variable shroud would be limited.
2. The preliminary value of the rotor exit tip diameter would dictate a relatively low rotor inlet radius for rotor blade designs in the range of aspect ratios or number of blades normally employed. For low rotor-inlet radius, the inlet annulus area available between this radius and the shaft would limit the high-speed operation by inlet choking.
3. An introduction of prewhirl would introduce a significant reduction in stable operating range.

Therefore, Frame 1 size double-entry configuration (F1-ROC-D) was sized with constant rotor passage width, axial flow inlet, and rotor exit radii considerably higher than that of the preliminary design. As in the case of centrifugal compressors, a single entry unit was also sized as a scaled version of one side of the double-entry configuration with about 13 per cent increase in the diameters and 35 per cent in the axial width of the rotor. The resulting over-all geometry and design performance characteristics of these two Frame 1 size compressors (F1-ROC-S and F1-ROC-D) are given in Table XVI.

The detailed analysis of the axial compressors for sizing of the Frame 1 compressor was performed with the use of NREC Program ZORBA (Ref 7). For the initial analysis, the preliminary basic design configuration

(B-AC51) was scaled up for Point A and analyzed. The analysis confirmed the earlier conclusion that it is, indeed, possible to design a five-stage compressor for the dynamometer of specified requirements within the initial limitation of 48 in for the over-all diameter. However, the preliminary blading details of Table XII were found to require considerable modifications from considerations of stage matching. Therefore, a 5-stage constant hub diameter compressor, which offers some advantage in terms of common blading between stages, was sized based on previous designs for industrial compressors. In this design, comparatively high aspect ratios were employed for the blade rows to help offset the additional weight associated with higher tip diameters for the front stages. The initial configuration thus obtained was analyzed by Program ZORBA. From the results of the analysis, the Frame 1 size compressor was finalized as a shroud-cut version of the initial design to match the Frame 1 size power absorption. The over-all geometry and design performance characteristics of this compressor (F1-AC5-H) are given in Table XVII. This compressor has common blading as shown in Figure 14 - the stator and rotor blade angles are independent of stages and are a function of the radius only.

Range with Inlet and Exit Valves

The Frame 1 size centrifugal and radial outflow compressor configurations were analyzed by Program PREDM at various rotational speeds for operation between surge and choke points. The surge points for these compressors were established based on NREC surge criteria using the detailed flow conditions at the impeller inlet and diffuser inlet. The choke points were established based on the maximum flow capacities of the inducer and exducer portions of the impeller. At low speeds where there is no choking for pressure ratios above one, the choke point was taken to be the point at which the pressure ratio is one. The results of the analysis were used to obtain the performance characteristics (Fig 15 thru 19) pertinent to the dynamometer application.

At each rotational speed, the variation of power with flow is very nearly linear (Fig 15, 16 and 17) for centrifugal compressors. This reflects the fact that, for radial impellers, the temperature rise across the impeller would not vary significantly with flow at a fixed rotational speed. Blades such as used in radial outflow compressors have forward slopes (in the direction of rotation). The temperature rise across the stages utilizing forward-sloped blades would increase at a given rotational speed when the flow is increased from surge to choke. This accounts for the rate of power increase higher than that of flow as shown in Figures 18 and 19 for the radial outflow compressors.

The axial compressor configuration was analyzed by Program ZORBA to arrive at the performance characteristics shown in Figure 20 for various rotational speeds between surge and choke operating points. The surge point was based on NREC stall criteria for axial compressors and the choke point was based on detailed flow calculations at the inter-blade row stations. As for the centrifugal compressors, the choke point for low speeds was taken to be the point at which the pressure ratio is one.

Unlike the centrifugal compressors, the power for a fixed rotational speed, decreases with increase in flow rate as shown in Figure 20 for the axial compressor sized for the dynamometer application. This results from a rate of decrease temperature rise across the stages greater than the rate of increase of flow rate. This effect is very pronounced at higher rotational speeds. The above power-flow relationship is akin to that of centrifugal compressors with high backward-sloped impellers or rotor blades.

The performance characteristics for the six compressors were obtained with standard inlet conditions. Therefore, the power range shown in the figures (Fig 15 thru 20) can be achieved by an exit valve as it can be used to vary the operating point from choke to surge by closing the valve area. With an exit valve, the inlet conditions to the compressor correspond to the ambient conditions.

For a given rotational speed and exit valve setting, the compressor would operate at a fixed corrected flow rate ($\dot{m}\sqrt{T_0}/\dot{g}_0 = P_{STD} \dot{m}\sqrt{T_{To}}/\sqrt{T_{STD}} P_{To}$). The actual flow rate is proportional to the inlet pressure level, P_{To} . Therefore, an inlet valve could be used to decrease the flow rate and, hence, the power absorption. The range of power modulation by an inlet valve, however, is set by the stage pressure ratio with the lower limit of inlet pressure approximately equal to the ambient pressure divided by the stage pressure ratio.

The minimum power achievable at a rotational speed depends on the power-pressure ratio relationship of a compressor. For the centrifugal and radial outflow compressors, the minimum power (with only exit valve) occurs at surge points where the pressure ratio is also maximum. Therefore, the minimum power with inlet and exit throttling for these compressors would occur at surge points. For the axial compressor in which the minimum power (with only exit valve) occurs at choke point, the minimum power with both valves could occur anywhere between the two limiting operating points. However, the minimum power for F1-AC5-H was found to occur at or very close to the surge points. Therefore, the minimum power with inlet and exit valves for all the six compressors were defined as the power with standard inlet conditions divided by the pressure ratio at the surge point for a given rotational speed. With the above definition and the performance characteristics of Figures 15 through 20, the variation of power range with inlet and exit valves for various rotational speeds were obtained (Fig 21 thru 26).

Number of Frame Sizes and Dynamometers

With the established power range characteristics for the six Frame 1 size compressors, an analysis was conducted for the minimum number of frame sizes and dynamometers required to meet all seven engine design operating points. The different frame sizes were obtained from Frame 1 size by appropriate scaling factors. In each frame size, different dynamometers were obtained by changes to the shroud dimensions to increase or decrease the flow capacity and, hence, the power absorption to meet the requirements of

operating points. At each operating point, the required power reduction is set at the specified minimum range of 2:1 with 10 per cent margin for surge and choke. This resulted in a requirement of at least 2.44:1 power range for the centrifugal and ROC dynamometers at the rotational speed of an operating point with the maximum power at choke equal to or greater than 1.1 times the operating point power.

With the above set requirements, the minimum number of frame sizes and dynamometers required to meet all operating points were obtained for the compressor systems. The performance envelopes of the frame sizes and dynamometers are given in Figures 27 through 32. It can be seen from the figures that, for a given compressor system, the performance envelopes of different dynamometers are identical except for the relative shift in their positions. The relative shifts of these envelopes are along lines of constant blade speed ratios (see Fig 10) when the basic shroud contour is not changed. A change in the shroud contour would move the envelopes up or down (along constant rpm lines) depending upon whether the change in shroud contour was introduced to increase or decrease the flow rate. The relative position of an envelope is, therefore, dictated by the linear scale factor, S_L , and the relative change in area, S_A , resulting from the shroud change.

The minimum speeds of these envelopes correspond to 50 per cent of the design equivalent speed, N_d . The maximum speeds correspond to the blade speed of the frame size obtained for Point B. The equivalent design speed, N_d , is given by

$$N_d = 7000 / S_L \quad (20)$$

where S_L is the linear scale factor employed to obtain the required frame size from Frame 1, whose design rotational speed is 7,000 rpm. At equivalent design speeds, the different frame sizes would, therefore, operate at the same blade speed.

The details of the frame sizes and dynamometers are listed in Tables XVIII through XXIII. The details include the linear scale factor (S_L) applied to Frame 1 size to obtain other required frame sizes and the relative change in area (S_A) introduced to the scaled frame size to obtain a dynamometer to meet the requirements of a specific operating point or points if more than one operating point could be covered by a single dynamometer. The tables also list the design equivalent speed, the operating point or points covered by a dynamometer and the operating speeds relative to the design equivalent speed at operating points covered by the dynamometer.

ANALYSIS OF RANGE EXTENSION WITH OTHER POSSIBLE METHODS

Introduction

Apart from the analysis of the six Frame 1 size compressors for range extension with inlet and exit valves, selected and applicable compressors were analyzed for range extension by various other methods. The various methods studied are:

1. Bleed Control
2. Recirculation
3. Water Injection
4. Variable Geometry

Both axial and tandem centrifugal compressors were analyzed for the range extension with bleed control. For the effect of recirculation on power range, both the radial outflow compressor configurations were used. The single-stage centrifugal compressor was analyzed for the effect of water injection on the range extension. Under variable geometry, two different concepts were studied: variable (rotatable) stator vanes and variable (axially movable) shrouds. The former concept is used to vary the total power by varying the power absorption per pound of flow rate while the later is used to vary the flow and, hence, the total power absorption. An axial compressor and two centrifugal compressor configurations (double-entry and tandem) were analyzed with variable vanes. The variable shroud concept, which is suitable only for the radial outflow compressors, was studied with both single and double-entry configurations.

The results of these various analyses are given and discussed in this section.

Bleed Control

Axial Compressor

Interstage bleeds are used in multistage axial compressors to adjust the blade row operating conditions relative to one another and thus extend the range of the unit at a fixed speed. For the compressor (F1-AC5-H) sized for the Navy dynamometer application, power range can be increased if bleed results in the absorption of either higher power at the compressor surge point or lower power at the choke point or both.

At design speed, the last stage controls surge while all five stages are operating with near maximum flow capacity of the choke point. The limiting mass flow is, however, set by the last stage. At 60 per cent of design speed, the second stage controls the surge mass flow while, once again, the maximum flow is set by the last stage. Hence, at design speed

it is possible that interstage bleed can be used to decrease the minimum power absorbed, while at part speed the range can be extended in both directions. At higher than design speeds, the flow capacity of the unit is limited by the inlet Mach numbers to the first and second rotors, and the last stage continues to control the surge characteristic of compressor. Interstage bleed would, therefore, be completely ineffective as a power range extension technique at speeds higher than design.

Individual stage characteristics were used to obtain some quantitative values of range extension at design (7,000 rpm) and at 60 per cent speed. It was determined that, at design speed, bleeds are ineffective in reducing the minimum power. Due to the stage power mass flow characteristics, all combinations of bleeds investigated resulted in higher power outputs. As a result, it was then assumed the bleed system would be specifically designed to operate at part speeds. Bleeds could be located behind the second, third, and fourth stages to make the downstream stages operate at their surge points with the second stage operation at surge. Such an operation with bleed was found to result in only about 4.3 per cent increase in power. In addition, it was found that the use of bleeds to decrease the power near choke is not possible since, for effective decrease in power, the unit would have to operate at pressure ratios less than 1.0.

Centrifugal Compressor

As in axial compressors, interstage bleed could be used in multi-stage centrifugal compressors. Therefore, a preliminary tandem centrifugal unit sized for Point A was analyzed for the effect of bleed on range extension at 7,000 rpm and the results of the analysis are shown in Figure 33.

The bottom line in the figure shows the variation of first-stage exit corrected flow with the inlet corrected flow. The minimum exit flow of 50.3 lbm/sec is set by the second-stage surge. For any exit flow from the first stage, the maximum bleed and, hence, the maximum reduction in power is set by the second stage surge. The variation of maximum bleed that can be obtained with second stage operating at surge point and the corresponding variation of total power absorbed by the two stages are also shown in the figure along with the variation of power without bleed. It can be seen from the figure that the maximum power range corresponds to 45 per cent bleed when the first stage is made to operate at choke and the second stage at surge. The resulting maximum power ratio (hp_{max}/hp_{min}) that can be realized with bleed control is then 1.25 (11,900 hp to 9,500 hp) compared to a power ratio of 1.32 (11,900 hp to 9,000 hp) with exit valve alone.

When there is no bleed, the second-stage operation at surge corresponds to the maximum pressure ratio across the first stage. With maximum bleed to have the first stage operate at choke and the second stage at surge, the pressure ratio across the first stage is at the minimum value. Hence, the bleed is equivalent to a partial throttling by a valve at the second-stage inlet from the pressure at the first-stage surge point to the

pressure at the first-stage choke point. With simple inlet throttling, the power could be reduced by a factor of 2.76 at the surge point. Also, the inlet throttling or valve could be combined with exit valve to effect a total power variation of 3.64:1.

The bleed, on the other hand, cannot be combined with exit valve to effect further extension in range since the minimum total power absorption with bleed is always higher than that which could be obtained with exit valve (Fig 33). The inlet valve, however, could be combined with bleed to increase the power range. But the effect of inlet valve would be less since the pressure ratio across the two stages with bleed is reduced due to the first-stage operation at choke. The combined range that can be realized is 2.5:1 compared to a range of 3.64:1 with inlet and exit valves. Also, an exit valve may be required along with bleed and/or an inlet valve to help set the operating points for the maximum potential range. Hence, bleed control is not an effective method for extending the range of power absorption in the tandem centrifugal compressor unit.

Recirculation

If part of the high temperature flow at the exit of the impeller is recirculated back to the inlet, the inlet temperature of the mixed flow would increase resulting in higher temperature rise across the impeller. Such an increase in temperature rise would increase the power absorption per pound of air entering and leaving the compressor. The increase in temperature of the mixed flow entering the impeller would, however, decrease the actual mass flow rate entering the impeller. Therefore, the increase in total horsepower depends on the degree to which the effect of temperature rise predominates over that of decrease in mass flow rate.

An accurate estimation of the power increase by such a recirculatory flow system is unnecessary unless it proves to be a promising concept for power range extension. Therefore, an approximate assessment of this effect on power for both the radial outflow compressor configurations (F1-ROC-S and F2-ROC-D) was made based on the following assumptions:

1. The inlet total corrected flow, $\dot{m}V\bar{\theta}_1/\bar{s}_1$, remains constant.
2. The recirculatory flow mixes with the inlet flow without any pressure loss.
3. The temperature ratio, T_R , across the rotor is unaltered.

With the above assumptions, the following relationships for the power ratio and the exit temperature can be obtained:

$$R_p = (1 + R_w T_R) / (1 + R_w) \quad (21)$$

$$T_{T2,R} = (1 + R_w T_R) / (1 + R_w) \quad (22)$$

where R_p = Power with recirculation/Power without recirculation

and R_w = Recirculatory flow/inlet flow

With the above relationships, an analysis was made for the effects of recirculation on the power and exit temperature of the compressors at the design operating point (Point A). The results of the analysis shown in Figure 34 indicate that the increase in power is less than 15 per cent even for recirculatory flow rate equal to the system inlet flow rate when 50 per cent of the exit flow is recirculated through the impeller. Also, as shown by the temperature limiting line for the use of aluminum (Ref 8), recirculation would necessitate the use of titanium or steel ductings for recirculatory flow in addition to titanium or steel impellers even for comparatively small increase in power absorption. The results are also not expected to be significantly different for other compressor systems. Therefore, recirculation is not a viable concept for range extension of dynamometers with air compressor as the power absorber.

Water Injection

The single-stage centrifugal compressor (F1-CC-S) was used to analyze the effect of water injection on the range extension. For the analysis, it was assumed that the air enters and leaves the impeller at saturated conditions. The effect of evaporation was calculated to decrease the inlet temperature by 24 degrees and the exit temperature by 165 degrees. The inlet and exit temperature drops correspond to humidity ratios (mass of water vapor/mass of dry air) of 0.005 and 0.039, respectively, for the inlet and exit flows.

The decreased temperature level would result in increased flow capacity of the machine. Since the maximum flow capacity of the unit is set by inducer choke, the increase in maximum flow would only result from the decrease in inlet temperature. An analysis by the NREC design analysis program (Ref 6) indicated that such an increase in maximum flow based on inducer choke would amount to only 2.1 per cent. However, the evaporation between the inlet and exit of the impeller is calculated to be 3.4 per cent of the air. Therefore, the actual increase in maximum mass flow of air-vapor mixture leaving the impeller is 5.5 per cent for complete saturation.

The power absorption is, of course, directly proportional to the flow and the work per pound of moist air. The gas properties of moist air are different from those of the dry air and the exit temperature of the flow is considerably reduced due to evaporation within the impeller. Nevertheless, these changes were found to be insignificant in work per pound of the moist air. Hence, the maximum increase in power that can be realized by water injection for complete saturation of air at the exit of the impeller is only 5.5 per cent. Therefore, water injection in single-stage centrifugal units does not result in significant improvement in range. It is also expected that range extension with interstage water injection would not be significant in multistage units. Hence, water injection would not be an effective method for significant range extension required of compressors for dynamometer applications.

Variable Geometry

Axial Compressor with Variable Stator Vanes

Variable blade-row stagger settings can be used to adjust compressor stage matching at constant speed, and hence, to vary the power absorption. The matching adjustment can be accomplished by varying any combination of rotor and stator rows. For the Navy dynamometer application, it has been assumed that only the stator rows are variable due to the mechanical complexity (i.e. cost, weight and reliability) of variable rotors. The last row acts only as a throttle to the preceding rotor; as such it is not considered in the power range extension by variable geometry. The achievable range extension by adjusting the inlet guide vane and first four stator-row stagger angles on the configuration F1-AC5-H was analyzed using the NREC axial compressor program ZORBA, Reference 8. For the analysis, it was also assumed that the stator vanes would be opened or closed in unison; this would provide mechanical simplicity while providing a good estimate of the maximum range achievable from an aerodynamic point of view. The maximum power absorbed by the compressor can be increased by opening the stators while continuing to operate the machine near the surge point; the minimum by closing the vanes at low levels of back pressure. Therefore, variable geometry could only be considered with an exit throttle system for range extension.

From the analysis, it was found that the maximum power achievable with design settings could be increased by 8 per cent when the vanes are opened by 7 degrees. Further increase in power is not possible since the rotor rows were found to operate at their limiting flow rate for this opening. The minimum power, however, could be decreased by 38 per cent when the vanes are closed by 15 degrees. Further closing of the vanes was found to result in flow instabilities for all operating points at 7,000 rpm. Therefore, the power range extension achievable solely due to the use of variable vanes is 1.74:1. Since this range extension is applicable to the already achievable range (1.53:1) with exit valve, the total range of power with variable vanes in conjunction with an exit valve is 2.66:1. This total range, however, is less than the 3.2:1 power range achievable with inlet and exit valves at 7,000 rpm. Also, the variable-vane concept would be mechanically more complex compared to a simple inlet valve for throttling. Therefore, the method of power modulation with variable vanes in combination with an exit valve is inferior to the method involving simple inlet and exit valves in the case of the axial compressor sized for the dynamometer application.

Centrifugal Compressors with VIGV

Double-Entry Configuration

The effect of variable inlet guide vanes (VIGV) in conjunction with an exit valve on range extension was investigated in the case of configuration F2-CC-D at 7,000 rpm. For this analysis, a free vortex type of swirl distribution was introduced at the impeller inlet. This type of swirl distribution would result if the IGV assembly is situated in a radial passage upstream of the rotor.

The variation of horsepower with inlet flow for various average flow angles at the impeller inlet is shown in Figure 35. The maximum opening is limited to -20 degrees since a higher flow angle would not result in a stable operating range. Similarly, a range of stable operation is not possible for flow angles much higher than +40 degrees caused by high negative incidences at the hub region. In general, the maximum possible variation in swirl is limited to 60 degrees in centrifugal compressors.

It can be seen from Figure 35 that the maximum range achievable with VIGV and exit valve is 3.18:1. This range is about 21 per cent higher than the range obtainable with simple inlet and exit valves. It should be noted that the pressure losses across the IGV, which are not introduced in the analysis, would introduce some inlet throttling effect. Since this throttling effect would reduce power at both negative and positive swirl angle settings, the range would not be significantly affected by the IGV losses. Therefore, the method of power modulation with VIGV and exit valve offers a slight advantage over the method employing only inlet and exit valves.

Tandem (2-Stage) Configuration

As in the case of the double-entry configuration, the VIGV (upstream of the first-stage) could be used along with an exit valve in the tandem unit (F1-CC-T) for extension of power range. The range extension achievable in the tandem configuration would, however, be very limited as the second stage is found to control the surge and choke operation. To achieve the range of power approaching that obtainable in the double-entry configuration, would, therefore, require an additional set of variable vanes upstream of the second stage. This would introduce additional mechanical complexity. However, VIGV could be used to throttle the inlet in addition to effecting power modulation by varying the inlet swirl angle. Therefore, configuration F1-CC-T was analyzed at different rotational speeds with VIGV-throttle and exit-valve combination.

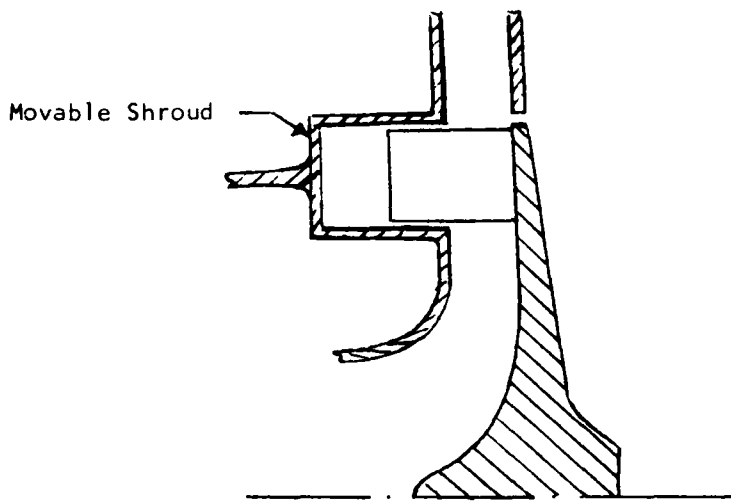
VIGV could be set either in a radial duct or in an axial duct upstream of the compressor. Introduction of swirl with radial vanes would result in nearly constant radial distribution of meridional velocity at the compressor inlet. The swirl angle would, however, not be uniform radially and its distribution would be very close to that corresponding to a free-vortex type of flow.

On the other hand, the radial distribution of swirl angle introduced by axial vanes would be very nearly uniform and the distribution of meridional velocity would be dictated by the radial equilibrium conditions. As a result, the radial distribution of flow conditions at the impeller inlet with radial vanes would be different from those with axial vanes for a constant mean swirl angle. An initial investigation indicated that axial vanes would have a larger operating range. Therefore, the VIGV were assumed to be axial vanes for the analysis of range by NREC design analysis Program PREDM (Ref 6).

The results of the analysis are shown in Figure 36. The top two lines in the figure show the maximum variation in average swirl angle that can be introduced without introducing flow instabilities. A comparison of the ranges with and without VIGV for inlet throttling indicates that the range with VIGV inlet throttling is not significantly greater than that which can be achieved with inlet throttling by a simple inlet valve. However, the required number of dynamometer units could be reduced with this modest increase in range which remains at about 20 per cent up to 7,000 rpm and then decreases to a lower value of 8 per cent when the rpm is increased to 9,100 rpm.

Radial Outflow Compressors with Variable Shroud

The Frame 1 size radial outflow compressors could be provided with a movable shroud as illustrated below for power modulation by means of flow variation.



In an ideal compressor with such a variable shroud, the power would be proportional to the flow width. In an actual compressor, however, the power reduction would be less than the reduction in flow path area due to several effects: recirculation within the closed impeller passages, recirculatory effect associated with the flow leakage from exit to inlet, and disk friction. The disk friction was calculated to be too small to effect any significant change in power variation within the range of power reduction of interest. The effect of leakage flow - mixing of exit leakage flow with the inlet flow - can be assessed on a very approximate basis with the simple relationships (Equations 21 and 22) developed earlier for the effect of recirculatory flow from exit to inlet.

A rigorous analytical investigation of the effect of complex recirculation within the closed impeller passages is very nigh impossible. Nevertheless, a crude estimate of this effect can be made by the following simplifying assumptions:

1. The impeller exit corrected flow remains constant
2. The temperature rise across the stage is given by $(1 + R'_W)$
3. The pressure ratio across the stage is unaffected

The above simplifying assumptions result in the following expressions for the power ratio and the exit temperature

$$\begin{aligned} R'_P &= (1 + R'_W) \left\{ \frac{T_R}{1 + (T_R - 1)(1 + R'_W)} \right\}^{1/2} \\ T'_{T2R} &= T_{T1} \left\{ 1 + (T_R - 1)(1 + R'_W) \right\} \end{aligned} \quad (24)$$

where R'_P = Power with passage-recirculation / Power with no recirculation

R'_W = Recirculatory flow/Inlet flow (\dot{m}_R/\dot{m})

T_R = Temperature ratio across the rotor without any recirculation

Figure 37, based on these relationships, shows that the effect of recirculation on power absorption is almost independent of the configuration at the design operating point; however, the effect on exit temperature is slightly higher for the single-stage configuration. Also, for high recirculation - either due to a high value of R'_W or smaller R'_W with regenerative flow pattern with n pattern for which the temperature rise could be increased by $(1 + nR'_W)$ - the exit temperature could even reach the limiting temperature for titanium alloys.

A comparison of this recirculation effect with that due to leakage (Figure 34 vs Figure 37) indicates that the effect of former (passage-recirculation) in increasing the power absorption is several times higher than that due to the latter. For instance, the increase in power for 100 per cent recirculation within the blade passages is about five times that associated with leakage-recirculation. Also, unlike the leakage-recirculation effect, the blade-recirculation effect does not taper off for large increases in recirculatory flows.

From the relationships for the two types of recirculation, the power range for a reduction in axial width of the rotor passage from b_1 to b_2 can be expressed as

$$\frac{HP_1}{HP_2} = \frac{b_1}{b_2} \times \frac{R'_{P1} \times R'_{P1}}{R'_{P2} \times R'_{P2}} \quad (25)$$

and the resulting exit temperature as

$$T'_{T2,2} = T_{T1} \left\{ (1 + T_R R'_W) / (1 + R'_W) \right\} \left\{ 1 + (T_R - 1) (1 + R'_W) \right\} \quad (26)$$

where T_{T1} is the inlet temperature without any recirculation

The above relationships could be used to arrive at an estimate of the achievable power range and the associated exit temperature level if the variations with the shroud movement of leakage and passage-recirculatory flow are known. The amount of leakage could be calculated after a detailed design. The passage-recirculatory flow is, however, difficult to estimate even after the completion of a detailed design. Nevertheless, the potential range attainable with the variable-shroud concept could be assessed with some assumptions about the leakage and recirculatory flow fractions. For such an analysis, the following assumptions were made:

1. The leakage and passage-recirculatory flow fractions are equal: $R_W = R'_W$
2. At the design maximum opening of the rotor blade passage, the leakage and recirculatory flows amount to 2 per cent of the inlet flow: $R_W = R'_W = 0.02$
3. The flow fractions are inversely proportional to the blade passage width

With the above relationships and assumptions, the effects of width reduction on power range and exit temperature were obtained (Fig 38) based on design operating conditions. As shown in Figure 38, the power range is independent of the configuration and it is about 25:1 for a 50:1 reduction in the axial width of the rotor. The maximum reduction is, of course, controlled by the practical limit on running clearances.

For the single-stage unit, a reasonable clearance value would be 0.10 in., for which the width reduction is 48:1 and the associated power range is close to 25:1. This range, however, could not be achieved with titanium alloys, as indicated by the temperature limiting line in Figure 38. Even for this temperature limitation, a 23:1 power range could be achieved.

If we reduce the clearance value assumed for the single-stage unit proportional to the rotor exit diameter, then the available width reduction would be 40:1 for the double-entry unit. This reduction would correspond to a power range of 22:1.

In essence, the above analysis based on what were judged to be reasonable assumptions indicates that the variable-shroud concept has the potential of a 20:1 power range. Even if the various effects and limits associated with this concept are much larger than those assumed for the analysis, a power range of 10:1 seems to be a definite possibility.

SELECTION AND DETAILED ANALYSIS OF THREE COMPRESSOR SYSTEMS

Introduction

Based on the feasibility and preliminary analysis of various compressor concepts, six compressor systems representing three types (centrifugal, radial outflow, and axial) of dynamic rotary compressors were selected. These selected compressor systems were then studied for range extension and required number of dynamometers with inlet and exit valves. In addition, selected and applicable compressor systems were studied for range extension with other possible methods.

The results of the above analyses indicate that compressor systems in each type do not differ as much between them as they do compared to the compressor systems of other types. Therefore, one in each of the three types of compressor systems with promising methods of power range extension was selected for further analysis. The three selected compressor systems are:

1. Tandem centrifugal compressor with VIGV-throttle and exit valve.
2. Single-stage radial-outflow compressor with variable shroud.
3. Axial compressor with inlet valve.

The three selected compressor systems were then analyzed for the number of dynamometers required to cover the range of specified engine design points. In addition, preliminary mechanical design and analysis, including layout of the selected compressor systems, was conducted. Also conducted was a preliminary analysis of the control systems mainly dealing with the sizing of inlet and exit valves.

Included in this section are the results of the above analyses dealing with, one, the selection of compressor systems; two, the number of dynamometer units required of the selected compressor systems; three, the control system; and four, the preliminary mechanical design and analysis.

Selection of Compressor Systems for Further Analysis

The physical details and operational characteristics of the six Frame 1-size compressor systems are listed in Table XXIV. Of the various range extension methods other than the simple inlet and exit valves, only the variable geometry was found to be effective. Therefore, the range with VIGV for centrifugals and variable shroud for radial outflow compressors are listed in Table XXV along with the range and required number of dynamometers with inlet and exit valves for the six compressor systems. A comparison of the required number of frame sizes and dynamometers indicates that the configuration CC-T is superior to the rest of the configurations, since it requires only 3 frame sizes instead of 4, and only 5 different dynamometers instead of 6 or 7 required by other configurations to cover the seven operating points. This mainly results from higher range in the required range of operating speeds, as evidenced by Figure 39.

A comparison of this configuration with configuration CC-D indicates that CC-D does not offer any other advantage in terms of size or weight. Also, the maximum range of CC-D with VIGV and exit valve (3.18) is also less than the range of CC-T with simple inlet and exit valves (3.75). Configuration CC-S has less weight compared to CC-T, but it is bigger in size (maximum casing diameter). Also, the growth potential of CC-S to high speed-high power application is limited, since the range of Frame 1 size starts to decrease beyond 8,400 rpm ($N/N_d > 1.2$ for other frame sizes), as shown in Figures 15 and 39. Further, the range extension in CC-S with VIGV and exit valve is estimated to be less than the corresponding range extension obtainable in CC-D, for the maximum range for CC-S with exit valve is only 1.268 compared to a value of 1.482 for CC-D. Therefore, configuration CC-T was selected from among the three centrifugal compressor configurations for further study. Since the increase in range achievable with the use of VIGV also as an inlet valve for throttling could be used to still reduce the number of dynamometers, the centrifugal dynamometer system was selected as the compressor configuration CC-T with VIGV-throttle and exit valve.

A comparison of the two ROC configurations indicates that they are similar in many respects: range with inlet and exit valves, range with VIGV and exit valve, potential range with variable shroud, and required number of frame sizes and dynamometers with inlet and exit valves. The configuration ROC-S is, however, lighter in weight but has a larger casing diameter. The configuration selected from these two should, of course, be used with variable shroud, which offers a very high potential range. Introduction of variable shroud in ROC-D could, however, present a more complicated mechanical problem, for two separate shroud structures must be moved in unison. An inlet valve could also be combined with variable shroud to help ensure the range level appears achievable with variable shroud alone. Therefore, ROC-S with inlet valve and variable shroud was selected for further study.

The required number of frame sizes and dynamometers is comparatively high for configuration AC5-H. Also, the range at part speed is very limited, as shown in Figure 39. However, it offers advantages both in weight and maximum diameter. As opposed to centrifugal and ROC compressor systems, the number of stages in axial compressors could be readily increased to improve the part-speed performance. Further, the maximum available range with both inlet and exit valves could be very nearly achieved by inlet throttling alone. Apart from these considerations, it represents an alternative concept to the other two selected systems. Therefore, configuration AC5-H with inlet valve was also selected for further study.

Number of Frame Sizes and Dynamometers for the Selected Compressor Systems

Tandem Centrifugal with VIGV-Throttle and Exit Valve

From the variation of maximum power with speed (Fig 17) and the variation of range with speed shown in Figure 36, the minimum number of frame sizes and dynamometers required to cover all engine design points were obtained. The performance envelopes and the details of the frame sizes and dynamometer

units are shown in Figure 40 and Table XXVI. A comparison of these details with those for dynamometers with simple inlet and exit valves (Table XX) indicates that the use of VIGV for inlet throttling results in a reduction of one dynamometer, requiring only four dynamometers out of the three required frame sizes.

Single-Stage ROC with Variable Shroud

Due to the wide variation in rotational speeds of the engine design points, the number of frame sizes and, hence, the number of dynamometers cannot be reduced below three even if an infinite power range (0 to maximum) is possible. To reduce the number of different dynamometers to three, however, requires a range of only 6:1; a range which can be easily achieved in ROC equipped with a variable shroud. Therefore, the performance envelopes and the details of the three dynamometers (Figure 41 and Table XXVII) were obtained using a 6:1 power variation. Since the variation of maximum power with speed for ROC-S is essentially the same as that for ROC-D, the performance envelopes and the details given in Figure 41 and Table XXVII are applicable to both single-stage and double-entry configurations.

Five-Stage Axial Compressor with Inlet Valve

Earlier, the range associated with inlet valve was taken nominally to be equal to the pressure ratio at surge point, as it is the most determining factor controlling the amount of inlet throttling. If the compressor is made to operate at or near surge point for maximum inlet throttling, then the power range extension for zero downstream losses will be equal to the pressure ratio at the surge point. However, the surge point or an operating point with a required surge margin and the corresponding inlet corrected flow will remain constant only up to a certain inlet throttling. Closing of the inlet valve beyond this throttling point will result in reduced inlet corrected flow and, hence, change in operating point with reduced surge margin. If an exit valve is used in conjunction with the inlet valve, the exit valve could be opened to maintain the nondimensional operating point with the required surge margin. In the case of systems with inlet valve only, the initial operating point (without inlet throttling) could be made to have high surge margin (near choke) by proper sizing of the exhaust duct and orifice. In this way, the effective range could be extended from what could be obtained with an initial operating point at the minimum required surge margin. Therefore, the maximum effective range with inlet valve depends on the minimum or surge flow operating point and the initial operating point.

The exhaust duct and orifice which set the initial operating point at a particular pressure ratio and corrected exit flow will require a certain pressure drop downstream of the compressor at or near surge point where the exit corrected flow is less. Hence, the amount of inlet throttling at or near surge will be less than the pressure ratio across the compressor. If we assume that the inlet throttling is carried up to the surge point, then the maximum effective range is given by

$$\frac{HP_{\max}}{HP_{\min}} = \frac{HP_0}{HP_s} \times \frac{P_{R,s}}{P_{R,e}} \quad (27)$$

where HP_0 is the horsepower at the initial operating point

HP_s is the horsepower at surge without inlet throttling

$P_{R,s}$ is the compressor pressure ratio at surge

and $P_{R,e}$ is the exhaust pressure ratio required by the duct and orifice at surge.

The maximum effective range thus achievable with inlet valve or the five-stage axial compressor (F1-AC5-H) was analyzed at 7,000 rpm. For the analysis, the exhaust duct and orifice were assumed to be represented by one single equivalent orifice. The results of the analysis are presented in Figure 42 as the variation of effective range from surge to choke with inlet corrected flow at the initial operating point. When surge is the initial operating point, $P_{R,e}$ is the minimum pressure ratio required for the equivalent orifice to operate at choked flow condition.

It can be seen from the figure that the maximum effective range with inlet valve is 2.28:1, and it is considerably less than the range (3.2:1) achievable with inlet and exit valve. This reduction in range results from the fact that, in addition to the effect of exhaust pressure ratio, the horsepower at the initial operating point for maximum effective range is less than the horsepower at surge point without inlet throttling. Even though the maximum effective range of 2.28:1 at 7,000 rpm would just meet the range criterion (the minimum power range should be at least 2:1 with about 10 per cent surge margin) for Point A, the effective range would be less for the dynamometers sized for other operating points which require the dynamometers to operate at blade speeds less than the design blade speed, as the reduction in range is significant for lower speeds (Fig 39). Therefore, it was concluded that the axial configuration AC5-H should only be considered with both inlet and exit valves.

Control System and Torque Measurement

Control Configuration

The function of a control system for air dynamometers is to match its power absorption with the engine power at the required testing conditions of the engine. The control can be considered at two levels of complexity. The first is a simple level where the operator can manually match the power by acting to close the control loop between the output parameters and the input signal. In the manual control mode the input signal would need some power amplification to cause the dynamometer to change power. In the second level the loop can be automatically controlled with either a torque or a speed input, depending upon whether it is a turboshaft engine or a turboprop engine. A possible control configuration is presented in Figure 43.

Weight of Controls with Valves

A preliminary assessment of the weights associated with the control system for the inlet and exit valves was based on the sizing of inlet and exit valves. The valves were sized for the six Frame I-size compressor systems using the design mass flow rate, \dot{m} ; pressure ratio, P_R ; and temperature ratio, T_R . The valves were assumed to be the coaxial cylinder type. The thickness of such a valve can be expressed as

$$t_v = (\pi D_v \Delta P_{v1}) / \sigma \quad (28)$$

where D is the valve diameter (ft)

σ is the allowable stress (psf)

and ΔP_{v1} is the maximum pressure drop across the valve (psf)

From the orifice equation, the maximum orifice area for the valve can be obtained as

$$A = \frac{\dot{m}}{C_d \{ 2 \rho_g g \Delta P_{v2} \}^{1/2}} \quad (29)$$

where C_d is the discharge coefficient

ρ_g is the density of gas (lbm/ft^3)

and ΔP_{v2} is the minimum pressure drop across the valve (psf)

If it is assumed that the valve skin area is equal to the maximum orifice area, then the weight of the valve is given by

$$W_v = \rho_m A t_v \quad (30)$$

where ρ_m is the density of the material (lbm/ft^3)

If the maximum and minimum pressure drops are related to the design pressure ratio, P_R , and the ambient pressure, P_a , by the following relations:

$$\Delta P_{v1} = (P_R - 1) P_a \quad (31)$$

$$\Delta P_{v2} = 0.01 (P_R - 1) P_a \quad (32)$$

then the weight of the valve can be expressed as

$$W_v = \frac{10 \pi}{C_d} \frac{\rho_m}{\sigma} \left\{ \frac{P_a (P_R - 1)}{2 \rho_g g} \right\}^{1/2} \dot{m} D \quad (33)$$

With the above formula, the following assumptions were used for the calculation of the weight of inlet and exit valves:

1. The value of C_d is 0.8.
2. The value of $\frac{f_m}{\sigma}$ is 8.0×10^{-5} lbm/lbf-ft.
3. The diameter of the inlet valve is equal to the rotor inlet tip diameter and that of the exit valve is equal to the rotor exit tip diameter.

The total weight of the valves thus calculated were multiplied by a factor of 4 to obtain an approximate estimate of the weight of the control system which will include support, controls, and power supply in addition to the valves. The weights of the control system shown in Table XXVIII for the various compressor systems indicate that the control system would not significantly affect the weight of the compressor systems, as they are less than 15 per cent of the preliminary values of the compressor weights shown in Table XIV.

Torque Measurements

The torque sensing means can be by a rotating torque sensor, a load cell acted upon by a trunnion-mounted dynamometer, or a flexure pivot table upon which the dynamometer is mounted. The rotating torque sensor has the advantages that it is insensitive to any extraneous torques and that it is simply installed on any dynamometer. Rotating torque sensors are relatively expensive, as they require high speed bearings, slip rings, or rotary transformers. Slip ring brushes must be replaced periodically, but a simple procedure is involved. Trunnion bearings have inherent friction and require elaborate mounting design for the dynamometer. Both the trunnion and flexure pivot mounts must contend with extraneous torques due to supply lines and momentum flux from inlet and exit flows. Flexure pivot tables are not usually found in the large size required by the dynamometers of interest.

Preliminary Mechanical Design and Analysis

A preliminary mechanical design and analysis were conducted for the three selected compressor systems. Based on the analysis, the preliminary design layouts of the dynamometer systems were obtained as shown in Figures 44, 45, and 46. The analysis included the estimation of weight and cost, the calculation of important stresses, and an assessment of the design complexity.

Weight Analysis

Using the preliminary design drawings shown in Figures 44, 45, and 46, the volume of the various components was calculated and then multiplied by the appropriate density to estimate their weight. The materials are taken to be steel for shafts, titanium for the stressed rotating parts, and aluminum for all stationary parts.

The weights of the systems thus calculated and shown in Table XXIX indicate that these values are considerably higher than those estimated earlier for these compressor systems. In addition to the weight of the inlet and exhaust ductings which were not considered earlier, the increase in weight also

results from various other factors: use of steel rather than titanium for shafts, use of titanium for all rotating parts rather than for stages with high temperatures, and a casing thickness of around 0.8 in instead of 0.5 in assumed earlier.

Cost Estimation

The cost of the materials was the basis for the estimation of cost for the different compressor systems. The material cost of a component is determined from

$$C_M = WMF_W F_T \quad (34)$$

where W is the weight of the component

M is the material cost (\$1.50/lbm for steel, \$1.25/lbm for aluminum, and \$2.00/lbm for titanium)

F_W is the wastage factor (1.1)

and F_T is the tooling factor (1.1)

The usual manufacturing cost for a component purchased from an outside source is about five times the material cost. Therefore, the total cost for a component is given by

$$C = 6 C_M \quad (35)$$

The summation of the component costs thus calculated was used to arrive at the cost of the compressor systems shown in Table XXIX.

Stress

The important stresses in the compressor systems are the stresses in the disk and in the blades. In a disk with a central hole, the maximum stress is the tangential stress, and it occurs at the inner radius of the disk. For the centrifugal and radial outflow compressors, the maximum tangential stress was obtained as 60 per cent of the stress calculated for a disk of uniform thickness--the percentage factor is based on the level of reduction achieved in previous NREC designs for proper profiling of the disk. Similar reduction was not done for the axial compressor to account for the disk rim stress caused by the blade centrifugal forces. The stresses thus obtained and shown in Table XXIX could be almost halved by a solid disk design.

The maximum blade stress is usually at the blade root. In a centrifugal compressor with radial blades, the maximum root stress is at the inducer. Therefore, the root stress for the centrifugal as well as the axial compressor was calculated employing simple relationships for centrifugal stresses based on annulus area, rotational speed, and material density.

In the case of the radial outflow compressor, the blade root stress mainly results from the bending moment caused by the centrifugal force associated

with the blade weight. Therefore, a preliminary blade shape of impulse turbine type with 20 per cent maximum thickness-to-chord ratio was obtained, and its sectional properties were calculated. From the sectional properties and the centrifugal force, the maximum root bending stress was obtained.

The values of root stress thus calculated and shown in Table XXIX do not include any effect of blade taper from root to tip. A 2:1 taper, for instance, would reduce the root stress of the centrifugal and the axial compressor blades by about 25 per cent and that of the radial outflow compressor blades by about 33 per cent. With a constant outer blade profile such as would be considered for the radial outflow compressor rotor, the taper can be introduced by the use of a hollow blade design.

Design Complexity

This analysis was mainly confined to the complexity associated with the design, detail, checking, and assembly of the systems. For this, the number of required parts, number of required drawings, and the man-hours required for design, details, and checking were obtained and listed in Table XXIX. The man-hours depend on the number of drawings as well as the size of each drawing. Depending on the complexity, a component is drawn on an "A" ($8\frac{1}{2}$ " x 11"), "B" (11" x 17"), "C" (17" x 22"), "D" (22" x 34") or an "E" (34" x 44") size drawing requiring 8, 16, 24, 32, or 40 man-hours.

DYNAMOMETER SYSTEM EVALUATION

Introduction

The first objective of the evaluation is to review the good and bad features of selected compressor systems. The second objective is to list recommendations as to the optimum system.

As discussed in the earlier section, three compressor systems were selected and analyzed in detail for performance, weight, cost, and operating stress levels. These are the tandem (2-stage) centrifugal with VIGV-throttle and exit valve, the single-stage radial outflow with a variable shroud, and the five-stage axial with inlet and exit valves. Initially, these three compressor systems were evaluated, and a relative rating of each system was established. The evaluation and subsequent ratings of these three systems indicated the desirability of evaluating the double-entry radial outflow as well as an axial compressor with increased number of stages. Therefore, a double-entry radial outflow with variable shroud and a ten-stage axial with inlet and exit valves were included in the rating analysis prior to the final recommendation as to the optimum system.

For the evaluation, six different categories are employed: applicability, controllability, cost effectiveness, configuration, safety, and environmental effects. Under each category, several different factors are used for the analysis of relative merits of the dynamometer systems. The relative rating of each system is performed by assigning numbers to each factor based on its importance and the available performance or design quantity associated with that factor.

Applicability

The applicability of a dynamometer system can be judged by three factors. These are the number of dynamometer units or models required to cover the specified range of engine design points, the power range possible at the design points, and the ability to change rotation.

Number of Frame Sizes

Ideally, it would be desirable to cover the specified range of design power and speeds with only one dynamometer model. This is not feasible with an air dynamometer because of the limitations of tip speed and air flow capacity. It is also recognized that the seven specified points (Points A to G) are not specific engine ratings but represent the centers of possible design points. The number of dynamometers required, therefore, may vary, dependent upon the exact design power and speeds to be handled. However, for the purposes of this evaluation, a good qualitative judgement can be made on the relative merits of each design by assuming the seven design points to be fixed.

With an assumed minimum power range of 2.4:1 at constant speed, four units or models of the tandem (2-stage) centrifugal dynamometers will be required to cover the seven design points (Fig 40). This can be done by only three frame sizes and by producing a smaller capacity machine by machining back the impeller shroud contours. This is not a significant advantage, as the reduced flow impellers and shroud components must be treated as additional parts in inventory. Since these components represent a major portion of the dynamometer cost, there is only a small savings in the initial tooling costs. Four separate dynamometer assemblies must still be kept in the Navy's test facility inventory.

The variable-shroud radial-outflow dynamometer (VSROC) required only three models to cover the seven design points for the 2.4:1 power range (Fig 41). Each of these models represents a frame size in itself.

The five-stage axial compressor requires seven different models to cover the seven design points (Fig 32). These seven models can be obtained from four basic frame sizes by using the shroud cut method to create three additional models. Again, the key factor to consider is that seven separate assemblies must be kept in inventory. Each of these machines will have a commonality of only a few minor parts. The key components such as the disks and the outer casings must be treated as noninterchangeable parts.

From the above it is apparent that the VSROC dynamometer is the most desirable concept because of the few models required.

Power Range

The minimum power range at each design point is specified to be 2:1. For the calculation of the required number of frame sizes and models, a power range of 2.4:1 was assumed to account for some operating margin away from surge and choke. However, the desirable power range is considerably larger. Turboshaft engines are required to hold constant speed from flight idle to full power. During the testing of such engines, it is desirable to operate transiently to insure the functioning of the acceleration and deceleration schedules and other limits within the controls. A dynamometer having 10:1 power range can, therefore, be used not only to check the full power capability of the engine but also to confirm that the control system is functioning properly. It was, therefore, concluded that an important feature of any dynamometer is its power range at constant speed.

The tandem centrifugal dynamometer has a power range of 4.4:1 at design speed. The average power range (average of the power ranges at all seven engine design points) is slightly higher at 4.6:1. However, the range for this dynamometer is reduced at speeds below the design value (Fig 36).

The VSROC dynamometer is required to have only 6:1 power range for the minimum number of models and frame sizes. The maximum potential range, however, is estimated to be around 20:1. Therefore, it is possible to obtain at least 10:1 power range in this dynamometer concept. Also, the 10:1 power range could be achieved at part speeds.

The five-stage axial has a maximum power range of 3.2:1 at design speed, and the average range is slightly less at a value of 3.0:1. In addition, the part-speed range for this dynamometer reduces drastically, as evident from Figure 39.

It has been concluded here that the power range at constant speed is a very important parameter and that the VSROC dynamometer is far superior to the other two types in this respect.

Direction of Rotation

It is desirable that a dynamometer be capable of loading engines having different directions of rotation. The three configurations selected must be always rotated in one direction. To permit bidirectional loading, all three designs must be arranged to permit an engine connection at either end of the dynamometer shaft. It is assumed that the dynamometer will be mounted on a fixed base and that the engine will be mounted on a structure grounded to this same base. To provide bidirectional loading, sufficient space must be provided at either end of the dynamometer to mount the engine. The shorter the dynamometer, the less will be the total space required.

The length of the tandem centrifugal dynamometer is shown to be 87 in in Figure 44. This length could be significantly reduced by the use of a shorter inlet duct and the elimination of exhaust ducting with either axial or radial flow exhaust. It is estimated that the length thus obtainable is 63 in.

The total length of the single-stage VSROC dynamometer is 72.6 in (Fig 45). Most of this length is associated with the inlet and exhaust ductings. A long inlet duct is used for the purpose of employing throttling by an inlet valve. Since an inlet valve is not needed for this system, it can be eliminated with considerable reduction in the length of the system. In addition, a radial exhaust would further reduce the total length. A preliminary design analysis of a double-entry version utilizing the above features resulted in a length of 39 in for the basic dynamometer system (Fig 47). It is expected that the length of the single-stage version would not exceed the length of the double-entry version. Therefore, the length of the single-stage VSROC dynamometer was taken to be 39 in.

The total length of the axial dynamometer system as shown in Figure 46 is 73 in. Even though some reduction could be accomplished in this length, the use of an exit valve which is not included in the preliminary design could require some additional length. As a result, the length of the axial dynamometer system is taken to be 73 in.

A comparison of the possible lengths for the different systems indicates that the single-stage VSROC would have an advantage over the other two systems.

Controllability

The control of a dynamometer can be considered at two levels of complexity. The first is a simple level where the torque produced is proportional to an

input signal but speed and ambient dependent. This means of control is analogous to the manual setting of a throttle valve. In this case the input signal would be considered sufficiently low that some sort of power amplification is required to cause the dynamometer to change load. The second level of control is where a desired torque or power signal is an input, and the control functions set and maintain the input value. This can be considered a closed-loop control and requires the measurement of the parameter controlled, such as torque or speed or both. In the normal operation of a dynamometer with a turboshaft engine, the dynamometer is operated at constant speed. This speed is set and controlled by the engine's power turbine governor. It is a dynamometer requirement that the torque produced is some function of a collective pitch signal that is also used as an engine control input. In a turboprop application, the dynamometer control must act to maintain a constant dynamometer speed. The load torque, therefore, should automatically adjust to match the power setting of the machine. Therefore, the evaluation of a dynamometer concept with respect to controllability should consider the suitability of the dynamometer to automatic control. For this, several factors associated with the controls have been selected: torque gain characteristics, number of control functions, friction and force level, polar moment of inertia, and the limit functions required.

Torque Gain

The torque gain of a dynamometer is the partial of load torque with respect to control device movement. For example, if a throttling valve is used, the gain can be expressed as the ratio of torque change to valve position change for small position increments. It is necessary to limit the gain change during dynamometer operation. An excessive or high gain or sensitivity value can cause a control system instability; a low value will cause inaccuracies in the set point. The air dynamometer load torque is primarily proportional to the air mass flow. A throttle valve, therefore, will have a low gain or sensitivity at large openings and a high gain at small openings. The sensitivity of a throttle valve can be made uniform by controlling the area schedule or by shaping networks in the valve position controller. In any case, the use of a throttle valve for torque control requires special treatment or control complexity to obtain a uniform and predetermined level of gain. Inlet guide vanes are also highly nonlinear in their gain characteristics. Again, at large openings the gain or sensitivity is low; at small openings the reverse is true. The tandem centrifugal machine requires both an inlet guide vane and an exit throttle valve. Both of these components must have compensation means to limit the band width of sensitivity.

The VSROC design would have a constant gain or torque sensitivity level for most of its operating range. However, at low power settings where there is a significant flow passage closure, the gain or sensitivity may decrease. This may be undesirable and some compensation may be needed.

The five-stage axial compressor must have both an inlet throttle and an exit throttle valve. Both of these components require some gain compensation or correction.

From the above considerations it appears that the VSROC design will have the most constancy to its torque/input position gain, and if compensation is required, it will be less critical or complex than the other two concepts. Therefore, it would have a definite advantage over the other two based on torque gain characteristic.

Number of Control Functions

Both the two-stage centrifugal and the five-stage axial dynamometers require two functions to be modulated. The phasing and scheduling of these two functions will increase the control complexity and promote rigging problems in the field. The single control function of the VSROC machine, therefore, appears more attractive.

Friction and Force Level

High levels of friction in the controlled mechanism can cause instability and erratic behavior in a closed-loop control system. High force levels for control device actuation dictate high control power, thus more costly components. The inlet guide vanes of the centrifugal machine will have low friction levels because of the absence of sliding surfaces. The actuation force levels will also be moderate because of the absence of friction and the ability to balance the vanes aerodynamically. The above statements are also true for butterfly-type throttle valves. The two-stage centrifugal machine, therefore, will have low friction and actuation force levels in the mechanisms needed to control torque.

The radial out-flow machine may have both high friction levels and forces. The design shown in Figure 45 has a complex annular piston geometry. The radial position of this ring must be controlled accurately. The close clearances plus the expected high seal friction can produce unpredictable control hysteresis. This must be compensated for, and thus, the control complexity will be increased. The control ring is also aerodynamically unbalanced in the axial direction in its simplified configuration. Either this unbalance must be compensated for by a more complex geometry using an air pressurized balanced chamber, or high activation forces must be provided.

The five-stage axial dynamometer is shown in Figure 46 with a flat plate inlet throttle valve. This valve is totally unbalanced and will have high friction levels in partially closed positions. Again hysteresis compensation will be required in the control systems, and a high power will be required for actuation. Even if butterfly-type valves could be used for inlet and exit throttling, they have to contend with large flow rates.

Based on the above observation, it appears that the tandem centrifugal dynamometer will have the least control problems related to friction and actuation.

Polar Moment of Inertia

The polar moment of inertia of a dynamometer is important. Ideally, it is desirable to duplicate the load polar moment of inertia which the engine

is designed to operate with. The inertia is an important part of the total system dynamics and can affect the stability. Duplicating the equivalent installation load inertia may not be a practical thing to do. However, if a dynamometer is designed to have the smallest possible polar moment of inertia, then inertia can be added if required by a specific engine. For this reason, the best dynamometer under this evaluation factor would be the VSROC. The tandem centrifugal will have an inertia higher by 70 per cent, and the axial, higher by 85 per cent.

Limit Functions

It is necessary that unstable aerodynamic operation be prevented if smooth dynamometer operation is to be achieved. The devices used to vary the power must be limited in their effect so as to prevent operation in unstable aerodynamic regimes. For example, if the exit throttle valve of the tandem centrifugal machine is permitted to close excessively, surge will occur. The valve must, therefore, have a limit stop. This stop may have to be continuously reset if a wide range of test speeds are to be encountered and the power or torque range maximized. A similar stop is also needed on the discharge throttle valve to prevent operation in the choke regime of the dynamometer. The inlet throttle valve minimum area must also be limited if surging is to be prevented. Again this limit may have to be continuously adjustable if the machine power range is to be maximized.

The five-stage axial dynamometer will require a similar but more precise limit functions, as the performance characteristics of the axial compressor are steeper than those of the tandem centrifugal. Also, the axial compressors are generally more sensitive to surge and choke than the centrifugals.

The VSROC, however, does not need any adjustable limits. The only limit expected is that necessary to prevent the shroud from being driven into the impeller. This need not be a precise stop and, therefore, can be built in as a natural limit in the actuator.

Summary

Based on the above five evaluation parameters, it appears that the VSROC dynamometer is the more controllable concept. However, the friction inherent in the movable shroud mechanism may be troublesome and, therefore, would need special development attention.

Cost Effectiveness

The cost effectiveness or life cycle cost of a dynamometer can be judged by four factors: first cost, scheduled maintenance costs, mean time to failure, and life. The following is a qualitative comparison of the three selected dynamometer concepts without the automatic controls.

First Cost

Even when made in small quantities, the first cost of similar devices can be estimated to be a function of weight and raw material costs. Using

this method, it was found that the five-stage axial dynamometer had the smallest first cost (Table XXIX). The VSROC dynamometer was 29 per cent greater in cost, and the two-stage tandem centrifugal, 23 per cent greater. However, these preliminary weights are based on preliminary design layouts. Most of the dynamometer weight is associated with the static structure. Also, the shafts, which are assumed to be solid and made of steel, could be shortened. Therefore, a design optimization might produce significant changes to the weight of the dynamometer systems. The rotor weights, however, will not change with design optimization and the materials involved are the most costly. Therefore, the rotor weights without the shaft could be a better index of the final package weight and the total cost. Based on this approach, the five-stage axial will have the lowest first cost; the radial out-flow will be only 23 per cent higher; and the two-stage centrifugal, 124 per cent higher.

The total cost to equip the Navy with dynamometers covering the specified range of powers and speeds is probably the best way to examine the first cost. Summing the scaled costs for all the individual dynamometer models needed, it is found that the VSROC dynamometer will have the lowest total first cost. The five-stage axial group will cost 98 per cent more, and the two-stage tandem, 211 per cent more.

Scheduled Maintenance Costs

This factor has to do with the costs associated with planned service and maintenance work. Items such as bearing and seal replacement, blade cleaning, control linkage adjustment, and torque calibration are typical of the service functions performed on dynamometer-type devices. The rotor system bearing and seal replacement and servicing will be about the same for all of the designs. The control linkage and bearings for the variable guide vanes of the tandem centrifugal and the control linkage for the VSROC dynamometer will require more service than the two throttle valves of the axial. However, the five-stage axial will require more frequent cleaning of the gas path components. It was, therefore, concluded that the three designs would have approximately the same maintenance costs.

Mean Time to Failure

The mean time to failure is indicative of those costs created by the non-availability of the machine and the costs to repair.

Such failures are usually associated with the mechanical complexity of the machine and the matureness of the design. The tandem centrifugal and the five-stage axial are expected to be equal in this regard. The VSROC would be worse due to the novelty and complexity of the movable shroud mechanism.

Life

The total life expected from a machine before a complete replacement is needed is another cost factor. It was concluded that all three designs would probably have the same life span. The VSROC design may be slightly better because of its simpler rotor system construction.

Configuration

The configuration advantages of the three dynamometer designs can be discussed in terms of weight, diameter length, and ducting complexity.

Weight

The preliminary studies of the largest frame size (Frame 1 size) resulted in a weight of 4,130 lbm for the tandem centrifugal, 3,870 lbm for the VSROC, and 2,780 lbm for the axial. Based on the possible reduction in length discussed earlier, it is estimated that the tandem centrifugal weight could be reduced to 3,450 lbm. The weight of the single-stage VSROC is estimated to be 2,860 lbm based on that of the optimized configuration for the double-entry version. Since the axial would need an exit valve with associated ductings, it is expected that its weight would remain at 2,780 lbm estimated earlier.

Diameter

The diameters of the three designs will determine the compactness of the installation design. Based on the preliminary design layouts, the axial is the smallest at 44 in, the tandem centrifugal is the next at 52.9 in, and the VSROC is the largest at 56.6 in. In all cases, the diameters may be reduced, but the relative diameters will remain about the same.

Length

Approximate lengths of the three machines were also established by the preliminary mechanical designs. However, this dimension was not optimized, and therefore, a best or minimum installed length for each machine was estimated and given earlier under Direction of Rotation. These values are 39 in for the VSROC, 63 in for the tandem centrifugal, and 73 in for the axial.

Ducting Complexity

It is assumed that the dynamometer air ducting must be arranged to prevent the ingestion of ground contamination, reingestion of the exhaust, and protection of personnel from both. This implies that at a minimum the exhaust air must be collected and discharged vertically. Both the tandem centrifugal and the VSROC designs lend themselves to this arrangement. The five-stage axial dynamometer will require extra length if a vertical discharge is required.

Safety

An air dynamometer will have an enormous amount of stored energy in its rotor system when operating. A mechanical failure that permits the release of part or all of this energy could be very hazardous to nearby operating personnel. The relative safety of the three chosen dynamometer designs was evaluated using the disk and blade stresses, rotor system complexity, and debris sensitivity.

Since safety cannot be compromised, the less safe systems may require more ancillary protective equipment and/or a burst shield. The cost or complexity of such equipment has not been considered in this evaluation.

Rotor Stress Levels

The average tangential stress in a rotating disk as compared to the ultimate strength of the material used is a good indication of the safety or burst margin. The preliminary design study of the three selected compressor systems shows (Table XXIX) that the VSROC has the highest maximum tangential stress value at 39,000 psi followed closely by a value of 35,900 psi for the tandem centrifugal. The value of 24,900 psi for the axial is considerably lower than the values for the other two designs. These stresses can be reduced to about one half of these values if the center bore holes in the designs shown are eliminated. If it is assumed that the average tangential stress is about one half of the calculated maximum stress, then the burst margins for the three designs will be about 6.5 for the tandem centrifugal, 6.3 for the VSROC, and 10.4 for the axial. These burst margins are more than ample, and therefore, all disk designs can be considered safe. However, it is obvious that the axial has much more margin and could be classed as the most safe.

Excessive blade tensile and bending stresses can be the cause of a failure less dangerous than that of a disk. Such failures can still be considered a safety hazard. The maximum tensile stress in the blading of the tandem centrifugal is 29,900 psi. The maximum blade stress in the VSROC design is 41,900 psi, and that of the axial is 22,300 psi. The blade stress in the VSROC is high, and it could be reduced by about one third by the use of a hollow blade design. Even then, this design could become marginal for the Frame 2 size at operating Point B if there are any significant vibratory stresses.

Rotor System Complexity

A rotor system built up of many parts may not be dimensionally stable. This can occur due to dimensional errors during manufacture, incorrect heat treatment, and poor assembly practices. A shift in alignment can, therefore, cause a significant unbalance and possibly a destructive failure. The simplicity of the rotor system assembly is, therefore, an indicator of safety.

The two-stage tandem centrifugal machine has two massive impellers that must be joined. This joint will have to be at midspan at the location of the maximum system deflections. The five-stage axial will have five disks that must be joined. Both rotor systems, therefore, can be considered complex and prone to rotor failures. In contrast, the VSROC rotor lends itself to a one-piece construction with an integral shaft. This rotor system can be considered the simplest and safest of the group.

Debris Sensitivity

Foreign objects invariably find their way into the gas path of high speed turbomachinery. Failures can occur ranging from a few pieces of a

blade passing out of the machine to a catastrophic rotor system fracture. Of the three dynamometer designs, the five-stage axial is most susceptible to foreign object damage because of the fragility of the blading and the high solidity. The single-stage VSROC is probably next in sensitivity because of the high bending stresses in the blading and the high solidity. The two-stage tandem centrifugal appears to be the least sensitive one because of the large flow passages between the blades and the general ruggedness that is practical for this type of blading.

Environmental

The environmental advantages of the different dynamometer designs can be assessed on the basis of noise and vibration level.

Noise

There are three major sources of noise in these compressor systems. The first source is associated with the passing of the downstream blades through the wakes of the upstream blades. Both centrifugal and axial will be subjected to this kind of a noise. In the tandem centrifugal, the impeller blades will be passing through the wakes of the inlet guide vane.

The second source of noise is associated with the aerodynamics of air flow past the blades. This noise level depends on the tip speed and the relative Mach numbers. The blade speeds of the three compressors are within 10 per cent of each other. The relative Mach number, however, is comparatively high for the axial compressor.

The third source is associated with the shearing interaction of a high velocity jet of air with the surrounding air. This noise level can be related to the amount of air flow passing through the compressor system. The air flow through the single-stage VSROC is 14 per cent greater, and the air flow through the five-stage axial is 53 per cent higher than the two-stage tandem centrifugal design.

Apart from these sources, unsteady or unstable aerodynamic flow will be a noise generator. It does appear that the flow through the VSROC configuration will be more stable than the other two because of the variable shroud. The other two depend on throttling, a noisy process, and will tend to operate both near the surge and choke areas. These areas imply unsteady or separated flow phenomena which will generate noise.

From the above it appears that the VSROC will be the one with the least noise level, and the axial, the one with the highest noise level.

Vibration

The mechanical vibration energy level of the dynamometer can be transmitted into the supporting structure and the test engine. The energy level can be assumed to be a function of the rotor system weight and complexity. The VSROC has a very low rotor weight and can be of one-piece construction.

This system is expected to have the least vibration. The high rotor weight and the complex construction of the two-stage tandem centrifugal implies that this system will have a higher vibration level than the five-stage axial. In the axial, however, the probability of resonance or near resonance operation is several times higher than that of the centrifugal due to the higher number of blade rows.

Rating

The three dynamometers were rated on a comparative basis for each of the six categories by assigning numbers to the associated factors. The average number for each factor is based on the assumed importance of that factor. An initial investigation indicated that the single-stage variable-shroud radial outflow design would rate at or near the top in each category. Therefore, integral numbers were used for the values of rating factors of that design. The values of rating factors for other designs were obtained by using simple relationships based on the related values of the design parameters given and discussed earlier under that factor. In the absence of such values, integral numbers were also applied to the other two systems based on the qualitative discussion included earlier in this section.

The various relationships employed for the several rating factors are as follows:

Number of Units

$$F_N = 10 \left(\frac{1}{n_F} + \frac{2}{n_M} \right) \quad (36)$$

where n_F is the number of frame sizes

and n_M is the number of different models

Power Range

$$F_{PR} = R_a \quad (37)$$

where R_a is the arithmetic average of the power ranges of the different models at the rotational speeds of the seven design points

Direction of Rotation and Length

$$F_{DR} \notin F_L = \frac{2}{L} \quad (38)$$

where L is the estimated minimum length normalized with respect to that of the VSROC

Polar Moment of Inertia

$$F_{PM} = \frac{3}{I_p} \quad (39)$$

where I_p is the normalized polar moment of inertia

First Cost

$$F_c = 7/C_T \quad (40)$$

where C_T is the relative total cost of the required number of dynamometers obtained as

$$C_T = C_1 \sum_n S_{L_n}^3 \quad (41)$$

where C_1 is the relative cost per unit of the Frame I size unit

n is the required number of dynamometers

and S_{L_n} is the linear scale factor

Weight

$$F_w = \frac{3}{W} \quad (42)$$

where W is the normalized total weight of the compressor system

Diameter

$$F_D = \frac{3}{D} \quad (43)$$

where D is the normalized maximum diameter of the compressor system

Rotor Stress Levels

$$F_s = (D_{BM} + \frac{1}{\sigma_b}) \quad (44)$$

where D_{BM} is the normalized value of the disk burst margin

and σ_b is the normalized value of the blade root stress

The values of rating factors obtained from the above relationships as well as from qualitative judgement are listed in Table XXX for the three systems.

It is evident from the table that the single-stage VSROC rates the highest in over-all rating as well as in all categories except in safety. A double-entry version is expected to have a high rating in this category also, owing to the reduced stress levels resulting from the lower rotor tip diameter and blade axial length. A comparison of the over-all percentage rating indicates that the tandem centrifugal is second with about 30 per cent less rating than the VSROC; the axial is third with 42 per cent less rating.

The poor rating for the five-stage axial mainly stems from its comparatively low power range and consequent increase in the number of units required. A significant improvement in these factors for axial compressors could be achieved by an increase in the number of stages. The decrease in over-all rating of the tandem centrifugal results from more or less equal decrease in rating under each category except for safety where it has a slightly better rating than that of the single-stage VSROC. The over-all rating for other types of centrifugal compressors is not expected to be significantly different from the rating of the tandem configuration. Therefore, the double-entry radial outflow (F1-ROC-D) with variable shroud and a ten-stage axial were analyzed for comparative rating prior to the selection as well as to aid in the selection of the optimum system.

Analysis of Two Alternate Compressor Systems

Double-Entry Radial Outflow Compressor With Variable Shroud

As indicated earlier in this section, the length of the VSROC can be reduced drastically with the elimination of the inlet throttle ducting and by employing a vertical exhaust. Also, an integral shaft rotor system can be easily introduced in this configuration with consequent increase in burst margin by a factor of about 2. Introducing the above desirable features for the physical details of the Frame 1 size configuration (F1-ROC-D, Table XXIV), a preliminary design of the double-entry VSROC was obtained as shown in Figure 47.

Since the variation of maximum power with speed and the range are essentially the same for both VSROC versions, the number as well as the details of the required frame sizes would be almost identical. Therefore, the performance envelopes of single-stage dynamometers shown in Figure 41 and the details of them given in Table XXVII are equally applicable to the double-entry version.

The estimated cost and mechanical design details of the two ROC configurations are compared in Table XXXI. Most of these values are estimated from the preliminary design layout of an optimum configuration for the double-entry version (Fig 47). Even though the rotor system weight of the single-stage is higher than that of the double-entry, the total weights of the two compressor systems are assumed to be the same due to the less ducting required for the single-stage version. As mentioned earlier, the cost is assumed to be proportional to the weight of the rotor system.

Ten-Stage Axial Compressor

An increase in the number of stages would increase the pressure ratio across the compressor. A higher pressure ratio would result in less number of frame sizes and dynamometers. An initial analysis indicated that the number of stages has to be doubled to reduce the required number of frame sizes from four to three with inlet and exit valves. Therefore,

the power absorption characteristics with rotational speed for a ten-stage compressor with inlet and exit valves were obtained with the following simplifying assumptions:

1. The first five stages are scaled versions of the five-stage compressor stages and control surge and choke flows
2. $(HP)_{10} = 2 (HP)_5 \times (S_L)^2$ at constant blade speed,
where HP_5 is the horsepower of the basic five-stage compressor (F1-AC5-H)
and S_L is the appropriate linear scale factor applied for the basic compressor stages to obtain the Frame I size ten-stage compressor (F1-AC10-H)
3. The polytropic efficiency is independent of the number of stages.

The power absorption and range characteristics thus obtained for the ten-stage axial compressor were then employed for the analysis of the required number of frame sizes and dynamometers. The details of the frame sizes and dynamometers are listed in Table XXXII; the performance envelopes of the dynamometers are given in Figure 48. The cost and mechanical design details of the ten-stage axial are estimated from and listed along with those of the five-stage axial in Table XXXIII.

Selection of the Optimum System

From the design details established as given in the above section, the two alternate compressor systems were rated based on the simple relationships (Equations 36-44). For factors for which relationships were not established, the rating was based on the rating of the same type of compressor given in Table XXX. To be consistent, the relevant rating factors of the ten-stage axial were related to the disk stress and diameter values of the single-stage VSROC configuration initially used rather than the stress value for the integral shaft design and the scaled diameter value listed in Table XXXI; the over-all rating would differ very little even if the latter values were employed.

The ratings thus obtained for the two alternate configurations for each of the six categories are listed in Table XXXIV along with the ratings established earlier for three other compressor systems. As anticipated, the double-entry VSROC configuration has a higher rating than that of the single-stage version. The increase in rating of about 8 per cent results mainly from the reduced rotor system weight and stress level. Also, the ten-stage axial has about 10 per cent higher over-all rating than that of the five-stage. This relative increase in rating is mainly due to the superior power range and the consequent reduction in the required number of dynamometer models.

A comparison of the over-all rating of the five compressor systems indicate that the double-entry radial outflow ranks first with close to a 108 per cent rating, and the single-entry version used as reference for per cent rating ranks second with 100 per cent rating. The two-stage tandem ranks third with about 30 per cent reduction in rating from that of the single-stage radial outflow dynamometer. The fourth one, the ten-stage axial,

has a rating only 2 per cent less than that of the third one, the tandem centrifugal. A small uncertainty in the rating or additional considerations could make the ten-stage axial rank third. The five-stage axial is at the bottom of the list with only 58 per cent rating.

It is evident from the ratings that the variable shroud radial outflow compressors would still top the list of feasible concepts even if we allow for great uncertainties in the rating system employed or, for that matter, even if an elaborate rating system is to be employed with additional categories and factors. Among the radial-outflow configurations, the double-entry configuration is equal or superior to the single-stage configuration in all categories.

The only major disadvantage associated with the double-entry version is that two separate shroud structures must be moved in unison. This may be done with a single actuator and linkage mechanisms or by two separate position control servo loops. Another disadvantage could be due to any cross-coupled aerodynamic excitation between the two flow paths resulting in premature surge. This may not be a problem since the compressor need not operate near surge. Any such problem that might appear at very high closing of the flow passage could be eliminated by a mechanical separator in the discharge area.

The major problems associated with the single-entry version are high blade stress, thrust balance, and narrow range of stable operation at higher speeds. The high blade stress may dictate some blade treatment for the operation of the Frame 2 dynamometer at Point B where the stress levels would be about 60 per cent higher than the design values. Even with a hollow blade design to reduce the stress level, the higher temperature rise across the stage (about 30 per cent greater than the double-entry version) may not allow power modulation of the order of 10 and beyond at high speed operation. The very narrow range exhibited by its performance characteristics at 130 per cent speed (9,100 rpm, Fig 18) would limit its growth potential to future engines with still higher power or speed or both. Also, the available flow area at the inlet of the stage would be a limiting factor at higher blade speeds. The axial thrust will be very high in the single-entry version requiring excessive clearances; an excessive clearance would limit the realization of the potential maximum range achievable in this type of configuration with the variable shroud for power modulation.

From the above considerations, it is judged that the double-entry configuration is the better of the two radial-outflow configurations with the variable shroud for power modulation. Therefore, it is recommended as the optimum system for the dynamometers of the Navy's future as well as present engines. For the recommended configuration, Table XXXV lists the over-all dimensions, stress levels, and the estimated weights of the three dynamometers required to cover the specified seven engine design points. Even though the length and diameters will be directly scaled based on the linear scale factor, some of the component thicknesses may not be scaled to arrive at the two lower frame size dynamometers.

Therefore, an index of 2.5 rather than 3 was used in Equation 7 for the weight calculation, assuming that only about 50 per cent of the component thicknesses is scalable.

ANALYSIS OF EXPERIMENTAL PROGRAM REQUIREMENTS

Introduction

The analytical investigation of various types of compressors with various means of power modulation has established firmly that the radial-outflow type compressors with a variable shroud or shrouds for power modulation would be the best concept for the development of air dynamometers to meet the needs of the Navy's future engines and growth versions of the present engines. Of the two versions of the radial-outflow type compressors, the double-entry version is preferred over the single-stage version and is, therefore, recommended as the optimum system.

As a logical next step to the analytical investigation, a program is needed for the experimental evaluation of the optimum concept and to solve the technical problems that could not be analytically studied. Therefore, a brief summary of the problem areas to be solved and the possible solutions to them are given in this section.

Low Power Operation

The unique feature of the radial-outflow variable-shroud dynamometer is its potential for a wide operating range. However, the behavior of the system at low power absorption where the flow path has been significantly closed down is not fully understood. A leakage flow can occur from the impeller discharge around the outer blade shroud to the inlet. This leakage will contribute to the flow being pumped, thus limiting the minimum power. The relationship between this leakage and the minimum achievable power should be developed. Having such a relationship, even if approximate, is necessary to set the mechanical design standards for the impeller running clearance and the practical limit for shroud closure.

The recirculation effects within the impeller blade system will also limit the minimum achievable power. This recirculation is a function of the blade solidity and the clearance volume around the covered portion of the blades (Ref 9). These effects should be analyzed, and the design guide lines should be set for blade solidity and clearances.

When the flow rate is altered across the stage, the operating point on the nondimensional compressor characteristic would change due to the fixed exhaust duct and orifice requiring some range of operation at a fixed speed. The operating range would also be affected by the variation in leakage and recirculation when the flow path width is closed. Further, there could be some cross-coupled aerodynamic excitation between the two flow paths which might reduce the range of operation by inducing premature surge. Therefore, these problems should be examined in detail analytically and, if necessary, experimentally. The cross-talk between the flow paths may be eliminated by a mechanical separator in the flow discharge area.

Shroud Seal

The leakage from the impeller discharge to its inlet around the outer blade shroud must be restricted. This can be done by decreasing the radial clearance between the outer blade shroud and the stator and/or increasing the restrictions in this leakage flow path.

The amount that the clearances can be reduced is limited. The radial excursions due to rotor system dynamics, the elastic deflections of the impeller disk and blades, and the relative thermal growth between the rotor and stator all must be considered. Some gains can be made if the rotor systems can be designed to operate below the first lateral critical speed.

This flow path restriction can be increased in many ways. Labryinth and visco type flow paths together with an abradable surface appear feasible. Another approach would be to operate the outer blade shroud with a fixed axial clearance. This then dictates that the outer throttle ring and the inner movable shroud be separate pieces. This approach looks very promising, but the synchronization and actuation may present difficulties.

From the above it appears that a detailed design study should be conducted to optimize the rotor seal and movable shroud structure and the actuation thereof. This should include configuration studies, stress, temperature and deflection analyses, and the synthesis of the actuation means.

Thrust Balance

In a single-stage (single-entry) configuration, the axial thrust levels will be high, requiring special schemes for thrust balance. The axial thrust of the rotor system in the double-entry configuration would be small, as it would be caused only by unequal operation of the two sides either due to a nonsymmetric inlet flow pattern or a nonsynchronous movement of the two variable shroud structures. Therefore, it is not necessary to introduce any thrust balancing schemes in the double-entry configuration.

Controls

The dynamometer control should be handled in two steps. The first is to solve the problems associated with shroud actuation and torque measurement. The second is to automate the control process so that the dynamometer becomes a useful field service tool.

It is expected that the shroud actuation device will have to overcome large friction and aerodynamic forces. This can best be done by a high pressure hydraulic system closing the loop around position. This does mean that a hydraulic power supply must be included as part of the dynamometer ancillary equipment. Another approach would be to use the pneumatic energy from the dynamometer discharge. This approach will dictate a large actuator size in order to get an adequate force margin. It also would not function during start-up. The third approach would be to use electric actuators powered from a storage battery.

Torque sensing can be done by sensing torque in the quill shaft between the test engine and the dynamometer or by measuring the reaction torque on the dynamometer. Sensing torque in the quill shaft requires either slip rings or a telemetry system to transmit the signal to a stationary source. The quill shaft is subject to considerable handling when changing engines and to changes in spring constant to match the system torsional dynamics. Measuring the reaction torque of the dynamometer is relatively straightforward except for the problem of aerodynamic reaction. The dynamometer exhaust air must pass through a commutator section with straightening vanes of high solidity to prevent this torque reaction from taking place.

Once the problems of actuation and torque measurement have been solved, it is a straightforward engineering task to design a suitable automatic control system for the dynamometer. This system in the turboshaft mode would have to produce a torque proportional to some given function of the input collection pitch angle. This signal would also be transmitted to the engine control. In the turboprop mode the dynamometer torque would be controlled to maintain the input speed value.

From the above discussion it appears that two control design phases should be done. One would solve the actuation control and torque measurement problems. The other would prepare the detail design of a completely automatic dynamometer control system.

Dynamometer Development

The problems discussed above are associated with the development of the dynamometers to be used for the testing of engines. Such a development, it is suggested, can be carried out in three phases: an experimental program for the evaluation of the concept, a demonstrator program, and a prototype program.

The first program would involve solving mainly the problems associated with the low power operation and provide important inputs to the design of the demonstrator dynamometer hardware with respect to mechanical design standards. The demonstrator program would be directed towards solving problems associated with the variable shroud mechanisms and the controls for the shroud actuation and torque measurements. The third phase will be the building of a dynamometer of particular frame size with a completely automatic control system and the demonstration of the dynamometer with an engine. The entire program could be completed within a span of four years with the first twelve months devoted to the concept demonstration and the remaining period distributed more or less equally between the other two phases.

For the concept demonstration and the demonstrator program, a suitable power source and test facility is needed. NREC has a test facility that can supply power up to at least 900 hp within a rotational speed range of 10,000 to 40,000 rpm. This facility is fully setup for semiautomatic data retrieval and processing. It is suggested that the concept demonstration and the demonstrator program be conducted in this test facility.

Even though it would involve additional hardware, the total development program could also be geared to the evaluation of the scaling effects associated with obtaining different frame sizes by scaling from a basic frame size. Also, the demonstration of the concept can be done by having only one side of a double-entry configuration. As a result, the concept demonstration at NREC's test facility could be accomplished in three ways:

1. Testing of the Frame 3 size double-entry compressor with inlet throttling
2. Testing of one side of the Frame 3 size double-entry compressor with inlet throttling
3. Testing of a lower diameter frame size with 0.3 linear scale factor

In the first, the testing would initially be done with standard inlet conditions up to the maximum available power, and then the inlet throttling would be employed to cover as much of the performance envelope as possible. At 21,500 rpm (equivalent Point B rotational speed), the inlet pressure could be throttled by more than 2:1. The second approach would be the same as the first one, except that it is possible to cover the entire performance envelope of the Frame 3 size including the equivalent Point B operation.

For the Frame 4 size ($S_L = 0.3$), the equivalent Point B rotational speed is 29,600 rpm, and the testing would be similar to the second approach, since the Frame 4 size would absorb about one half of the Frame 3 size power absorption at an equivalent speed. Unlike in the second approach, any cross-talk effect between the two flow paths could be investigated in the first and third approaches.

From the above considerations it appears that the third approach would be the best one for the Navy to follow in the demonstration of the variable-shroud radial-outflow compressor concept.

EXPERIMENTAL PROGRAM FOR CONCEPT DEMONSTRATION

Introduction

It has been suggested in the previous section that, for the Navy's future engines, the development of dynamometers with the double-entry version of the variable-shroud radial-outflow compressors should be undertaken in three phases: a concept demonstration program, a demonstrator dynamometer program, and a prototype dynamometer program. The concept demonstration program, as stated earlier, could be completed within a 12-month period using the NREC test facility. In this section, an outline of the experimental program required for the demonstration of the concept is given. The outline is presented in terms of specific tasks with a brief description of the effort associated with each task.

Outline of Experimental Program

Task 1 - Aerodynamic Design and Analysis

The main objective is the detailed design of the flow path and the rotor profile based on the over-all dimensions established earlier for Frame 1 size and the scaling factor mutually agreed upon by NREC and Navy personnel. The second objective is to analyze the effects of leakage and recirculation at low power operation.

The results from the design effort will be the detailed specification of flow path dimensions and rotor blade profile. The main results of the analysis will be the guidelines for aerodynamic and mechanical design with respect to desired solidity and clearance and any necessary flow conditions required for mechanical design. The results will also include the specification of instrumentation and rotational speeds for testing.

Task 2 - Mechanical Design of the Stage

The objective of this task is the mechanical design of the stage flow path components including selection of material and stress and vibration analysis of the critical components. The results will include the design and analysis data, detailed drawings for manufacturing, and material specifications.

Task 3 - Mechanical Design of the Auxiliaries and Test Fixture

The objective of the task is the mechanical design of the test fixture and auxiliary components necessary for the demonstration of the concept using NREC test facility with variable shroud setting. The results will be the design data, specification and detailed drawings for the manufacture of test fixtures and necessary auxiliary components including instrumentation and assembly drawing.

Task 4 - Procurement, Inspection, and Assembly

In this task, the drawings for the manufacture of components will be released and the necessary components procured and inspected. The task will also include the assembly of the test hardware and instrumentation.

Task 5 - Testing for Concept Demonstration

The testing will be conducted at rotational speeds established in Task 1. A minimum of three rotational speeds will be used, covering the equivalent speeds of Points A, B, and G of the three frame sizes. At each rotational speed, a minimum of five test points will be recorded with data at the shroud setting for maximum passage opening, three immediate settings, and the shroud setting for the maximum possible closing of the blade passage.

Task 6 - Data Analysis and Reporting

The test data would be reduced and analyzed for the variation of power with the shroud setting. Based on the analysis, desirable modifications to the stage and the resulting maximum performance envelopes possible for dynamometers with this concept will be obtained. In addition, an outline of the program associated with the demonstrator dynamometer will be prepared and included in the final report, which will contain the major results and conclusions resulting from the concept demonstration program.

REFERENCES

1. Rodgers, C., Technical Advances in Gas Turbine Design, Paper 5: A Cycle Analysis Technique for Small Gas Turbines, Institution of Mechanical Engineers, Warwick, England, April 9-11, 1969.
2. Shephard, D. G., Principles of Turbomachinery, The Macmillan Company, New York, 1956.
3. Cates, P. S., Peripheral-Compressor Performance on Gases With Molecular Weights of 4 to 400 (ASME Paper No. 64-WA/FE-25), The American Society of Mechanical Engineers, New York, September, 1964.
4. Performance Evaluation of Helical-Screw Compressors (NREC Report No. 1182-1), Northern Research and Engineering Corporation, Cambridge, Mass., February, 1972.
5. Scheel, L. F., "A Technology for Rotary Compressors", J. of Engineering for Power, July, 1970, pp. 207-216.
6. Program PREDM: Multistage Centrifugal Compressor Performance Evaluation (NREC Report No. 900AXA-1), Northern Research and Engineering Corporation, Cambridge, Massachusetts, July 1, 1974.
7. Axial-Flow Compressor Computing System - Volumes I through V (NREC Report No. 1110-1-5), Northern Research and Engineering Corporation, Cambridge, Massachusetts, October 24, 1966.
8. Sternlicht, B., "Design", Gas Turbine Engineering Handbook, Gas Turbine Publications, Inc., Stamford, Connecticut, 1966, page 88.
9. Mann, Robert W., and Marston, Charles H., Friction Drag on Bladed Disks in Housings as a Function of Reynolds Number, Axial and Radial Clearance, and Blade Aspect Ratio and Solidity (ASME Paper No. 61-Hyd-5), The American Society of Mechanical Engineers, New York, May, 1961.

TABLE I
OVER-ALL DETAILS OF CENTRIFUGAL COMPRESSOR STAGES FOR POINT A

Power = 10,000 hp
 Rotational Speed = 7,000 rpm

| Configuration | Single Stage | Double Entry (Parallel) | Tandem Units (Series) | | |
|---|--------------|-------------------------|-----------------------|----------|----------|
| | A-CC1 | A-CCD1 | I-Stage | II-Stage | Over-All |
| Flow Rate (lbm/sec) | 128.2 | 84.6* | 89.2 | 89.2 | 89.2 |
| Pressure Ratio | 1.893 | 1.763 | 1.781 | 1.479 | 2.634 |
| Efficiency | 0.452 | 0.525 | 0.516 | 0.553 | 0.502 |
| Exit Temperature (deg R) | 750 | 694 | 700 | 850 | 790 |
| Tip Speed (ft/sec) | 1252 | 1090 | 1109 | 1011 | --- |
| Absolute Mach Number at Impeller Exit | 1.026 | 0.911 | 0.925 | 0.745 | --- |
| Impeller Exit Diameter, D_2 (in) | 41.0 | 35.7 | 36.3 | 33.1 | --- |
| Maximum-to-Impeller Exit Diameter Ratio, $48.0/D_2$ | 1.17 | 1.35 | 1.32 | 1.45 | --- |
| Specific Speed, N_s | 0.13 | 0.13 | 0.13 | 0.13 | --- |

* Flow entering one side

TABLE II
OVER-ALL DETAILS OF CENTRIFUGAL COMPRESSOR STAGES FOR POINT B

Power = 10,000 hp
Rotational Speed = 12,000 rpm

| | Single Stage | Double Entry (Parallel) | Tandem Units (Series) | | | Over-All |
|---|--------------|-------------------------|-----------------------|----------|----------|----------|
| | | | B-CCT1 | B-CCT1-1 | B-CCT1-2 | |
| Configuration | | | | | | B-CCT1 |
| Flow Rate (lbm/sec) | 83.3 | 55.0* | | 61.4 | 61.4 | 61.4 |
| Pressure Ratio | 3.363 | 2.733 | | 2.884 | 1.675 | 4.831 |
| Efficiency | 0.609 | 0.645 | | 0.637 | 0.671 | 0.616 |
| Exit Temperature (deg R) | 874 | 788 | | 809 | 1000 | 1000 |
| Tip Speed (ft/sec) | 1553 | 1352 | | 1403 | 1142 | --- |
| Absolute Mach Number at Impeller Exit | 1.222 | 1.094 | | 1.128 | 0.780 | --- |
| Impeller Exit Diameter, D_2 (in) | 29.7 | 25.8 | | 26.8 | 21.8 | --- |
| Maximum-to-Impeller Exit Diameter Ratio, $48.0/D_2$ | 1.62 | 1.86 | | 1.79 | 2.20 | --- |
| Specific Speed, N_s | 0.13 | 0.13 | | 0.13 | 0.13 | --- |

*Flow entering one side

TABLE III

OVER-ALL DETAILS OF DOUBLE-ENTRY RADIAL OUTFLOW COMPRESSORS
FOR POINTS A AND B

| <u>Configuration</u> | <u>Point A</u> | <u>Point B</u> |
|---|----------------|----------------|
| Horsepower | 10,000 | 10,000 |
| Rotational Speed (rpm) | 7,000 | 12,000 |
| Weight Flow (lbm/sec) | 61.1 | 38.8 |
| Over-All Stage Pressure Ratio | 1.393 | 2.961 |
| Over-All Stage Efficiency | 0.214 | 0.498 |
| Stage Exit Absolute Total Temperature (deg R) | 761 | 900 |
| Rotor Exit Blade Speed (ft/sec) | 850 | 1067 |
| Relative Mach Number at Rotor Exit | 0.768 | 0.904 |
| Absolute Mach Number at Rotor Exit | 1.61 | 2.05 |
| Absolute Mach Number at Diffuser Exit | 1.10 | 0.83 |
| Rotor Exit Diameter (in) | 27.8 | 20.4 |
| Diffuser Exit Diameter (in) | 37.1 | 39.4 |
| Rotor Exit Passage Width (in) | 3.31 | 2.52 |
| Specific Speed, N_s | 0.09 | 0.09 |

Note: The weight flow and passage width correspond to one side of the double entry units.

TABLE IV
OVER-ALL DETAILS OF A CONSTANT-TIP THREE-STAGE AXIAL COMPRESSOR FOR POINT A

Power = 10,000 hp
 Rotational Speed = 7,000 rpm
 Flow Rate = 178 lbm/sec
 Tip Diameter = 35 in
 Tip Speed = 1,070 ft/sec

| | I-Stage | II-Stage | III-Stage | Over-All |
|--|----------|----------|-----------|----------|
| Configuration | A-AC31-1 | A-AC31-2 | A-AC31-3 | A-AC31 |
| Pressure Ratio | 1.345 | 1.312 | 1.284 | 2.001* |
| Efficiency | 0.835 | 0.842 | 0.848 | 0.691* |
| Exit Temperature (deg R) | 1035 | 1090 | 1145 | 1145 |
| Inlet Tip Relative Mach Number | 1.215 | 1.130 | 1.080 | --- |
| Flow Coefficient, ϕ_f | 0.665 | 0.600 | 0.590 | --- |
| Temperature Rise Coefficient, Ψ_t | 1.029 | 0.905 | 0.800 | --- |
| Hub-to-Tip Diameter Ratio, D_h/D_t | 0.50 | 0.60 | 0.70 | --- |
| Specific Speed, N_s | 0.50 | 0.45 | 0.409 | --- |

*Based on the assumption that the compressor exit dynamic head is lost.

TABLE V
OVER-ALL DETAILS OF A CONSTANT-TIP FIVE-STAGE AXIAL COMPRESSOR FOR POINT B

Power = 10,000 hp
 Rotational Speed = 12,000 rpm
 Flow Rate = 85.4 lbm./sec
 Tip Diameter = 21.5 in
 Tip Speed = 1,130 ft/sec

| | I-Stage | II-Stage | III-Stage | IV-Stage | V-Stage | Over-All |
|--|----------|----------|-----------|----------|----------|--------------------|
| Configuration | B-AC51-1 | B-AC51-2 | B-AC51-3 | B-AC51-4 | B-AC51-5 | B-AC51 |
| Pressure Ratio | 1.444 | 1.391 | 1.348 | 1.312 | 1.281 | 4.206 ^a |
| Efficiency | 0.835 | 0.844 | 0.849 | 0.850 | 0.846 | 0.765 ^a |
| Exit Temperature (deg R) | 1049 | 1118 | 1187 | 1256 | 1325 | 1325 |
| Inlet Tip Relative Mach Number | 1.350 | 1.195 | 1.088 | 1.018 | 0.965 | --- |
| Flow Coefficient, ϕ_t | 0.78 | 0.64 | 0.55 | 0.50 | 0.49 | --- |
| Temperature Rise Coefficient, Ψ_t | 1.226 | 1.118 | 1.018 | 0.935 | 0.860 | --- |
| Hub-to-Tip Diameter Ratio, D_h/D_t | 0.46 | 0.53 | 0.60 | 0.67 | 0.74 | --- |
| Specific Speed, N_s | 0.500 | 0.439 | 0.392 | 0.355 | 0.326 | --- |

*Based on the assumption that the compressor exit dynamic head is lost.

TABLE VI
OVER-ALL DETAILS OF DRAG COMPRESSORS FOR POINT B

Power = 10,000 hp
 Rotational Speed = 12,000 rpm

| | Configuration | | | | |
|----------------------------|---------------|-------|-------|-------|-------|
| | DC1 | DC2 | DC3 | DC4 | DC5 |
| Capacity Coefficient | 0.168 | 0.10 | 0.14 | 0.114 | 0.124 |
| Head Coefficient | 0.444 | 0.635 | 0.350 | 0.25 | 0.805 |
| Normalized Channel Width | 0.050 | 0.050 | 0.050 | 0.050 | 0.088 |
| Normalized Channel Height | 0.02 | 0.02 | 0.02 | 0.02 | 0.05 |
| Impeller Tip Diameter (in) | 22.14 | 22.14 | 24.19 | 26.33 | 22.14 |
| Impeller Tip Mach Number | 1.037 | 0.037 | 1.113 | 1.233 | 1.037 |
| Weight Flow (lbm/sec) | 0.980 | 0.585 | 1.068 | 1.121 | 1.532 |
| Tip Speed (ft/sec) | 1159 | 1159 | 1266 | 1378 | 1159 |
| Over-All Pressure Ratio | 1.814 | 2.317 | 1.755 | 1.616 | 2.821 |
| Over-All Efficiency | 0.118 | 0.099 | 0.097 | 0.074 | 0.221 |
| Specific Speed, N_s | 0.005 | 0.003 | 0.005 | 0.005 | 0.007 |
| Required Number of Units | 37 | 36 | 30 | 26 | 24 |
| | | | | | 18 |

OVER-ALL DETAILS OF VARIOUS POSITIVE DISPLACEMENT COMPRESSORS FOR POINT B

Power = 10,000 hp
 Rotational Speed = 12,000 rpm

| | Configuration | | | | | | | | | |
|--------------------------------|---------------|--------|--------|-------|-------|-------|-------|-------|-------|-------|
| | HS1 | HS2 | SA1 | SA2 | SL1 | SL2 | SV1 | SV2 | LL1 | LL2 |
| Pressure Ratio | 4 | 6 | 3 | 4.5 | 1.7 | 2.55 | 4 | 6 | 5 | 7.5 |
| Tip Mach Number | 0.35 | 0.525 | 0.12 | 0.18 | 0.05 | 0.075 | 0.05 | 0.075 | 0.06 | 0.09 |
| Characteristic | 0.0612 | 0.0918 | 0.1333 | 0.200 | 0.270 | 0.405 | 0.046 | 0.069 | 0.071 | 0.107 |
| Displacement Constant | | | | | | | | | | |
| Length-to-Diameter Ratio | 1.0 | 1.5 | 1.5 | 2.25 | 1.5 | 2.25 | 2 | 3 | 1.12 | 1.68 |
| Specific Speed, N _s | 0.018 | 0.030 | 0.009 | 0.019 | 0.007 | 0.012 | 0.001 | 0.003 | 0.001 | 0.003 |
| Required Number of Units | 58 | 7 | 648 | 58 | 10350 | 726 | 11240 | 905 | 4131 | 260 |

HS - Helical Screw

SA - Spiral Axial

SL - Straight Lobe

SV - Sliding Vane

LL - Liquid Liner

TABLE VIII
PRELIMINARY GEOMETRIC DATA AND STAGE CHARACTERISTICS OF
CENTRIFUGAL COMPRESSORS

| | <u>A-CCD2 or</u> <u>A-CCT2-1</u> | <u>A-CCT2-2</u> | <u>D-CC2</u> | <u>B-CCD2 or</u> <u>B-CCT2-1</u> | <u>B-CCT2-2</u> |
|--|-------------------------------------|-----------------|--------------|-------------------------------------|-----------------|
| Horsepower per stage or side | 5,000 | 5,000 | 2,500 | 5,000 | 5,000 |
| Rotational Speed (rpm) | 7,000 | 7,000 | 6,600 | 12,000 | 12,000 |
| Weight Flow (lbm/sec) | 84.6 | 84.6 | 47.6 | 54.7 | 54.7 |
| Pressure Ratio | 1.556 | 1.458 | 1.613 | 2.449 | 2.008 |
| Over-All Pressure Ratio | -- | 2.269 | -- | -- | 4.918 |
| Inducer Tip Radius (in) | 12.8 | 12.0 | 10.53 | 9.40 | 7.75 |
| Inducer Hub Radius (in) | 5.89 | 5.89 | 5.89 | 4.23 | 4.23 |
| Impeller Tip Radius (in) | 17.83 | 17.83 | 17.83 | 12.94 | 12.94 |
| Impeller Exit Passage Width (in) | 2.211 | 1.925 | 1.284 | 1.449 | 0.931 |
| Flow Angle at Inducer Tip (deg) | 61.5 | 60 | 56.5 | 62 | 57.2 |
| Flow Angle at Inducer Hub (deg) | 40.2 | 40.2 | 40.2 | 40.2 | 40.2 |
| Inducer Tip Relative Mach Number | 0.853 | 0.686 | 0.680 | 1.115 | 0.738 |
| Impeller Tip Speed (ft/sec) | 1,090 | 1,090 | 1,028 | 1,355 | 1,355 |
| Absolute Flow Angle at Impeller Exit (deg) | 61.5 | 61.3 | 61.3 | 61.4 | 61.6 |
| Absolute Mach Number at Impeller Exit | 0.913 | 0.805 | 0.868 | 1.099 | 0.919 |
| Specific Speed, N_s | 0.138 | 0.122 | 0.101 | 0.143 | 0.103 |

A(B)-CCD2 One side of a Double Entry Unit for Point A(B)

A(B)-CCT2-1 First stage of a Tandem Unit for Point A(B)

A(B)-CCT2-2 Second stage of a Tandem Unit for Point A(B)

D-CC2 Single stage Unit for Point D

TABLE IX
RESULTS OF THE SCALING ANALYSIS - CENTRIFUGAL COMPRESSOR

| Operating Point | Basic Unit (A-CCT2) | | Scaled Units | | | | |
|--|------------------------|--------|--------------|-------|-------|-------|--------|
| | A | B | C | D | E | F | G |
| Rotational Speed, N_s (rpm) | 7,000 | 12,000 | 12,000 | 6,600 | 6,600 | 7,000 | 19,500 |
| Linear Scale Factor, S_L | 1.0 | 0.724 | 0.653 | 0.785 | 0.863 | 0.903 | 0.410 |
| Design Rotational Speed, $N_{s,d}$ | 7,000 | 9,673 | 10,713 | 8,916 | 8,116 | 7,753 | 17,077 |
| Blade Speed Ratio, $\frac{U_b}{U_{s,d}}$ ($= \frac{N_s}{N_{s,d}}$) | 1.00 | 1.241 | 1.120 | 0.740 | 0.813 | 0.903 | 1.142 |
| Over-All Diameter (in) | 48 | 34.75 | 31.34 | 37.68 | 41.42 | 43.34 | 19.68 |
| Compressor Weight (lbm) | 2,020 | 767 | 562 | 977 | 1,298 | 1,487 | 139 |

TABLE XCOMPARISON OF OVER-ALL DIMENSIONS OF SCALED UNIT WITH
THOSE OF PRELIMINARY DESIGN - CENTRIFUGAL COMPRESSOR

| | <u>B-CCD2 or B-CCT2-1</u> | <u>Scaled Unit</u> |
|----------------------------------|-------------------------------|------------------------|
| Inducer Tip Radius (in) | 9.40 | 9.27 |
| Inducer Hub Radius (in) | 4.23 | 4.26 |
| Impeller Tip Radius (in) | 12.94 | 12.91 |
| Impeller Exit Passage Width (in) | 1.449 | 1.601 |

TABLE XI
RESULTS OF THE SCALING ANALYSIS - AXIAL COMPRESSOR

| | Basic Unit (B-AC51) | Scaled Units | | | | | |
|----------------------------------|---------------------------|--------------|--------|--------|--------|--------|--------|
| | | B | A | A | A | G | G |
| Operating Point | | B | A | A | A | G | G |
| Horsepower, P_s | 10,000 | 10,000 | 10,000 | 10,000 | 2,500 | 2,500 | 2,500 |
| Rotational Speed, N_s (rpm) | 12,000 | 7,000 | 7,000 | 7,000 | 19,500 | 19,500 | 19,500 |
| Number of Stages, n_s | 5 | 5 | 4 | 3 | 5 | 4 | 3 |
| Scaling Factor, S_L | 1.0 | 1.382 | 1.445 | 1.531 | 0.566 | 0.592 | 0.627 |
| Tip Diameter (in) | 21.5 | 29.7 | 31.1 | 32.9 | 12.2 | 12.7 | 13.5 |
| Blade Speed Ratio, $U_s/U_{b,d}$ | 1.0 | 0.806 | 0.843 | 0.893 | 0.920 | 0.962 | 1.019 |
| Length Ratio, L_s/L_b | 1.0 | 1.38 | 1.18 | 0.97 | 0.57 | 0.48 | 0.40 |
| Weight Ratio, W_s/W_b | 1.0 | 2.64 | 2.47 | 2.28 | 0.181 | 0.170 | 0.157 |
| Weight, W_s (lbm) | 636 | 1680 | 1570 | 1450 | 115 | 108 | 100 |

TABLE XII
PRELIMINARY BLADING DETAILS FOR THE AXIAL COMPRESSOR CONFIGURATION B-AC51

| <u>Stage</u> | <u>Diameter Ratio, $\frac{D}{DR}$</u> | <u>Section</u> | <u>Solidity</u> | <u>Camber Angle, ϕ (deg)</u> | <u>Inlet Blade Angle, β_1 (deg)</u> | <u>Stagger Angle, ξ (deg)</u> | <u>Exit Blade Angle, β_2 (deg)</u> |
|----------------------|--|----------------|-----------------|--|--|--|---|
| First (B-AC51-1) | 0.46 | Hub | 1.90 | 69.4 | 7.1 | 41.8 | -27.6 |
| | | Mean | 1.20 | 46.0 | 19.0 | 42.0 | -4.0 |
| | | Tip | 0.88 | 38.5 | 26.1 | 45.4 | 6.8 |
| Second (B-AC51-2) | 0.53 | Hub | 1.73 | 67.4 | 11.8 | 45.5 | -21.8 |
| | | Mean | 1.20 | 46.4 | 23.4 | 46.6 | 0.3 |
| | | Tip | 0.92 | 38.5 | 30.3 | 49.6 | 11.1 |
| Third (B-AC51-3) | 0.60 | Hub | 1.60 | 62.0 | 17.4 | 48.4 | -13.6 |
| | | Mean | 1.20 | 44.5 | 27.7 | 49.9 | 5.4 |
| | | Tip | 0.96 | 36.9 | 34.0 | 52.4 | 15.5 |
| Fourth (B-AC51-4) | 0.67 | Hub | 1.50 | 54.7 | 22.7 | 50.1 | -4.7 |
| | | Mean | 1.20 | 41.5 | 30.9 | 51.6 | 10.0 |
| | | Tip | 1.00 | 34.9 | 36.3 | 53.7 | 18.8 |
| Fifth (B-AC51-5) | 0.74 | Hub | 1.41 | 46.7 | 26.8 | 50.1 | 3.4 |
| | | Mean | 1.20 | 37.9 | 32.6 | 51.6 | 13.7 |
| | | Tip | 1.04 | 32.7 | 36.9 | 53.2 | 20.6 |

Note: The rotor and stator blade angles are equal in magnitude from design assumptions. For the rotor blade angles, the sign given in the table should be reversed for the sign convention which assigns negative values to the swirl component against the direction of rotation.

TABLE XIII
PRELIMINARY DESIGN DETAILS OF DRAG COMPRESSORS

| | <u>A-DC1</u> | <u>A-DC2</u> | <u>A-DC1</u> [*] | <u>B-DC2</u> ^{**} |
|--------------------------------|--------------|--------------|---------------------------|----------------------------|
| | A | A | B | B |
| Operating Point | | | | |
| Total Horsepower | 10,000 | 10,000 | 10,000 | 10,000 |
| Rotational Speed (rpm) | 7,000 | 7,000 | 12,000 | 12,000 |
| Capacity Coefficient | 0.168 | 0.100 | 0.168 | 0.10 |
| Head Coefficient | 0.444 | 1.160 | 0.444 | 1.16 |
| Normalized Channel Width (in) | 0.05 | 0.125 | 0.05 | 0.125 |
| Normalized Channel Height (in) | 0.02 | 0.080 | 0.02 | 0.080 |
| Rotor Tip Diameter (in) | 38.0 | 38.0 | 22.1 | 22.1 |
| Rotor Tip Mach Number | 1.037 | 1.037 | 1.037 | 1.037 |
| Weight Flow (lbm/sec) | 2.89 | 5.94 | 0.98 | 2.02 |
| Tip Speed (ft/sec) | 1159 | 1159 | 1159 | 1159 |
| Over-All Pressure Ratio | 1.81 | 4.12 | 1.81 | 4.12 |
| Over-All Efficiency | 0.12 | 0.32 | 0.12 | 0.32 |
| Specific Speed, N_s | 0.0053 | 0.0077 | 0.0053 | 0.0077 |
| Required Number of Units | 13 | 6 | 37 | 18 |

* Same as configuration DC1 of Table VI

**Same as configuration DC6 of Table VI

TABLE XIV
PRELIMINARY DESIGN DETAILS OF HELICAL SCREW COMPRESSORS

| | <u>A-HS1</u> | <u>A-HS2</u> | <u>B-HS1</u> | <u>B-HS2</u> |
|--------------------------------------|--------------|--------------|--------------|--------------|
| Operating Point | A | A | B | B |
| Total Horsepower | 10,000 | 10,000 | 10,000 | 10,000 |
| Rotational Speed (rpm) | 7,000 | 7,000 | 12,000 | 12,000 |
| Pressure Ratio | 4.0 | 6.0 | 4.0 | 6.0 |
| Tip Mach Number | 0.35 | 0.42 | 0.35 | 0.42 |
| Characteristic Displacement Constant | 0.0612 | 0.0673 | 0.0612 | 0.0673 |
| Length-to-Diameter Ratio | 1.0 | 1.5 | 1.0 | 1.5 |
| Male Rotor Diameter (in) | 12.8 | 15.4 | 7.5 | 9.0 |
| Weight Flow (lbm/sec) | 3.31 | 7.97 | 1.13 | 2.71 |
| Over-All Efficiency | 0.56 | 0.47 | 0.56 | 0.47 |
| Specific Speed, N_s | 0.018 | 0.022 | 0.018 | 0.022 |
| Required Number of Units | 20 | 5 | 58 | 15 |

TABLE XV
OVER-ALL GEOMETRY AND PERFORMANCE CHARACTERISTICS
FRAME 1 SIZE CENTRIFUGAL COMPRESSORS

Power = 10,000 hp
Rotational Speed = 7,000 rpm
Inlet Pressure = 14.7 psia
Inlet Temperature = 518.7 deg R

| Configuration | Single Stage | Double Entry* | Tandem** |
|---------------------------------|--------------|---------------|----------|
| | F1-CC-S | F1-CC-D | F1-CC-T |
| Total Mass Flow Rate (lbm/sec) | 143.1 | 172.6 | 86.4 |
| Pressure Ratio, P_R | 1.882 | 1.706 | 2.580 |
| Temperature Ratio, T_R | 1.394 | 1.326 | 1.651 |
| Inducer Tip Radius (in) | 15.01 | 12.70 | 11.8 |
| Inducer Hub Radius (in) | 6.41 | 5.84 | 5.84 |
| Inducer Tip Blade Angle (deg) | -61.5 | -61.5 | -60.0 |
| Inducer Hub Blade Angle (deg) | -40.2 | -40.2 | -40.2 |
| Impeller Tip Radius (in) | 19.58 | 17.86 | 17.86 |
| Impeller Tip Width (in) | 2.97 | 2.23 | 1.90 |
| Impeller Exit Blade Angle (deg) | 0.0 | 0.0 | 0.0 |
| Diffuser Exit Radius (in) | 21.735 | 19.825 | 19.825 |
| Diffuser Exit Width (in) | 2.97 | 2.23 | 1.90 |
| Maximum Casing Radius (in) | 27.19 | 24.0 | 24.0 |

*Width correspond to one side of the unit

**The dimensions listed are for the second stage and the first stage dimensions are the same as those of one side of the double entry unit

**Based on casing thickness of 0.5 in

TABLE XVI
OVER-ALL GEOMETRY AND PERFORMANCE CHARACTERISTICS
FRAME 1 SIZE RADIAL OUTFLOW COMPRESSORS

Power = 10,000 hp
 Rotational Speed = 7,000 rpm
 Inlet Pressure = 14.7 psia
 Inlet Temperature = 518.7 deg R

| Configuration | Single Stage | Double Entry* | F1-ROC-D |
|--------------------------------|--------------|---------------|----------|
| Total Mass Flow Rate (lbm/sec) | 98.1 | 120.3 | |
| Pressure Ratio, P_2/P_1 | 1.670 | 1.498 | |
| Temperature Ratio, T_2/T_1 | 1.575 | 1.468 | |
| Rotor Inlet Radius (in) | 14.1 | 12.5 | |
| Rotor Inlet Blade Angle (deg) | -60.0 | -60.0 | |
| Rotor Exit Radius (in) | 18.6 | 16.5 | |
| Rotor Exit Width (in) | 4.78 | 3.53 | |
| Rotor Exit Blade Angle (deg) | 60.0 | 60.0 | |
| Diffuser Exit Radius (in) | 19.87 | 17.68 | |
| Diffuser Exit Width (in) | 4.78 | 3.53 | |
| Maximum Casing Radius (in) ** | 28.32 | 24.0 | |

*Widths correspond to one side of the unit

**Based on casing thickness of 0.5 in

TABLE XVIIOVER-ALL GEOMETRY AND PERFORMANCE CHARACTERISTICS
FRAME 1 SIZE 5-STAGE AXIAL COMPRESSOR -- F1-AC5-H

Power = 10,000 hp
 Rotational Speed = 7,000 rpm
 Inlet Pressure = 14.7 psia
 Inlet Temperature = 518.7 deg R
 Total Mass Flow Rate, \dot{m} = 132.6 lbm/sec
 Over-all Pressure Ratio, P_R = 2.52
 Overall Temperature Ratio, T_R = 1.425

| Station* | | Axial Coordinate (in) | Hub Radius (in) | Tip Radius (in) |
|----------|-------|--------------------------|--------------------|--------------------|
| IGV | Inlet | 0.0 | 11.472 | 17.277 |
| IGV | Exit | 3.492 | 11.472 | 16.796 |
| 1R | Exit | 6.804 | 11.472 | 16.319 |
| 1S | Exit | 8.796 | 11.472 | 16.067 |
| 2R | Exit | 12.096 | 11.472 | 15.694 |
| 2S | Exit | 14.088 | 11.472 | 15.461 |
| 3R | Exit | 16.128 | 11.472 | 15.235 |
| 3S | Exit | 18.132 | 11.472 | 15.035 |
| 4R | Exit | 20.172 | 11.472 | 14.841 |
| 4S | Exit | 22.164 | 11.472 | 14.651 |
| 5R | Exit | 24.204 | 11.472 | 14.485 |
| 5S | Exit | 26.208 | 11.472 | 14.340 |

*Exit stations are located between two blade rows; therefore, they also represent the inlet stations to the following blade row

AD-A108 356

NORTHERN RESEARCH AND ENGINEERING CORP WOBURN MA

F/6 13/7

ANALYTICAL INVESTIGATION OF AIR DYNAMOMETER CONCEPTS FOR FUTURE--ETC(U)

N68335-75-C-2098

UNCLASSIFIED

NREC-1253-1

NL

2-2
4-2
5-2

END
DATE
FILED
4-82
RTIC

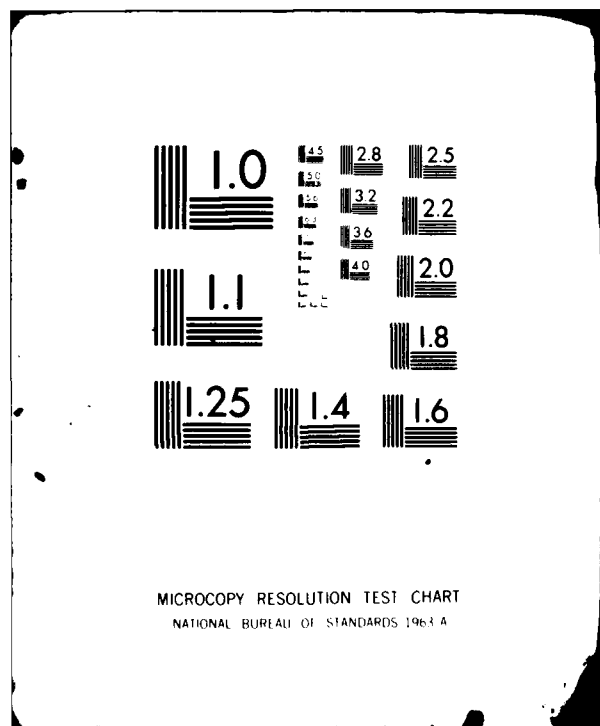


TABLE XVIII
OVER-ALL DETAILS OF DYNAMOMETERS WITH INLET AND EXIT VALVES
SINGLE-STAGE CENTRIFUGAL COMPRESSOR (CC-S)

| <u>Frame Size</u> | <u>Dynamometer</u> | <u>S_L</u> | <u>S_A</u> | <u>N_d</u> (rpm) | <u>Point</u> | <u>N/N_d</u> |
|-----------------------|--------------------|----------------------|----------------------|-------------------------------|--------------|------------------------|
| F1 | F1-1 | 1.0 | 1.0 | 7,000 | A | 1.00 |
| F2 | F2-1 | 0.891 | 1.0 | 7,860 | F | 0.891 |
| F2 | F2-2 | 0.891 | 0.76 | 7,860 | E | 0.840 |
| F2 | F2-3 | 0.891 | 0.48 | 7,860 | D | 0.840 |
| F3 | F3-1 | 0.737 | 1.0 | 9,500 | B | 1.263 |
| F3 | F3-2 | 0.737 | 0.60 | 9,500 | C | 1.263 |
| F4 | F4-1 | 0.414 | 1.0 | 16,900 | G | 1.154 |

S_L - Linear Scale Factor, L_{Fn}/L_{F1}

S_A - Relative Change in Area by Shroud Change

N_d - Equivalent Design Speed, $7,000/S_L$

N - Operating Point Speed, rpm

Note: See Figure 27 for performance envelopes of dynamometers.

TABLE XIX

OVER-ALL DETAILS OF DYNAMOMETERS WITH INLET AND EXIT VALVES
DOUBLE-ENTRY CENTRIFUGAL COMPRESSOR (CC-D)

| <u>Frame Size</u> | <u>Dynamometer</u> | <u>S_L</u> | <u>S_A</u> | <u>N_d</u> (rpm) | <u>Point</u> | <u>N/N_d</u> |
|-------------------|--------------------|----------------------|----------------------|-------------------------------|--------------|------------------------|
| F1 | F1-1 | 1.0 | 1.0 | 7,000 | A | 1.0 |
| F2 | F2-1 | 0.877 | 1.0 | 7,980 | F | 0.877 |
| F2 | F2-2 | 0.877 | 0.77 | 7,980 | E | 0.827 |
| F3 | F3-1 | 0.747 | 1.00 | 9,370 | B/D | 1.281/ 0.704 |
| F3 | F3-2 | 0.747 | 0.60 | 9,370 | C | 1.281 |
| F4 | F4-1 | 0.412 | 1.0 | 17,000 | G | 1.147 |

Note: See Table XVIII for explanation of symbols and Figure 28 for performance envelopes of dynamometers.

TABLE XX

OVER-ALL DETAILS OF DYNAMOMETERS WITH INLET AND EXIT VALVES
2-STAGE (TANDEM) CENTRIFUGAL COMPRESSOR (CC-T)

| <u>Frame Size</u> | <u>Dynamometer</u> | <u>S_L</u> | <u>S_A</u> | <u>N_d</u> (rpm) | <u>Point</u> | <u>N/N_d</u> |
|-------------------|--------------------|----------------------|----------------------|-------------------------------|--------------|------------------------|
| F1 | F1-1 | 1.0 | 1.0 | 7,000 | A | 1.0 |
| F1 | F1-2 | 1.0 | 0.6 | 7,000 | F/E | 1.0/ 0.943 |
| F2 | F2-1 | 0.768 | 1.0 | 9,120 | B/D | 1.317/ 0.724 |
| F2 | F2-2 | 0.768 | 0.588 | 9,120 | C | 1.317 |
| F3 | F3-1 | 0.408 | 1.0 | 17,160 | G | 1.136 |

Note: See Table XVIII for explanation of symbols and Figure 29 for performance envelopes of dynamometers.

TABLE XXI

OVER-ALL DETAILS OF DYNAMOMETERS WITH INLET AND EXIT VALVES
SINGLE-STAGE RADIAL OUTFLOW COMPRESSOR (ROC-S)

| <u>Frame Size</u> | <u>Dynamometer</u> | <u>S_L</u> | <u>S_A</u> | <u>N_d</u> (rpm) | <u>Point</u> | <u>N/N_d</u> |
|-----------------------|--------------------|----------------------|----------------------|-------------------------------|--------------|------------------------|
| F1 | F1-1 | 1.0 | 1.0 | 7,000 | A | 1.0 |
| F2 | F2-1 | 0.866 | 1.0 | 8,080 | F | 0.866 |
| F2 | F2-2 | 0.866 | 0.85 | 8,080 | E | 0.817 |
| F3 | F3-1 | 0.738 | 1.00 | 9,480 | B/D | 1.266/ 0.696 |
| F3 | F3-2 | 0.738 | 0.62 | 9,480 | C | 1.266 |
| F4 | F4-1 | 0.410 | 1.00 | 17,070 | G | 1.142 |

Note: See Table XVIII for explanation of symbols and Figure 30 for performance envelopes of dynamometers.

TABLE XXII

OVER-ALL DETAILS OF DYNAMOMETERS WITH INLET AND EXIT VALVES
DOUBLE-ENTRY RADIAL OUTFLOW COMPRESSOR (ROC-D)

| <u>Frame Size</u> | <u>Dynamometer</u> | <u>S_L</u> | <u>S_A</u> | <u>N_d</u> (rpm) | <u>Point</u> | <u>N/N_d</u> |
|-----------------------|--------------------|----------------------|----------------------|-------------------------------|--------------|------------------------|
| F1 | F1-1 | 1.0 | 1.0 | 7,000 | A | 1.0 |
| F2 | F2-1 | 0.860 | 1.0 | 8,140 | F | 0.86 |
| F2 | F2-2 | 0.860 | 0.90 | 8,140 | E | 0.811 |
| F3 | F3-1 | 0.738 | 1.0 | 9,480 | B/D | 1.266/ 0.696 |
| F3 | F3-2 | 0.738 | 0.65 | 9,480 | C | 1.266 |
| F4 | F4-1 | 0.408 | 1.0 | 17,160 | G | 1.137 |

Note: See Table XVIII for explanation of symbols and Figure 31 for performance envelopes of dynamometers.

TABLE XXIII
OVER-ALL DETAILS OF DYNAMOMETERS WITH INLET AND EXIT VALVES
5-STAGE CONSTANT HUB AXIAL COMPRESSOR (AC5-H)

| <u>Frame Size</u> | <u>Dynamometer</u> | <u>S_L</u> | <u>S_A</u> | <u>N_d</u> (rpm) | <u>Point</u> | <u>N/N_d</u> |
|-----------------------|--------------------|----------------------|----------------------|-------------------------------|--------------|------------------------|
| F1 | F1-1 | 1.0 | 1.0 | 7,000 | A | 1.0 |
| F2 | F2-1 | 0.875 | 1.0 | 8,000 | F | 0.875 |
| F2 | F2-2 | 0.875 | 0.760 | 8,000 | E | 0.825 |
| F2 | F2-3 | 0.875 | 0.475 | 8,000 | D | 0.825 |
| F3 | F3-1 | 0.642 | 1.839 | 10,910 | B | 1.100 |
| F3 | F3-2 | 0.642 | 1.540 | 10,910 | C | 1.100 |
| F4 | F4-1 | 0.395 | 1.222 | 17,730 | G | 1.100 |

Note: See Table XVIII for explanation of symbols and Figure 32 for performance envelopes of dynamometers.

TABLE XXIV
PHYSICAL DETAILS AND DESIGN OPERATIONAL CHARACTERISTICS OF COMPRESSOR SYSTEMS - FRAME I SIZE

Power = 10,000 hp
 Rotational Speed = 7,000 rpm
 Inlet Pressure = 14.7 psia
 Inlet Temperature = 518.7 deg R

| | Centrifugal | | | Radial Outflow Double Entry | Axial Constant Hub |
|------------------------------------|--------------|------------------|------------|-----------------------------|--------------------|
| | Single Stage | Double Entry (1) | Tandem (2) | | |
| Configuration | F1-CC-S | F1-CC-D | F1-CC-T | F1-ROC-S | F1-AC5-H |
| Total Mass Flow Rate, lbm/sec | 143.1 | 172.6 | 86.4 | 98.1 | 120.3 |
| Pressure Ratio, P_R | 1.882 | 1.706 | 2.580 | 1.67 | 1.498 |
| Temperature Ratio, T_R | 1.394 | 1.326 | 1.651 | 1.575 | 1.468 |
| Number of Stages | 1 | 1 | 2 | 1 | 5 |
| Design Maximum Blade Speed, ft/sec | 1196 | 1091 | 1091 | 1136 | 1007 |
| Rotor Inlet Tip Diameter, in | 30.02 | 25.4 | 23.6 | 28.2 | 25.0 |
| Rotor Exit Tip Diameter, in | 12.82 | 11.68 | 11.68 | 28.2 | 25.0 |
| Rotor Exit Width (Hub Dia), in | 39.16 | 35.72 | 35.72 | 37.2 | 33.0 |
| Diffuser Exit Tip Diameter, in | 2.97 | 2.23 | 1.90 | 4.78 | 3.53 |
| Diffuser Exit Width (Hub Dia), in | 43.47 | 39.65 | 39.65 | 39.74 | 35.36 |
| Maximum Casing Diameter, in | 2.97 | 2.23 | 1.90 | 4.78 | 3.53 |
| Total Weight, lbm | 1330 (3) | 2020 (3) | 2020 | 1360 (4) | 1970 |

(1) Widths correspond to one side of the unit

(2) The dimensions correspond to the second stage and the first stage dimensions are the same as those of one side of the double entry unit

(3) Estimates based on calculated weight of tandem unit

(4) Estimates based on calculated weight of double entry unit

(5) Estimates based on calculated weight of a 5-stage unit sized for Point B (10,000 hp, 12,000 rpm)

TABLE XXV
ACHIEVABLE RANGE WITH INLET AND EXIT VALVES AND VARIABLE GEOMETRY

| Configuration | Centrifugal | | | Radial Outflow | Axial Constant Hub |
|--|---------------------|---------------------|---------------------|---------------------|---------------------|
| | <u>Single Stage</u> | <u>Double Entry</u> | <u>Tandem Unit</u> | <u>Single Stage</u> | <u>Double Entry</u> |
| F1-CC-S | F1-CC-D | F1-CC-T | F1-ROC-S | F1-ROC-D | F1-AC5-H |
| Maximum Range with Exit Valve | 1.268 | 1.482 | 1.367 | 1.487 | 1.737 |
| Nominal Range with Inlet Valve ^{**} | 1.957 | 1.769 | 2.741 | 1.952 | 1.706 |
| Maximum Range with Inlet and Exit Valves | 2.481 | 2.621 | 3.747 | 2.902 | 2.963 |
| Maximum Range with Variable Vanes and Exit Valve | 3.01 ^{***} | 3.18 | 4.42 ^{***} | 3.52 ^{***} | 3.59 ^{***} |
| Potential Range with Variable Shroud | NA | NA | NA | 10-20 | 10-20 |
| Required Number of Frame Sizes with Inlet and Exit Valves | 4 | 4 | 3 | 4 | 4 |
| Required Number of Dynamometers with Inlet and Exit Valves | 7 | 6 | 5 | 6 | 7 |

NA=Not applicable

*Nominal range with inlet valve is taken to be the pressure ratio at surge point

**Based on the analysis of double-entry configuration

***Includes throttling with VIGV

TABLE XXVI

OVER-ALL DETAILS OF TANDEM CENTRIFUGAL DYNAMOMETERS
WITH VIGV-THROTTLE AND EXIT VALVE

| <u>Frame Size</u> | <u>Dynamometer</u> | <u>S_L</u> | <u>S_A</u> | <u>N_d</u> (rpm) | <u>Point</u> | <u>N/N_d</u> |
|-----------------------|--------------------|----------------------|----------------------|-------------------------------|--------------|------------------------|
| F1 | F1-1 | 1.0 | 1.0 | 7,000 | A/E | 1.0/0.943 |
| F1 | F1-2 | 1.0 | 0.6 | 7,000 | F/E | 1.0/0.943 |
| F2 | F2-1 | 0.768 | 1.0 | 9,120 | B&C/D | 1.317/0.724 |
| F3 | F3-1 | 0.408 | 1.0 | 17,160 | G | 1.136 |

Note: See Table XVIII for explanation of symbols and Figure 40 for performance envelopes of dynamometers.

TABLE XXVII
OVER-ALL DETAILS OF RADIAL OUTFLOW DYNAMOMETERS
WITH VARIABLE SHROUD

| <u>Frame Size</u> | <u>Dynamometer</u> | <u>S_L</u> | <u>S_A</u> | <u>N_d</u> (rpm) | <u>Point</u> | <u>N/N_d</u> |
|-------------------|--------------------|----------------------|----------------------|-------------------------------|--------------|------------------------|
| F1 | F1-1 | 1.0 | 1.0 | 7,000 | A&F/E | 1.0/0.943 |
| F2 | F2-1 | 0.74 | 1.0 | 9,460 | B&C/D | 1.268/0.698 |
| F3 | F3-1 | 0.414 | 1.0 | 16,900 | G | 1.154 |

Note: See Table XVIII for explanation of symbols and Figure 41 for performance envelopes of dynamometers.

TABLE XXVIII
WEIGHT OF CONTROL SYSTEMS WITH INLET AND EXIT VALVES

Power = 10,000 hp
 Rotational Speed = 7,000 rpm
 Inlet Pressure = 14.7 psia
 Inlet Temperature = 518.7 deg R

| Configuration | Centrifugal | | | Radial Outflow Double Entry | Axial 5-Stage |
|---|--------------|--------------|----------|--------------------------------|------------------|
| | Single Stage | Double Entry | Tandem | | |
| F1-CC-S | F1-CC-D | F1-CC-T | F1-ROC-S | F1-ROC-D | F1-AC5-H |
| Mass Flow Rate, \dot{m} (lbm/sec) | 143.1 | 172.6 | 86.4 | 98.1 | 120.3 |
| Pressure Ratio, P_R | 1.882 | 1.706 | 2.580 | 1.670 | 1.498 |
| Temperature Ratio, T_R | 1.394 | 1.326 | 1.651 | 1.575 | 1.468 |
| Inlet Valve Diameter, D_{vi} (in) | 30.02 | 25.4 | 25.4 | 28.2 | 25.0 |
| Exit Valve Diameter, D_{ve} (in) | 39.16 | 35.72 | 35.72 | 37.2 | 33.0 |
| Weight of Control System with Inlet and Exit Valves, W_C (lbm) | 187 | 180 | 128 | 113 | 107 |
| | | | | | 198 |

TABLE XXIX

RESULTS OF MECHANICAL DESIGN AND
ANALYSIS OF THREE SELECTED COMPRESSOR SYSTEMS

| | <u>Tandem Centrifugal</u> <u>(F1-CC-T)</u> | <u>Single-Stage Radial Outflow</u> <u>(F1-ROC-S)</u> | <u>5-Stage Axial</u> <u>(F1-AC5-H)</u> |
|--|---|---|---|
| Rotor System Weight without Shaft (lbm) | 1,220 | 670 | 545 |
| Rotor System Weight with Steel Shaft (lbm) | 1,670 | 1,050 | 780 |
| Compressor System Weight (lbm) | 4,130 | 3,870 | 2,780 |
| Cost Per Unit (Dollars) | 39,500 | 41,400 | 32,100 |
| Maximum Disk Tangential Stress (psi) | 35,900 | 39,000 | 24,900 |
| Blade Root Stress (psi) | 29,900 | 41,900 | 22,300 |
| Number of Parts | 72 | 64 | 318 |
| Number of Drawings | 48 | 52 | 58 |
| Man-Hours for Design, Details, and Checking | 1,592 | 1,672 | 1,936 |

TABLE XXX
RATING OF THREE SELECTED COMPRESSOR SYSTEMS

| | Tandem Centrifugal (VIGV&Inlet Valve) | Single-Stage Radial Outflow (Variable Shroud) | 5-Stage Axial (Inlet&Exit Valves) |
|-----------------------------------|---|---|---|
| <u>Applicability</u> (Total) | (14.1) | (22) | (9.5) |
| Number of Units | 8.3 | 10 | 5.4 |
| Power Range | 4.6 | 10 | 3.0 |
| Direction of Rotation | 1.2 | 2 | 1.1 |
| <u>Controllability</u> (Total) | (9.8) | (16) | (7.6) |
| Torque Gain | 2 | 4 | 2 |
| Number of Control Functions | 1 | 3 | 1 |
| Friction Source Level | 3 | 2 | 2 |
| Polar Moment of Inertia | 1.8 | 3 | 1.6 |
| Limit Functions | 2 | 4 | 1 |
| <u>Cost Effectiveness</u> (Total) | (7.3) | (12) | (8.5) |
| First Cost | 2.3 | 7 | 3.5 |
| Scheduled Maintenance | 2 | 2 | 2 |
| Mean Time to Failure | 2 | 1 | 2 |
| Life | 1 | 2 | 1 |
| <u>Configuration</u> (Total) | (8.9) | (10) | (9.1) |
| Weight | 2.5 | 3 | 3.1 |
| Diameter | 3.2 | 3 | 3.9 |
| Length | 1.2 | 2 | 1.1 |
| Ducting Complexity | 2 | 2 | 1 |
| <u>Safety</u> (Total) | (7.4) | (7) | (5.6) |
| Rotor Stress Levels | 2.4 | 2 | 3.6 |
| Rotor System Complexity | 2 | 3 | 1 |
| Debris Sensitivity | 3 | 2 | 1 |
| <u>Environmental</u> (Total) | (4) | (6) | (2) |
| Noise Level | 2 | 3 | 1 |
| Vibration | 2 | 3 | 1 |
| Over-All Rating | 51.5 | 73 | 42.3 |
| Percentage Over-All Rating | 70.5 | 100 | 57.9 |

* Includes inlet throttling by variable inlet guide vanes.

TABLE XXXICOMPARISON OF COST AND MECHANICAL DESIGN DETAILS
OF SINGLE-STAGE AND DOUBLE-ENTRY ROC CONFIGURATIONS

| <u>Configuration</u> | <u>Single-Stage</u> | <u>Double-Entry</u> |
|--------------------------------------|---------------------|---------------------|
| | FI-ROC-S | FI-ROC-D |
| Rotor System Weight (lbm) | 670 | 480 |
| Compressor System Weight (lbm) | 2,860 | 2,860 |
| Cost Per Unit (Dollars) | 41,400 | 29,700 |
| Maximum Disk Tangential Stress (psi) | 19,500* | 15,300* |
| Maximum Blade Root Stress (psi) | 41,900 | 22,800 |
| Maximum Diameter (in) | 63.2** | 56 |
| Maximum Length (in) | 39 | 39 |

*Integral Shaft Design

**Scaled from double-entry value based on rotor exit tip diameters

TABLE XXXII

OVER-ALL DETAILS OF DYNAMOMETERS WITH INLET AND EXIT VALVES
10-STAGE CONSTANT-HUB AXIAL COMPRESSOR (AC10-H)

| <u>Frame Size</u> | <u>Dynamometer</u> | <u>S_L</u> | <u>S_A</u> | <u>N_d</u> (rpm) | <u>Point</u> | <u>N/N_d</u> |
|-----------------------|--------------------|----------------------|----------------------|-------------------------------|--------------|------------------------|
| F1 | F1-1 | 1.0 | 1.0 | 7,000 | A & F | 1.0 |
| F1 | F1-2 | 1.0 | 0.5 | 7,000 | E & D | 0.943 |
| F2 | F2-1 | 0.75 | 1.0 | 9,330 | B & C | 1.286 |
| F3 | F3-1 | 0.41 | 1.0 | 17,070 | G | 1.142 |

Note: See Table XVIII for explanation of symbols and Figure 48 for performance envelopes of dynamometers.

TABLE XXXIIICOMPARISON OF COST AND MECHANICAL DESIGN DETAILS
OF 5-STAGE AND 10-STAGE AXIAL COMPRESSORS

| Configuration | <u>5-Stage</u> | <u>10-Stage</u> |
|--------------------------------------|----------------|-----------------|
| F1-AC5-H | F1-AC10-H | |
| Rotor System Weight (lbm) | 680 | 545 |
| Compressor System Weight (lbm) | 2,780 | 3,320 |
| Cost Per Unit (Dollars) | 32,100 | 40,100 |
| Maximum Disk Tangential Stress (psi) | 24,900 | 18,200 |
| Maximum Blade Root Stress (psi) | 22,300 | 16,300 |
| Maximum Diameter (in) | 44.0 | 37.6 |
| Maximum Length (in) | 73 | 91 |

TABLE XXXIV
FINAL RATING OF FIVE COMPRESSOR SYSTEMS

| | <u>2-Stage Tandem Centrifugal (VIGV-Throttle & Exit Valve)</u> | <u>Single-Stage Radial Outflow (Variable Shroud)</u> | <u>Double-Entry Radial Outflow (Variable Shroud)</u> | <u>5-Stage Axial (Inlet&Exit Valves)</u> | <u>10-Stage Axial (Inlet&Exit Valves)</u> |
|----------------------------|--|--|--|--|---|
| Applicability | 14.1 | 22.0 | 22.0 | 9.5 | 15.3 |
| Controllability | 9.8 | 16.0 | 17.3 | 7.6 | 7.8 |
| Cost Effectiveness | 7.3 | 12.0 | 14.8 | 8.5 | 9.1 |
| Configuration | 8.9 | 10.0 | 10.4 | 9.1 | 9.0 |
| Safety | 7.4 | 7.0 | 8.1 | 5.6 | 6.7 |
| Environmental | 4 | 6 | 6 | 2 | 2 |
| Over-All Rating | 51.5 | 73.0 | 78.6 | 42.3 | 49.9 |
| Percentage Over-All Rating | 70.5 | 100 | 107.7 | 57.9 | 68.4 |

TABLE XXXV
OVER-ALL DIMENSIONS, STRESS LEVELS, AND ESTIMATED WEIGHT OF DYNAMOMETERS
SINGLE-STAGE RADIAL OUTFLOW COMPRESSOR WITH VARIABLE SHROUD

| | <u>Frame 1</u> | <u>Frame 2</u> | <u>Frame 3</u> |
|---|----------------|----------------|----------------|
| Linear Scale Factor, s_L | 1.0 | 0.74 | 0.414 |
| Over-All Diameter (in) | 56.0 | 41.4 | 23.2 |
| Rotor Tip Diameter (in) | 29.0 | 21.5 | 12.0 |
| Over-All Length (in) | 39.0 | 21.8 | 16.1 |
| Rotor System Weight (lbm) | 480 | 226 | 53 |
| Compressor System Weight, w^* (lbm) | 2,860 | 1,350 | 315 |
| Critical Operating Point, X_{cr} | A | B | G |
| Rotational Speed at X_{cr} (rpm) | 7,000 | 12,000 | 19,500 |
| Horsepower at X_{cr} | 10,000 | 10,000 | 2,500 |
| Maximum Disk Tangential Stress at X_{cr} (psi) | 15,300 | 24,600 | 20,400 |
| Blade Root Stress at X_{cr} (psi) | 22,800 | 36,700 | 30,400 |

 $*w \propto s_L^{2.5}$

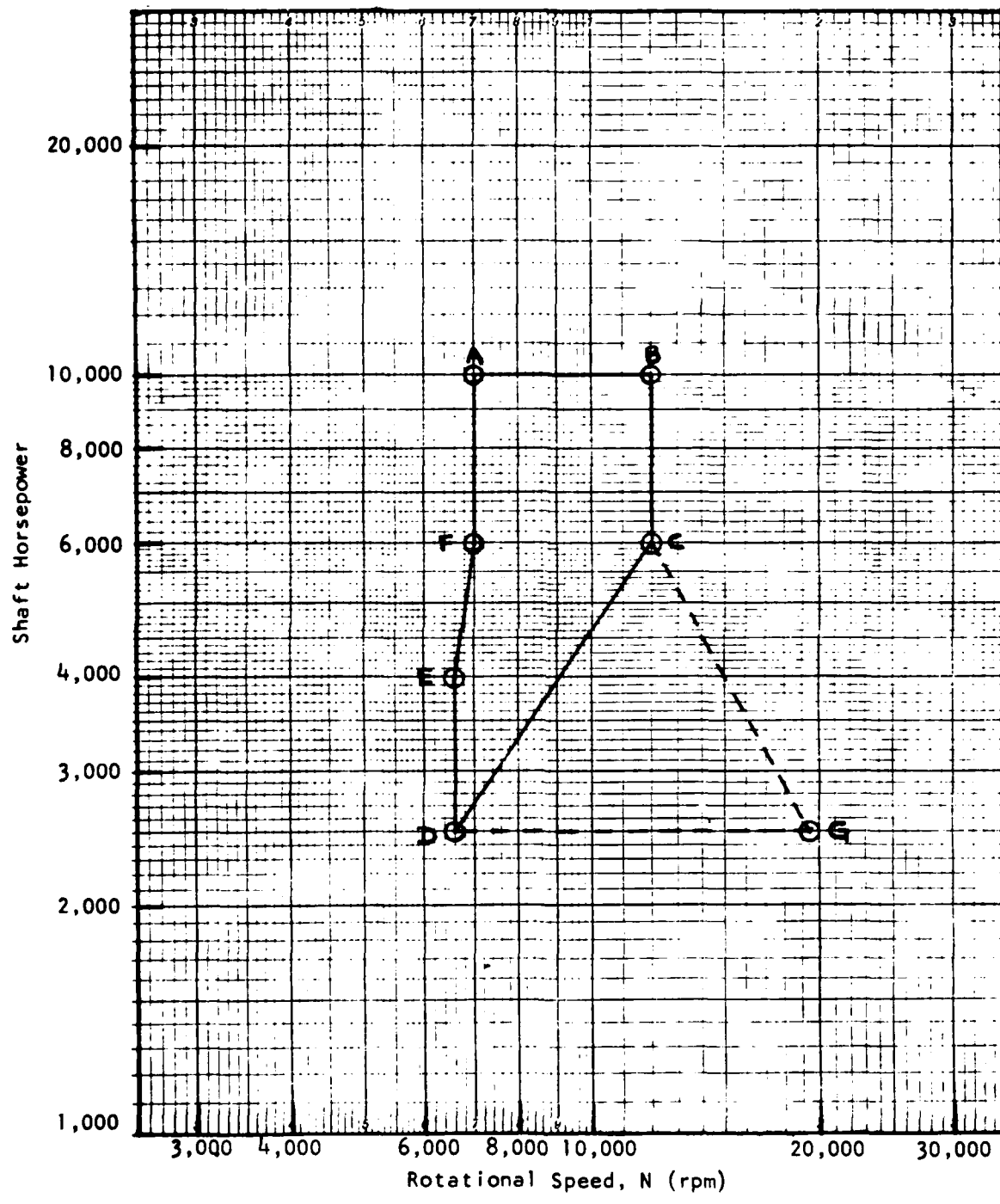


FIGURE 1 - ENVELOPE OF OPERATION

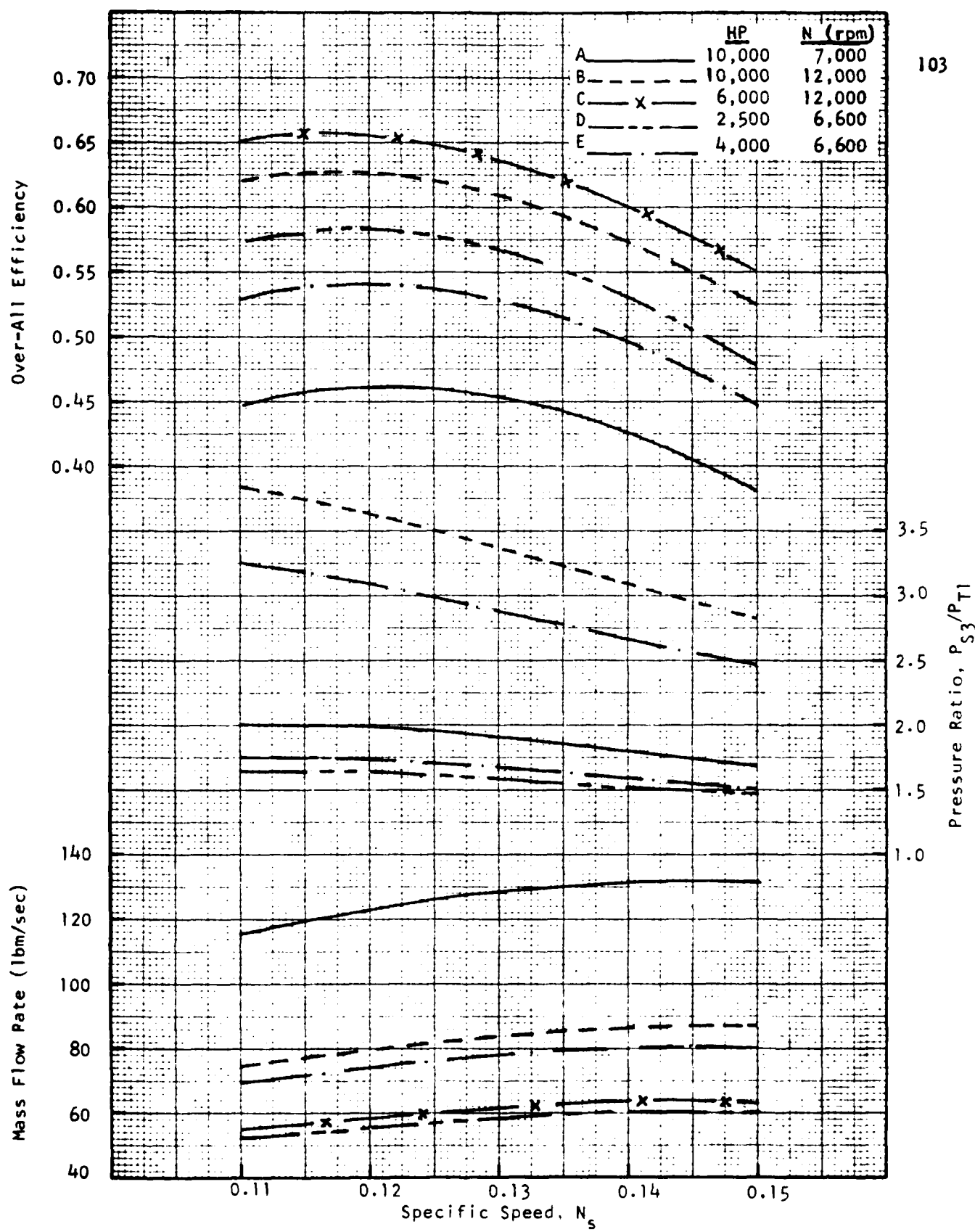


FIGURE 2 - EFFECT OF SPECIFIC SPEED ON FLOW RATE, PRESSURE RATIO AND EFFICIENCY FOR A SINGLE STAGE CENTRIFUGAL COMPRESSOR

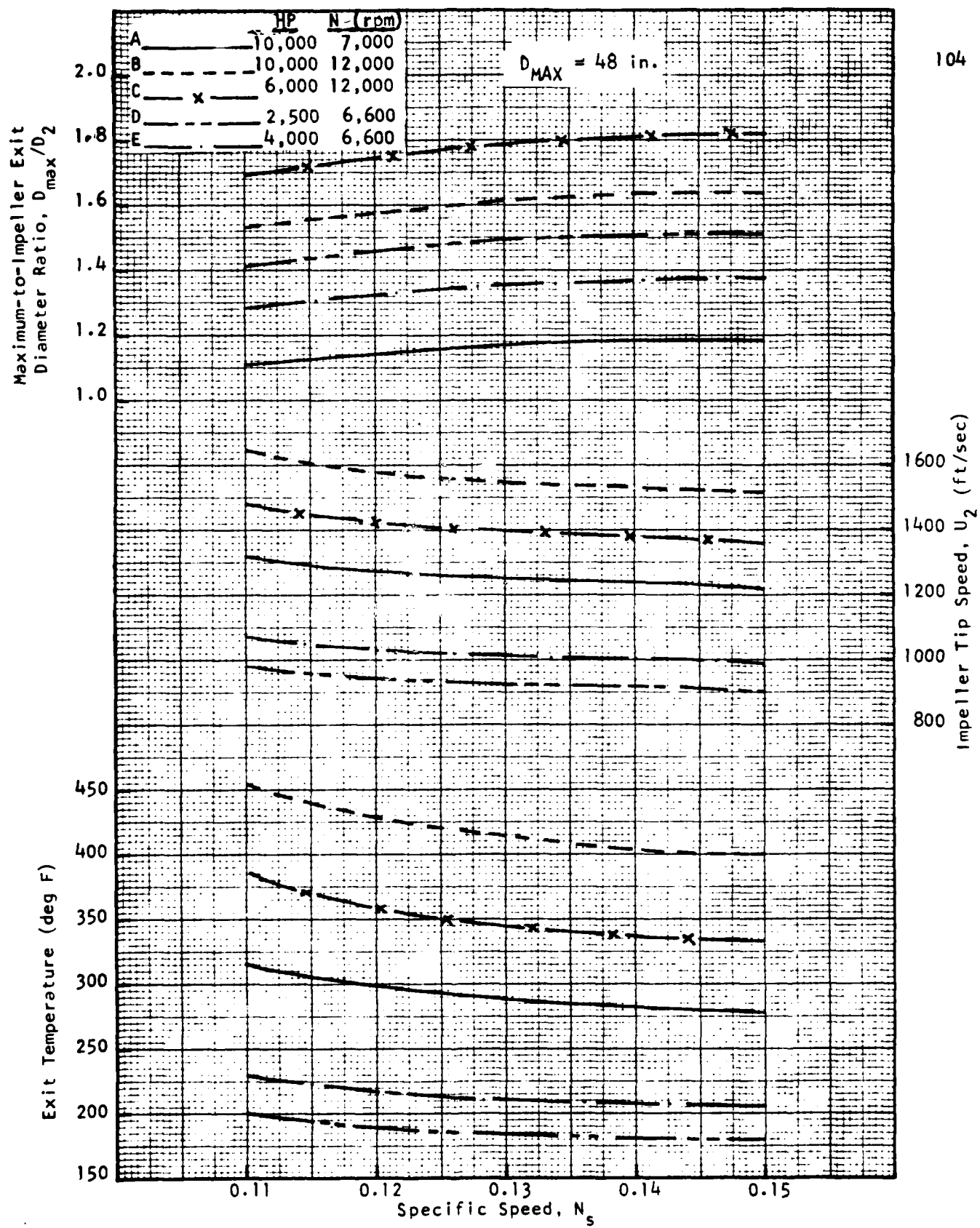


FIGURE 3 - EFFECT OF SPECIFIC SPEED ON EXIT TEMPERATURE, TIP SPEED, AND MAXIMUM-TO-IMPELLER EXIT DIAMETER RATIO FOR A SINGLE STAGE CENTRIFUGAL COMPRESSOR

Absolute Mach Number
at Diffuser Exit, M_3

Rotor and Diffuser Exit
Diameters, D_2 and D_3 (in)

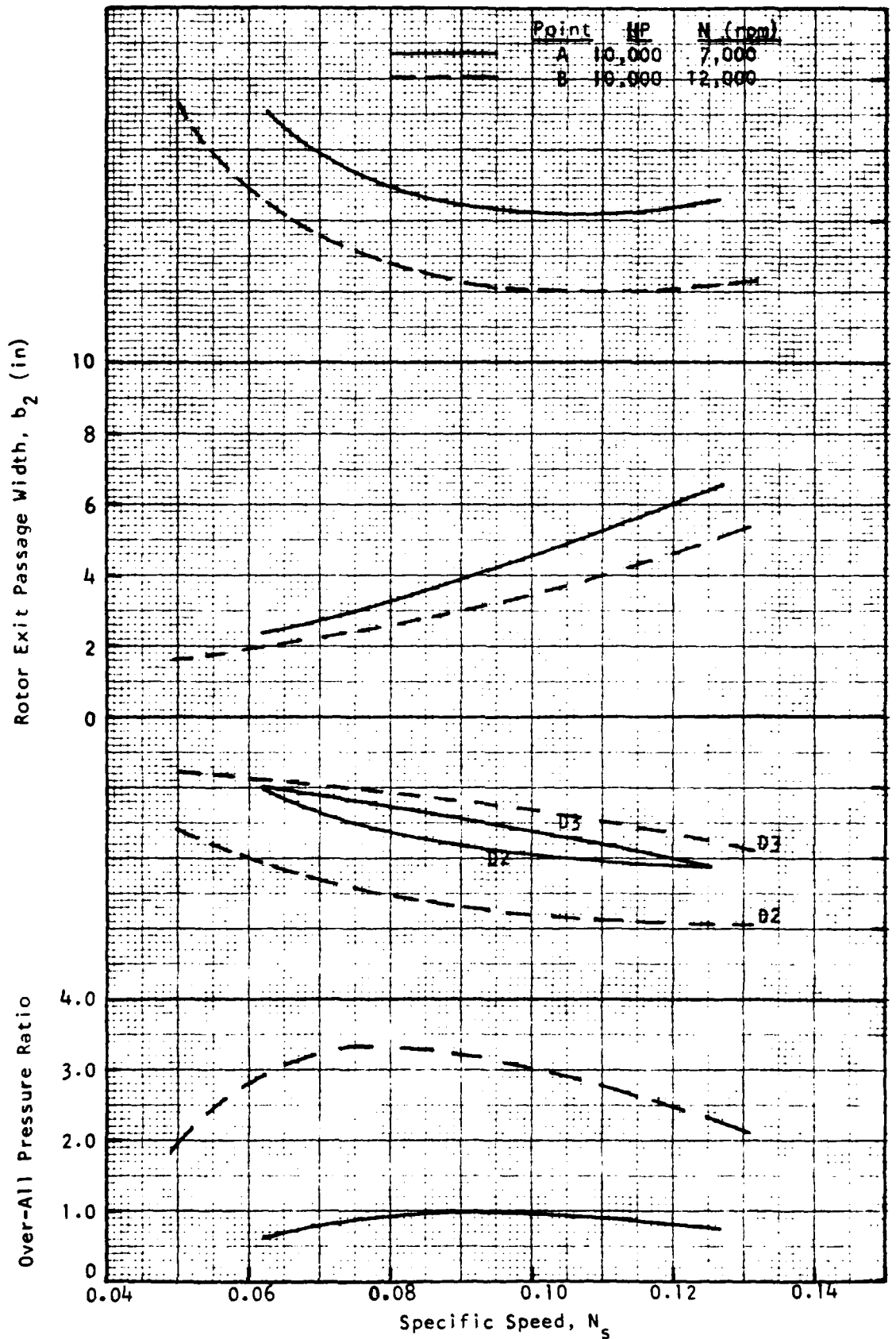


FIGURE 4 - EFFECT OF SPECIFIC SPEED ON OVER-ALL PRESSURE RATIO, OVER-ALL DIMENSIONS, AND EXIT MACH NUMBER - SINGLE STAGE RADIAL OUTFLOW COMPRESSOR

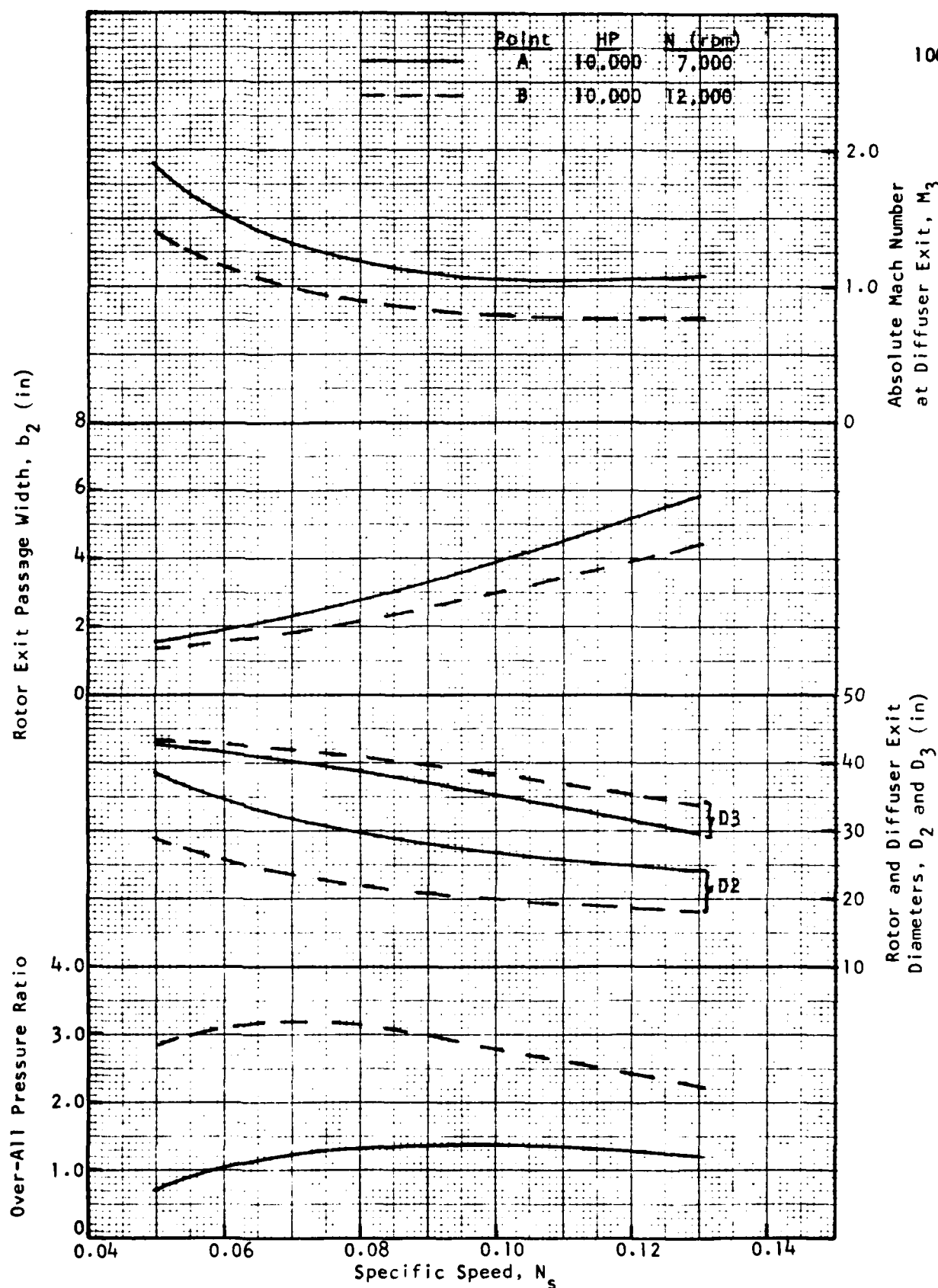


FIGURE 5 - EFFECT OF SPECIFIC SPEED ON OVER-ALL PRESSURE RATIO, OVER-ALL DIMENSIONS, AND EXIT MACH NUMBER - DOUBLE ENTRY RADIAL OUTFLOW COMPRESSOR

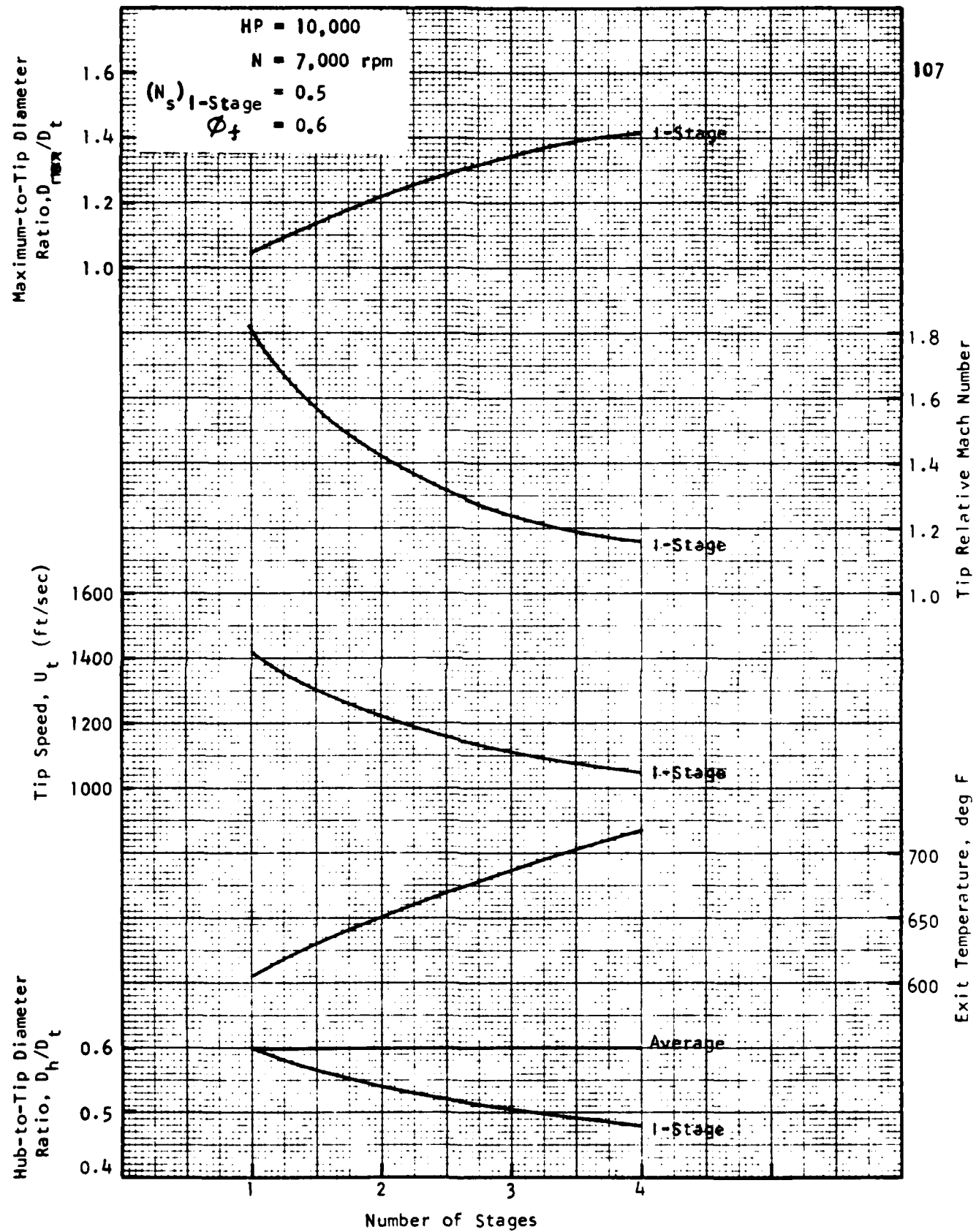


FIGURE 6 - EFFECT OF NUMBER OF STAGES ON VARIOUS MEAN STAGE-DESIGN QUANTITIES -
 AXIAL COMPRESSOR FOR POINT A

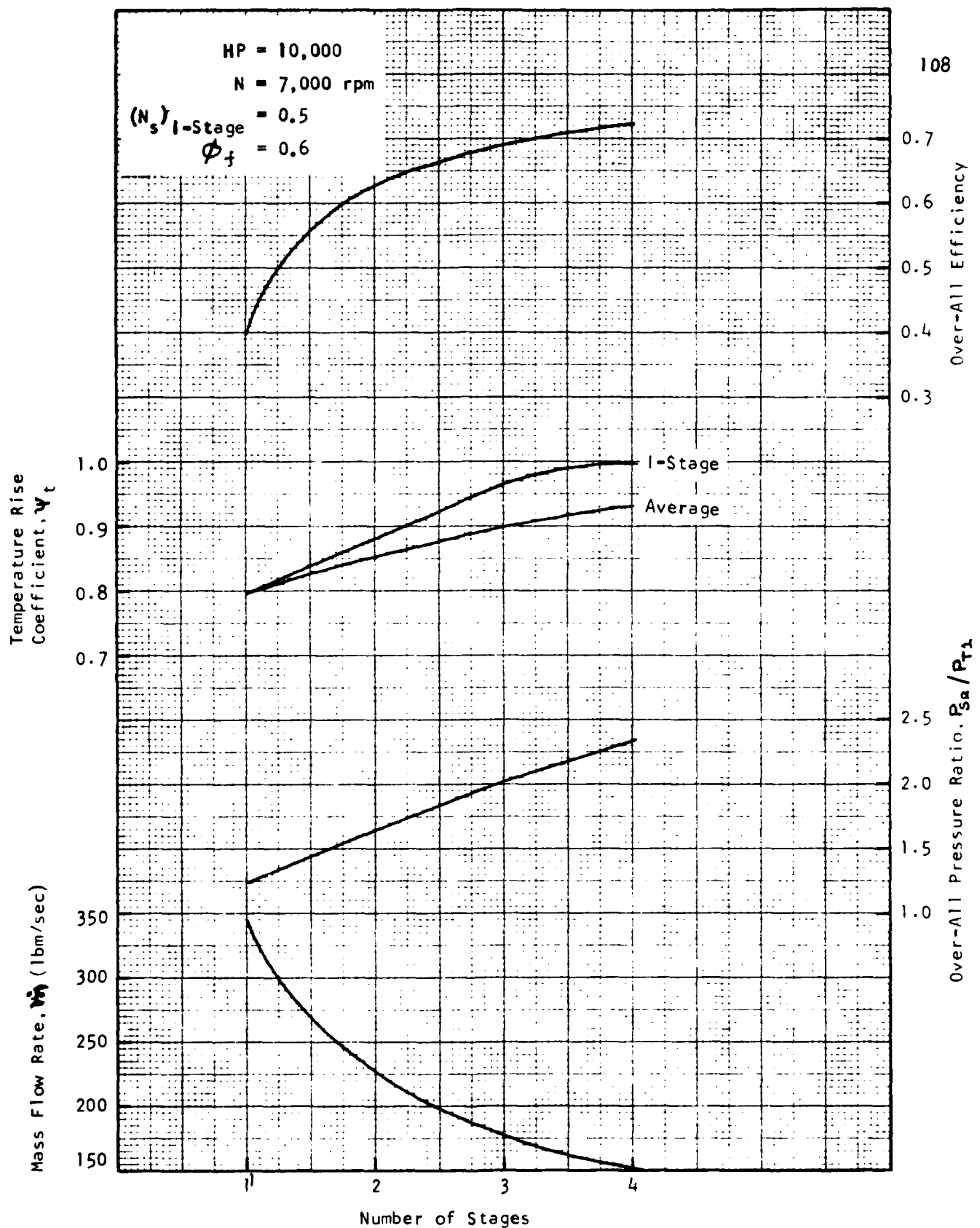


FIGURE 7 - EFFECT OF NUMBER OF STAGES ON VARIOUS MEAN STAGE-DESIGN QUANTITIES - AXIAL COMPRESSOR FOR POINT A

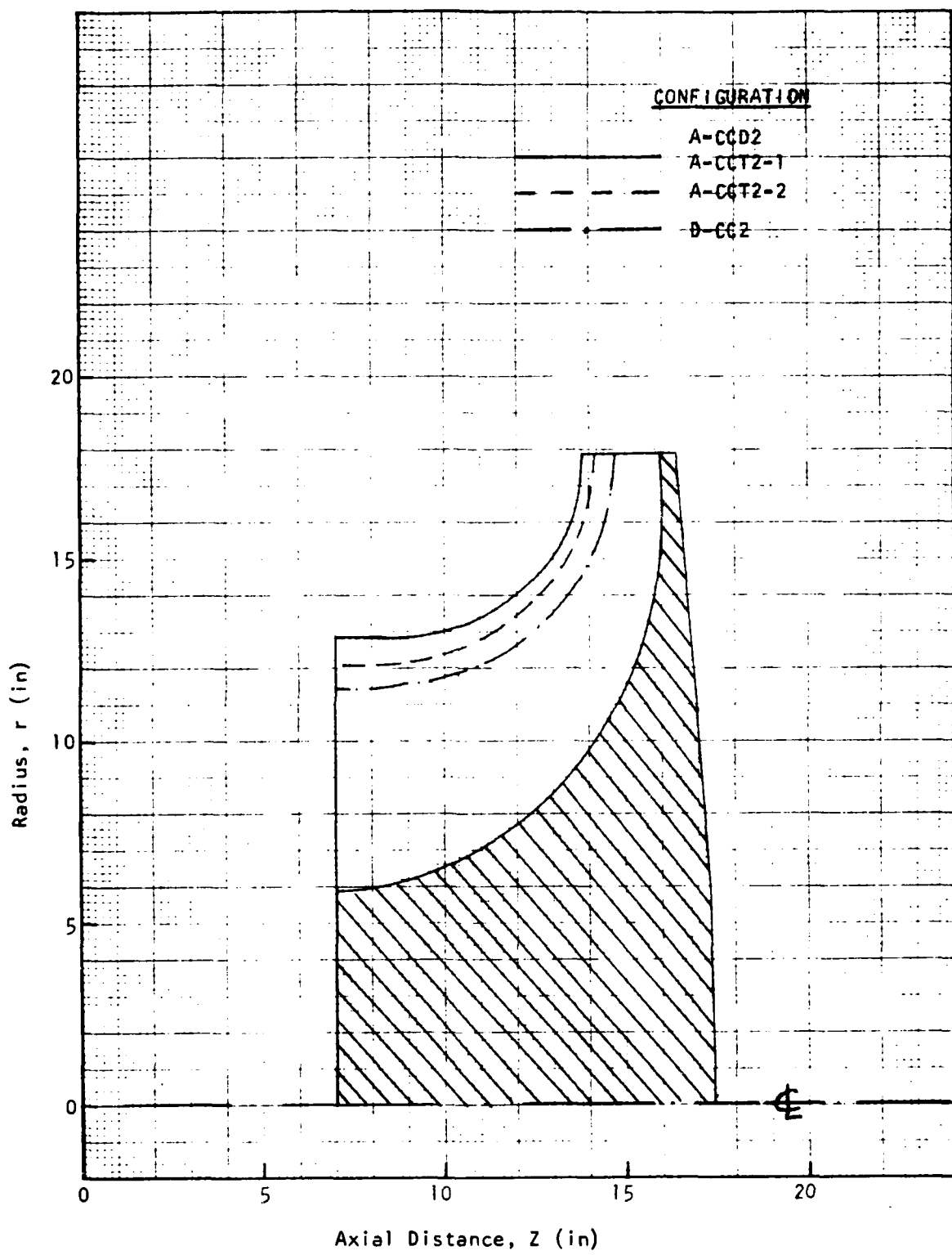


FIGURE 8 - ILLUSTRATION OF SHROUD-CUTS

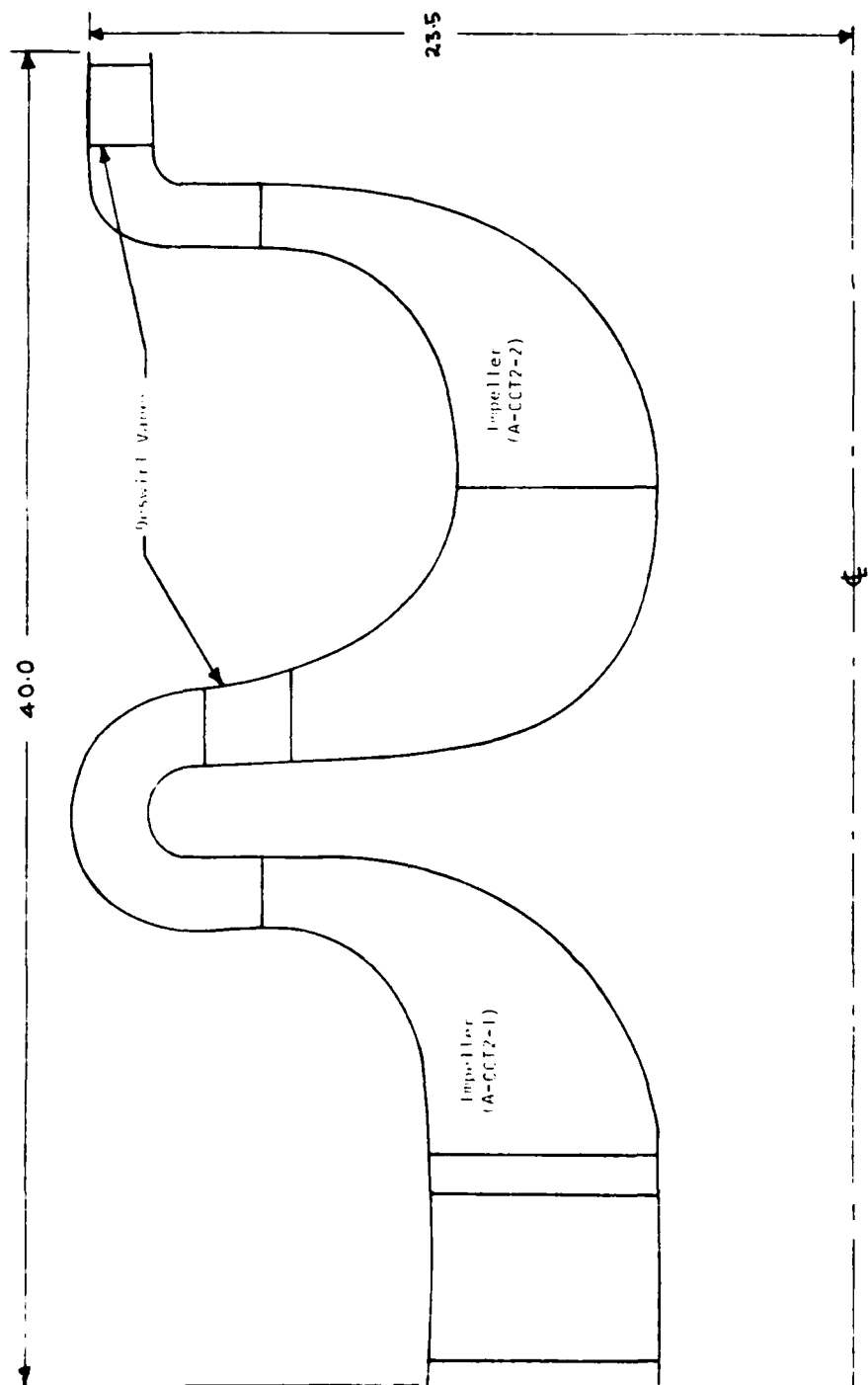


FIGURE 9 FLOW PATH OF TANDEM CENTRIFUGAL COMPRESSOR
FOR POINT A - CONFIGURATION A-CCT2

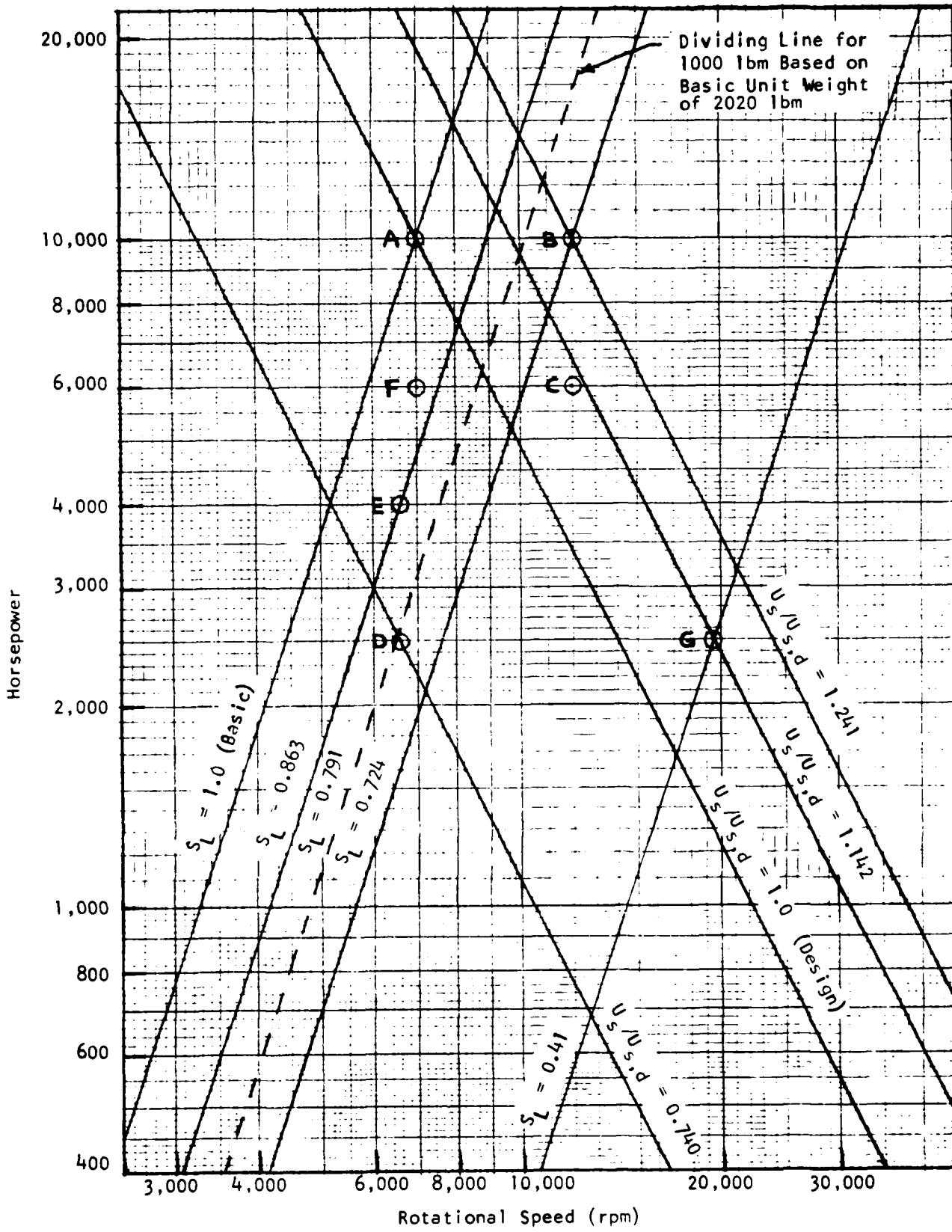


FIGURE 10 - POWER-SPEED CHARACTERISTICS OF VARIOUS SCALED UNITS

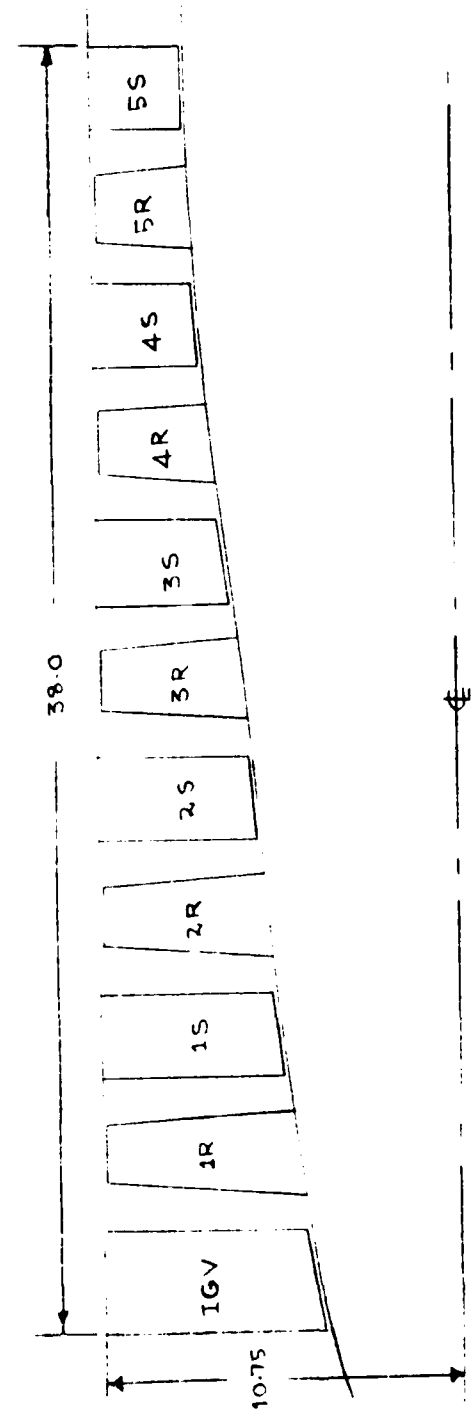


FIGURE 11 - FLOW PATH OF 5-STAGE AXIAL COMPRESSOR FOR
POINT B - CONFIGURATION B-AC51

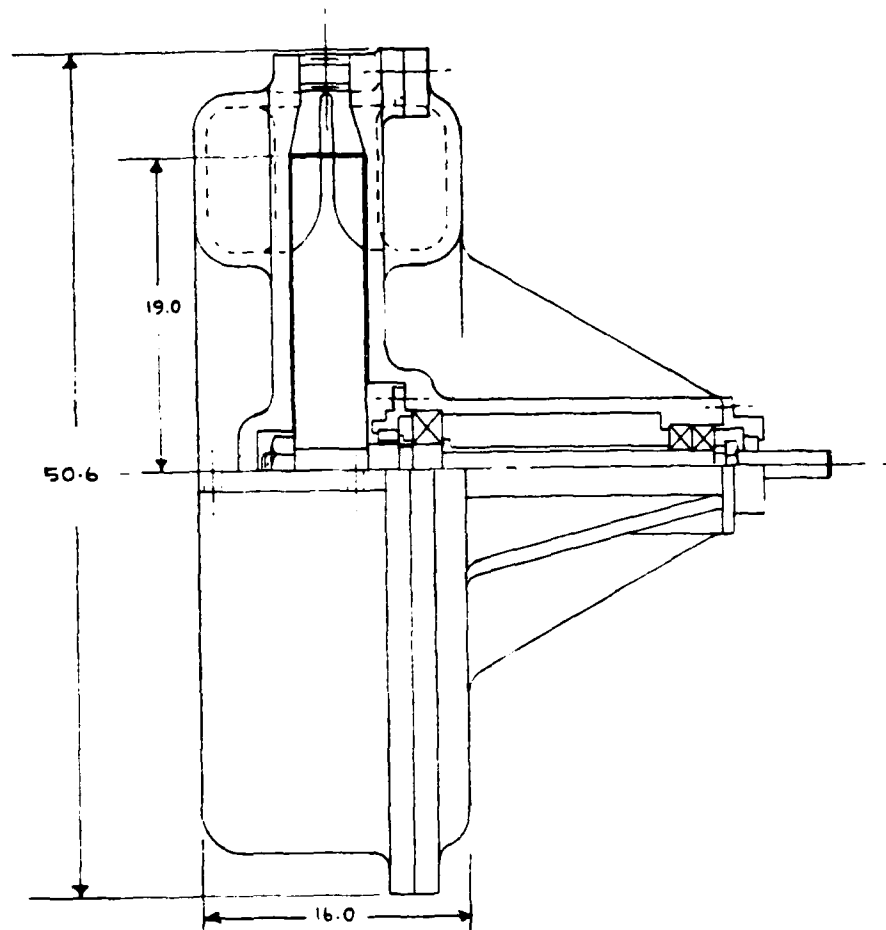


FIGURE 12 - A DRAG COMPRESSOR UNIT SIZED FOR
POINT A - CONFIGURATION A-DC2

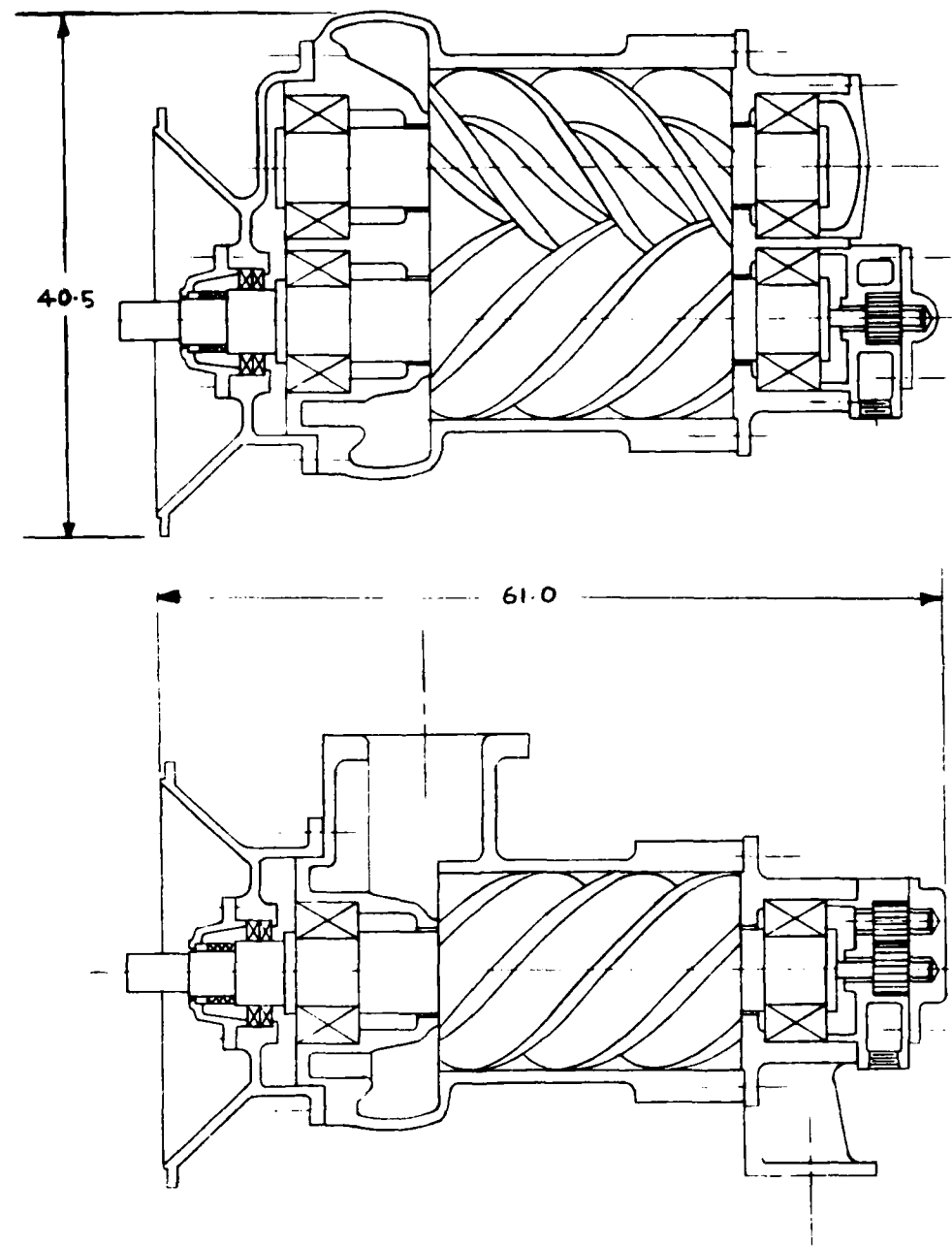


FIGURE 13 - A HELICAL SCREW COMPRESSOR SIZED FOR
POINT A - CONFIGURATION A-HS2

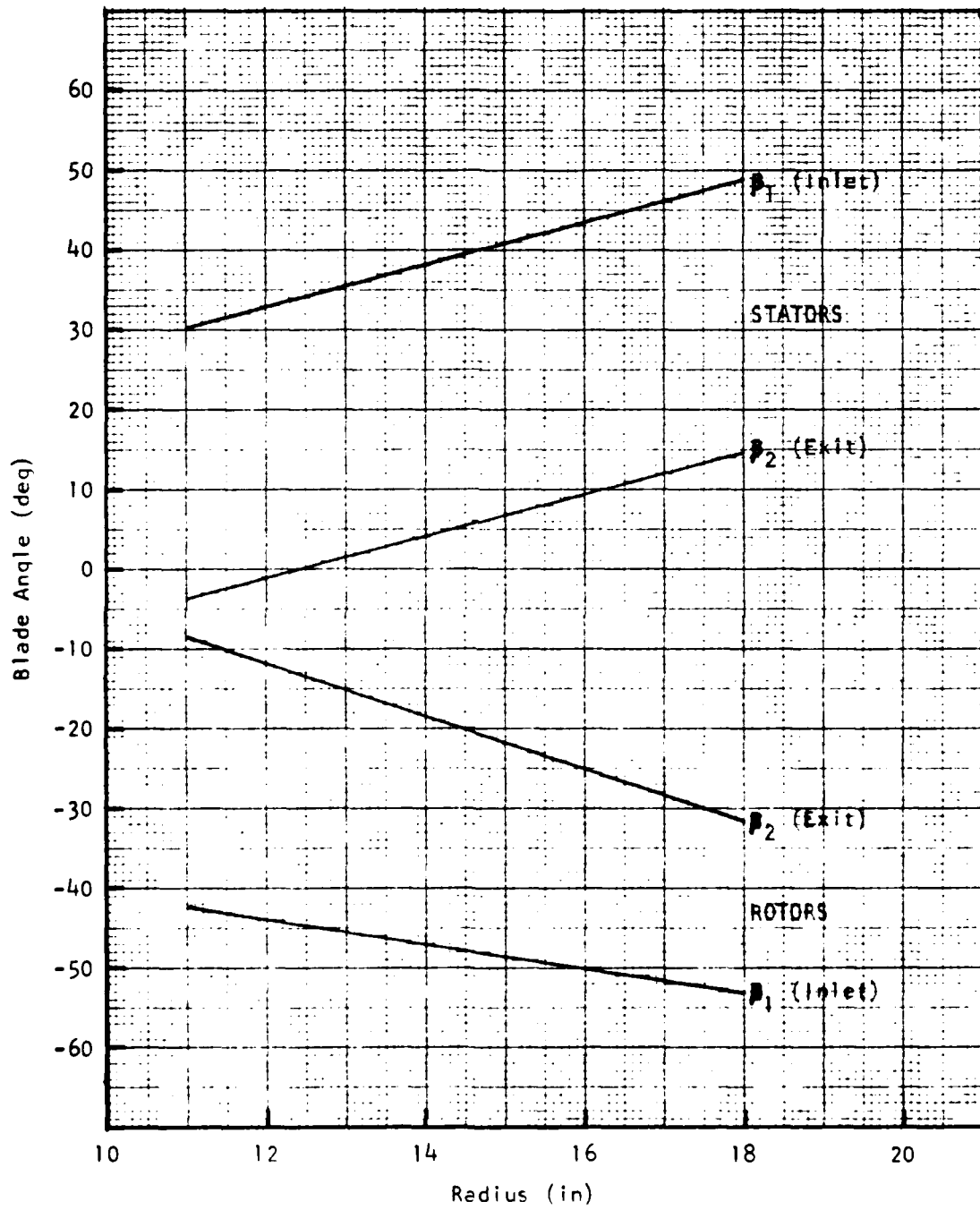


FIGURE 14 - RADIAL VARIATION OF BLADE ANGLES FOR
FRAME 1 SIZE AXIAL COMPRESSOR -- F1-AC5-H

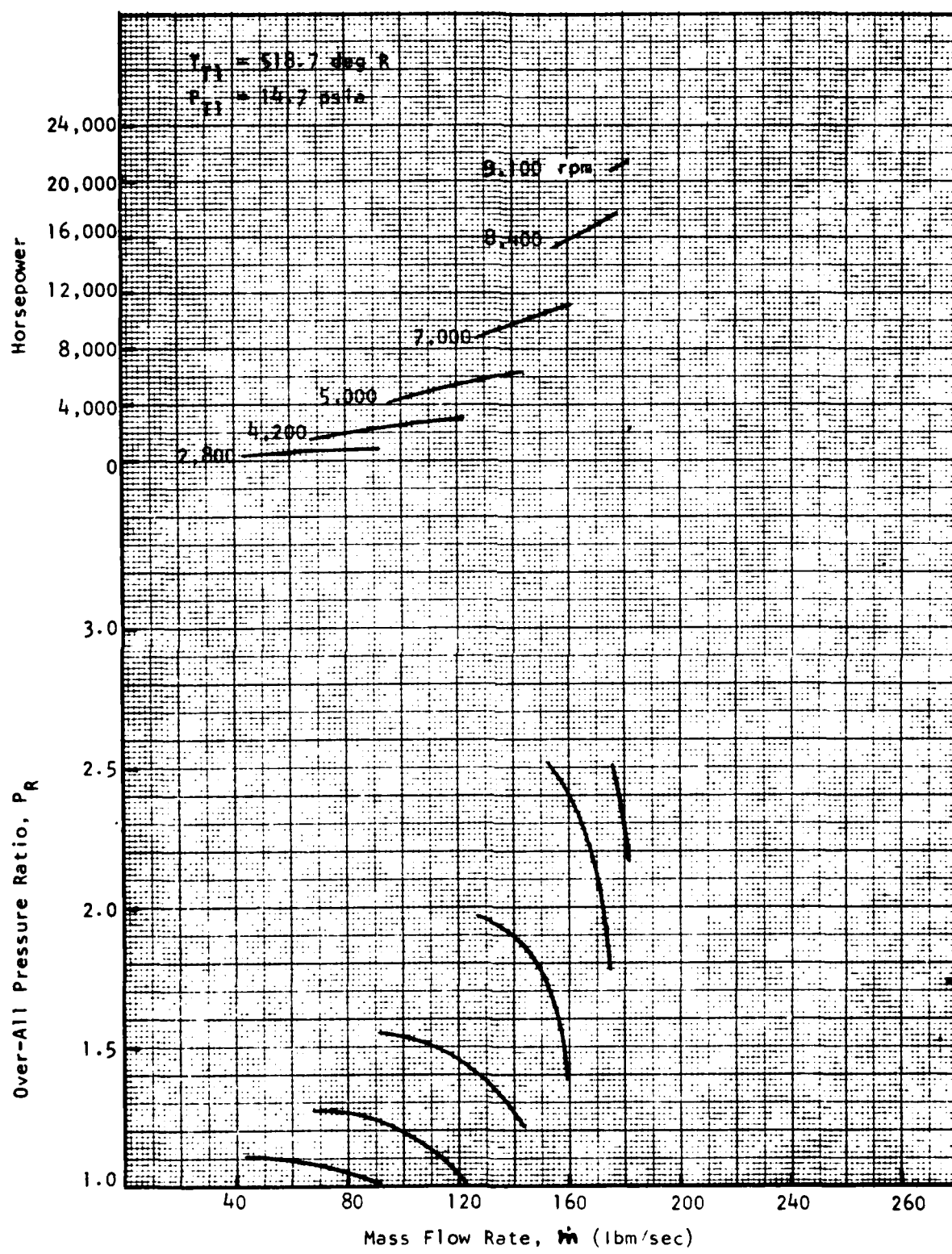


FIGURE 15 - PERFORMANCE CHARACTERISTICS OF SINGLE-STAGE
CENTRIFUGAL COMPRESSOR -- F1-CC-S

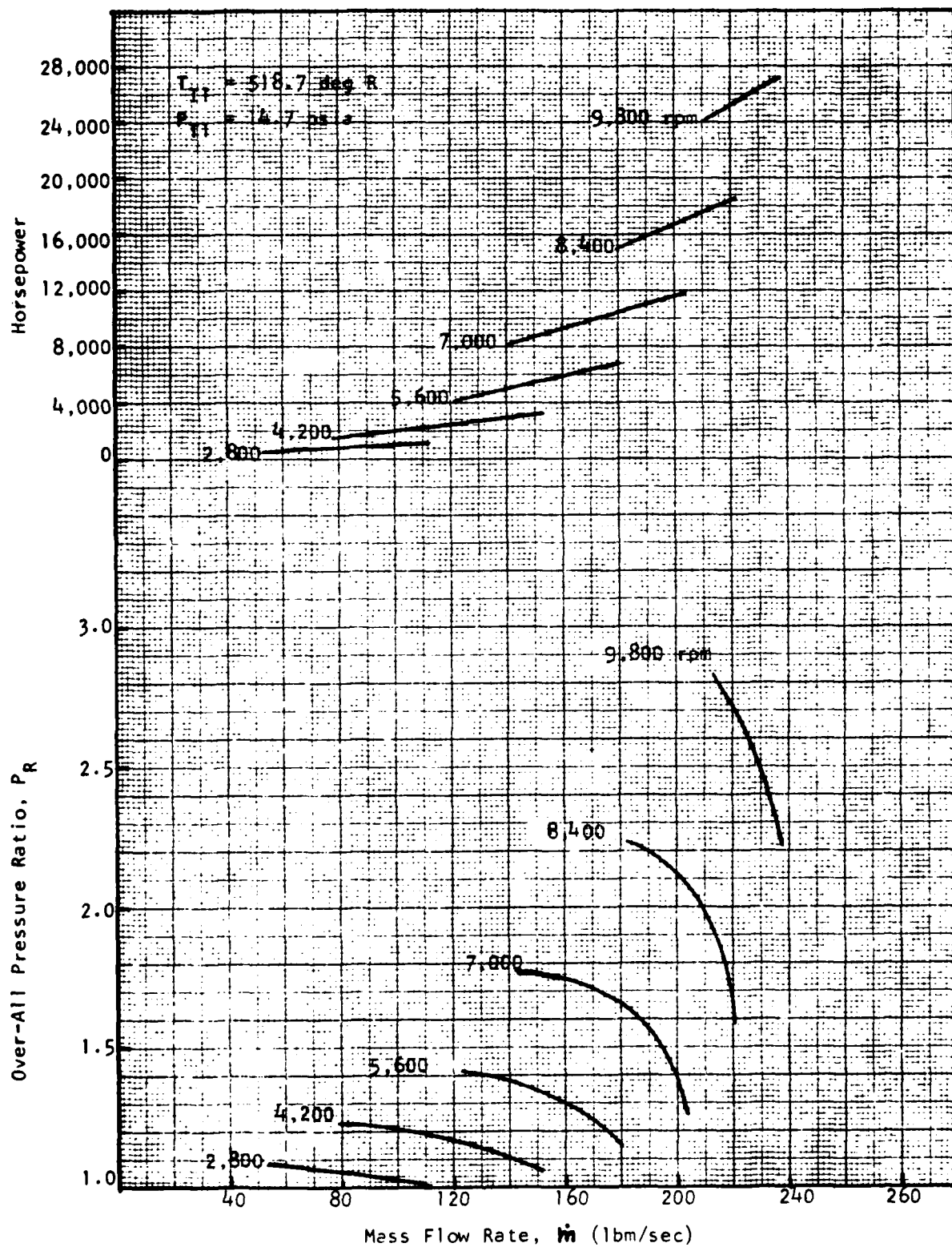


FIGURE 16 - PERFORMANCE CHARACTERISTICS OF DOUBLE-ENTRY CENTRIFUGAL COMPRESSOR -- F1-CC-D

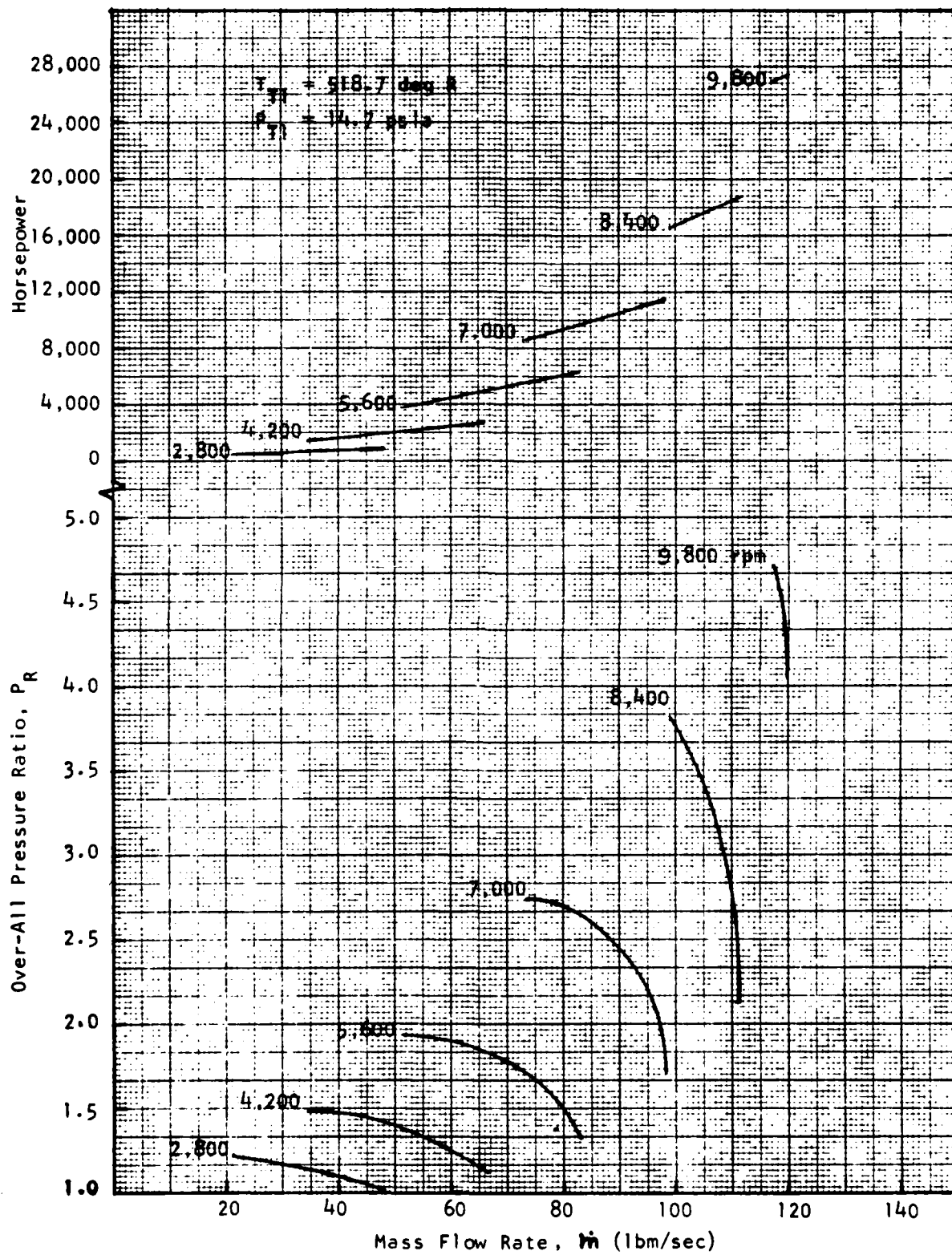


FIGURE 17 - PERFORMANCE CHARACTERISTICS OF TANDEM
CENTRIFUGAL COMPRESSOR -- F1-CC-T

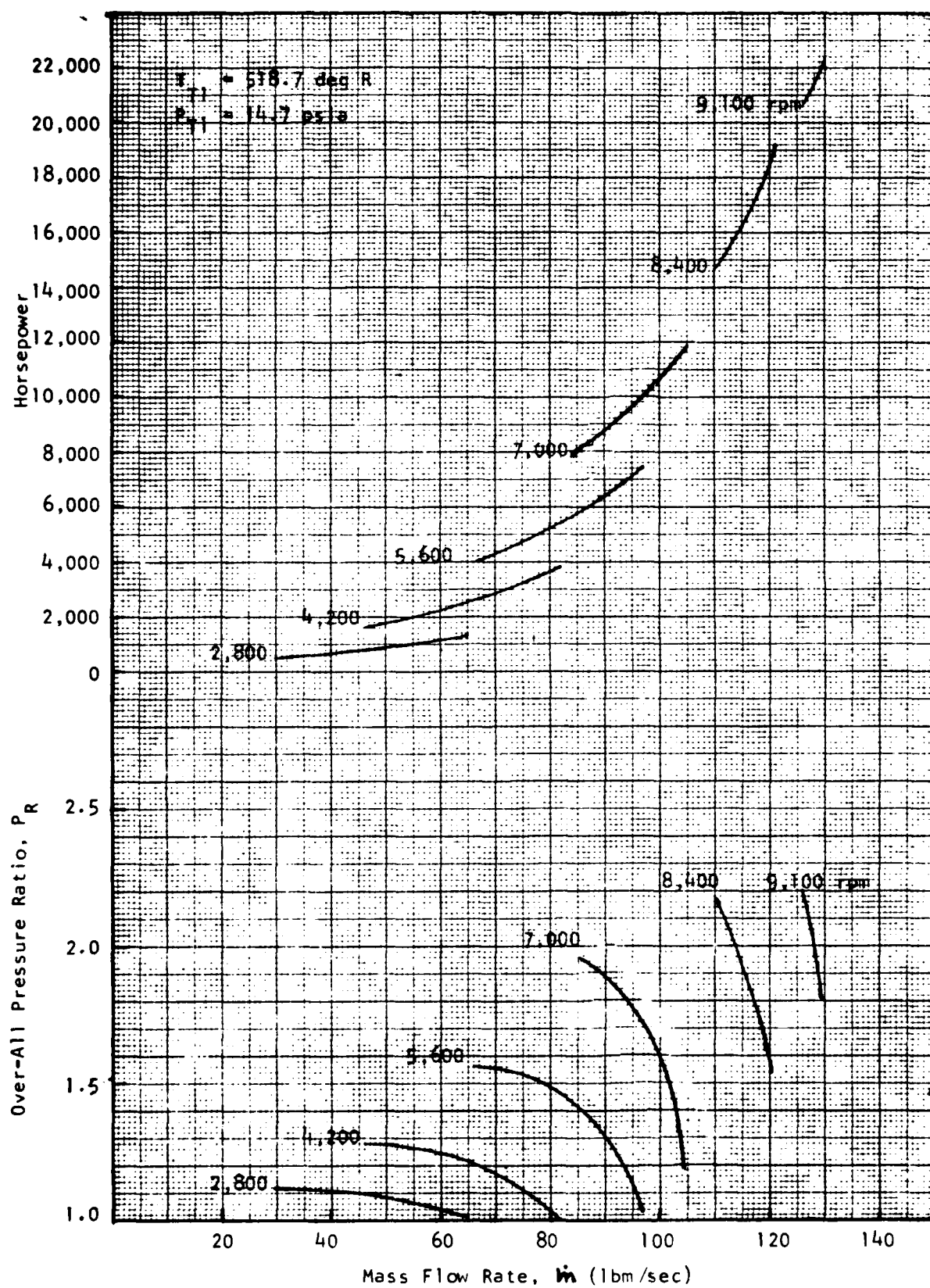


FIGURE 18 - PERFORMANCE CHARACTERISTICS OF SINGLE-STAGE
RADIAL OUTFLOW COMPRESSOR -- FI-ROC-S

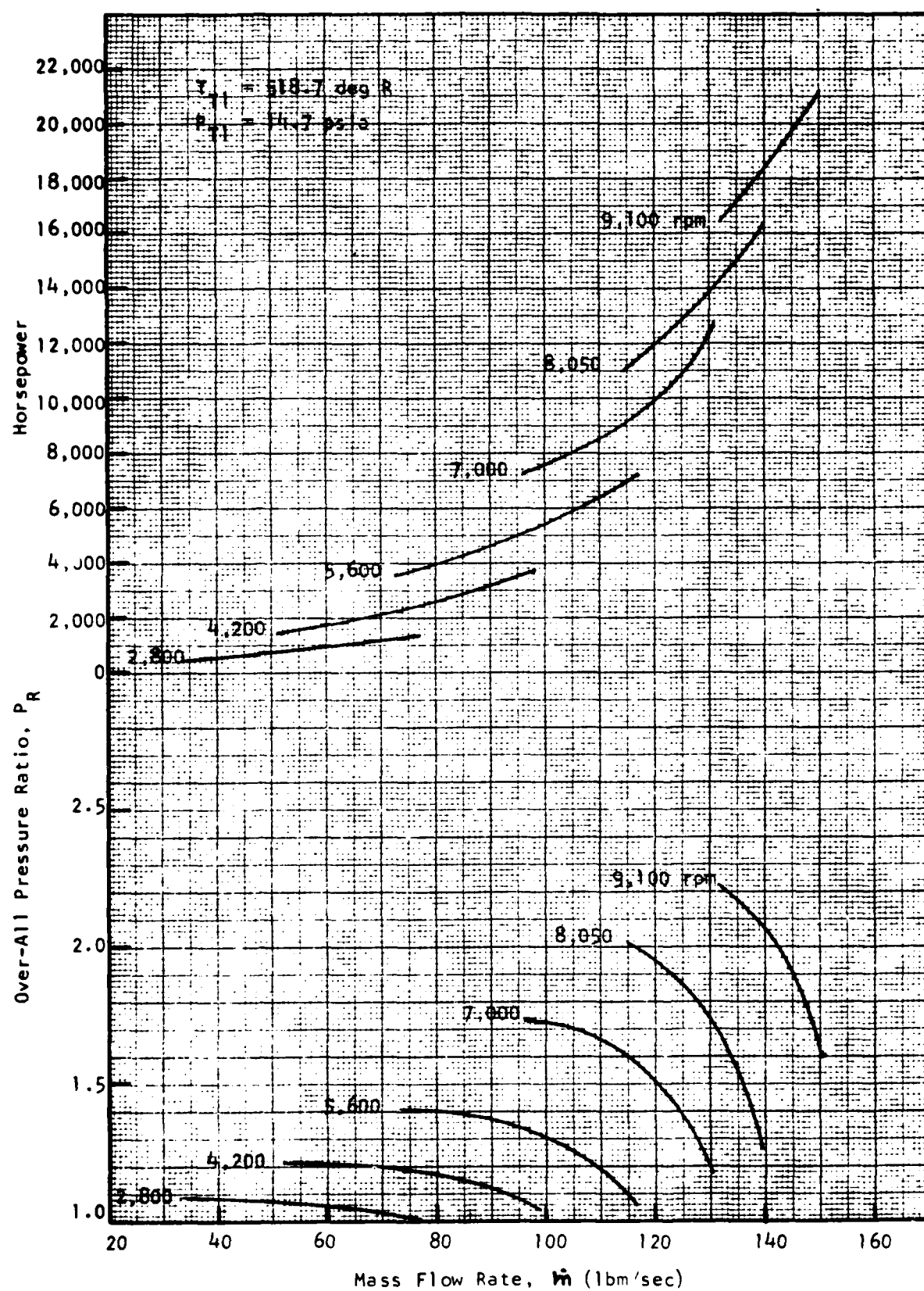


FIGURE 19 - PERFORMANCE CHARACTERISTICS OF DOUBLE-ENTRY
RADIAL OUTFLOW COMPRESSOR -- F1-ROC-D

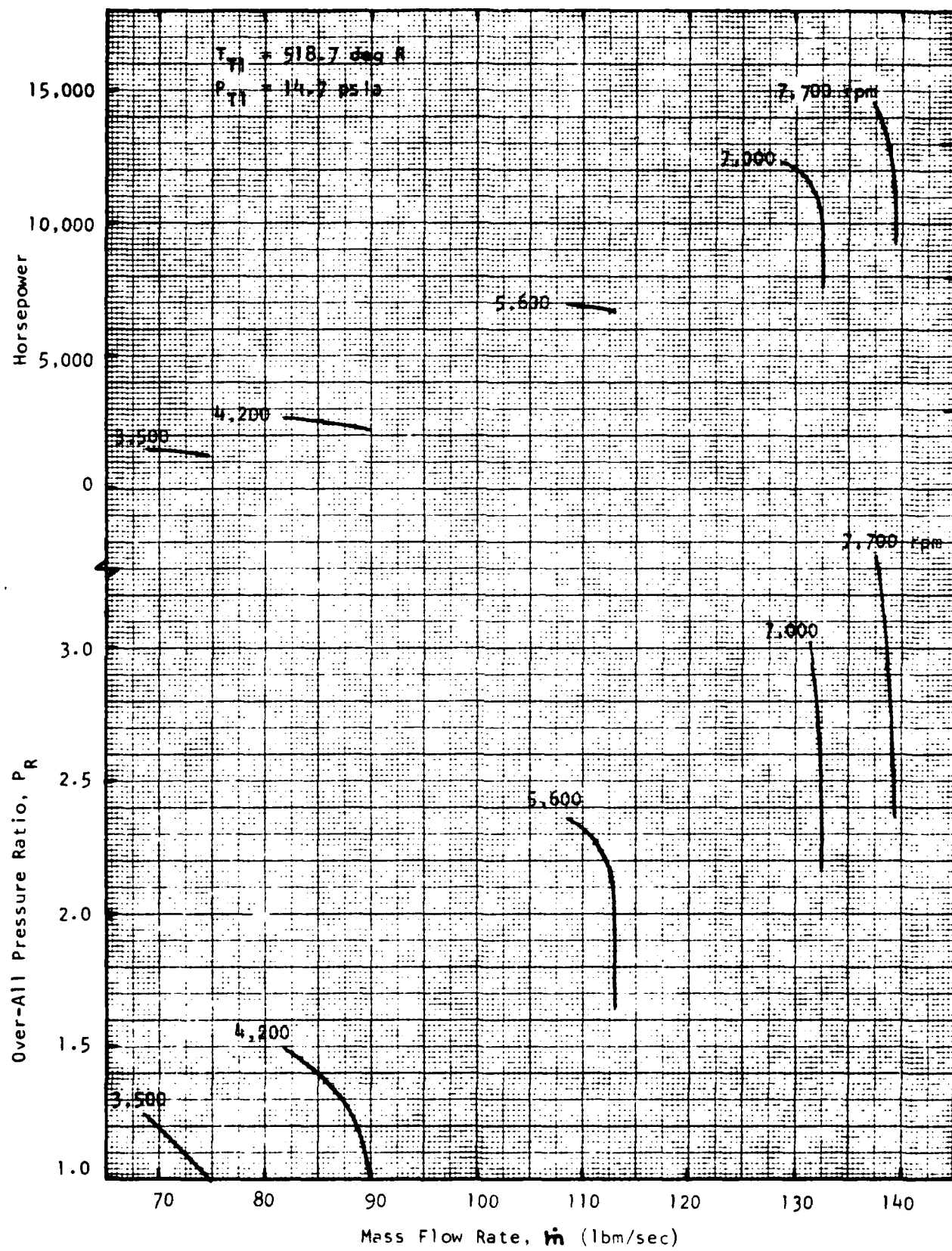


FIGURE 20 - PERFORMANCE CHARACTERISTICS OF
5-STAGE AXIAL COMPRESSOR -- F1-AC5-H

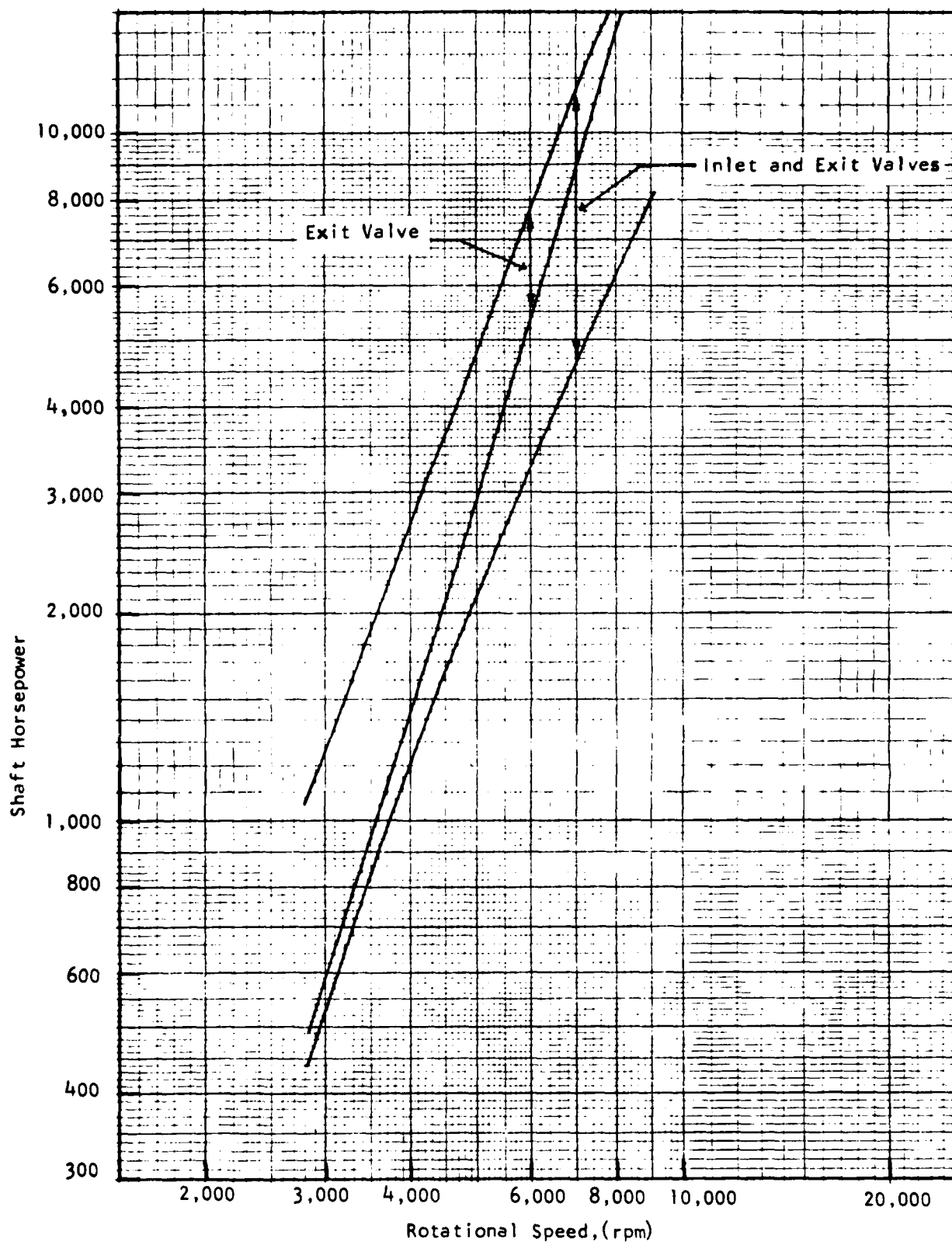


FIGURE 21 - EFFECT OF RPM, AND INLET AND EXIT VALVES ON POWER - SINGLE STAGE CENTRIFUGAL COMPRESSOR (F1-CC-S)

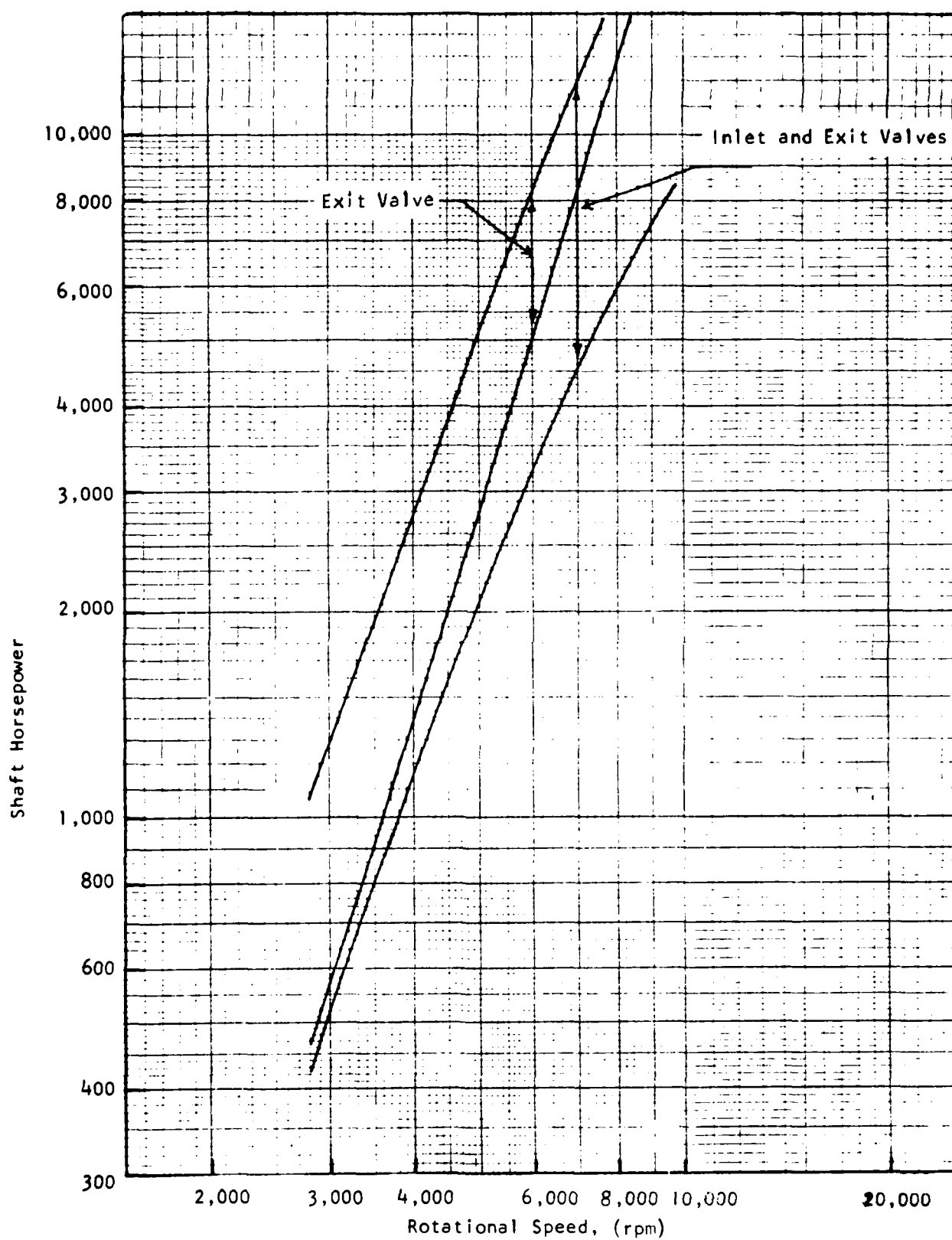


FIGURE 22 - EFFECT OF RPM, AND INLET AND EXIT VALVES ON POWER - DOUBLE ENTRY CENTRIFUGAL COMPRESSOR (F1-CC-D)

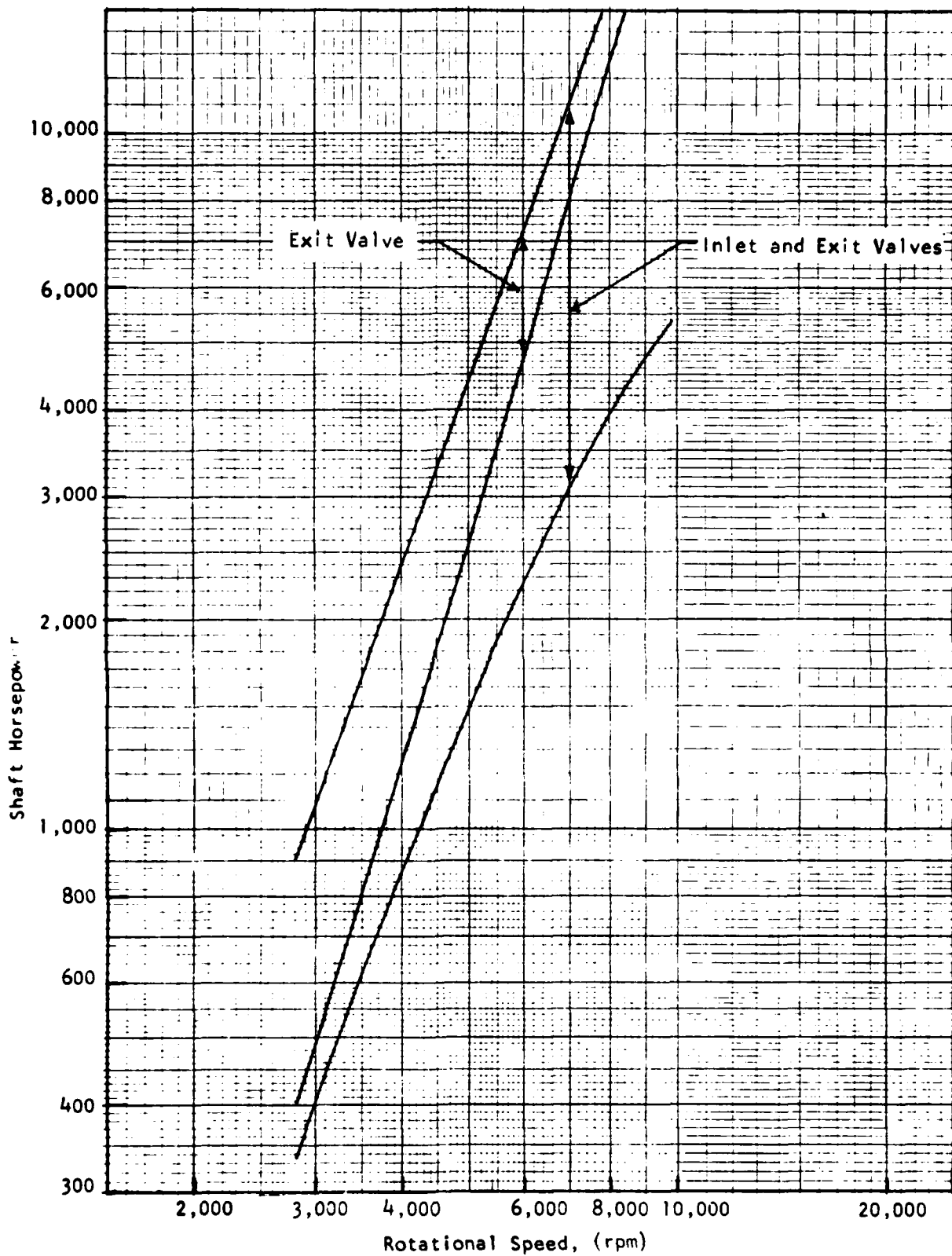


FIGURE 23 - EFFECT OF RPM. AND INLET AND EXIT VALVES ON POWER - TANDEM
CENTRIFUGAL COMPRESSOR (F)-CC-T)

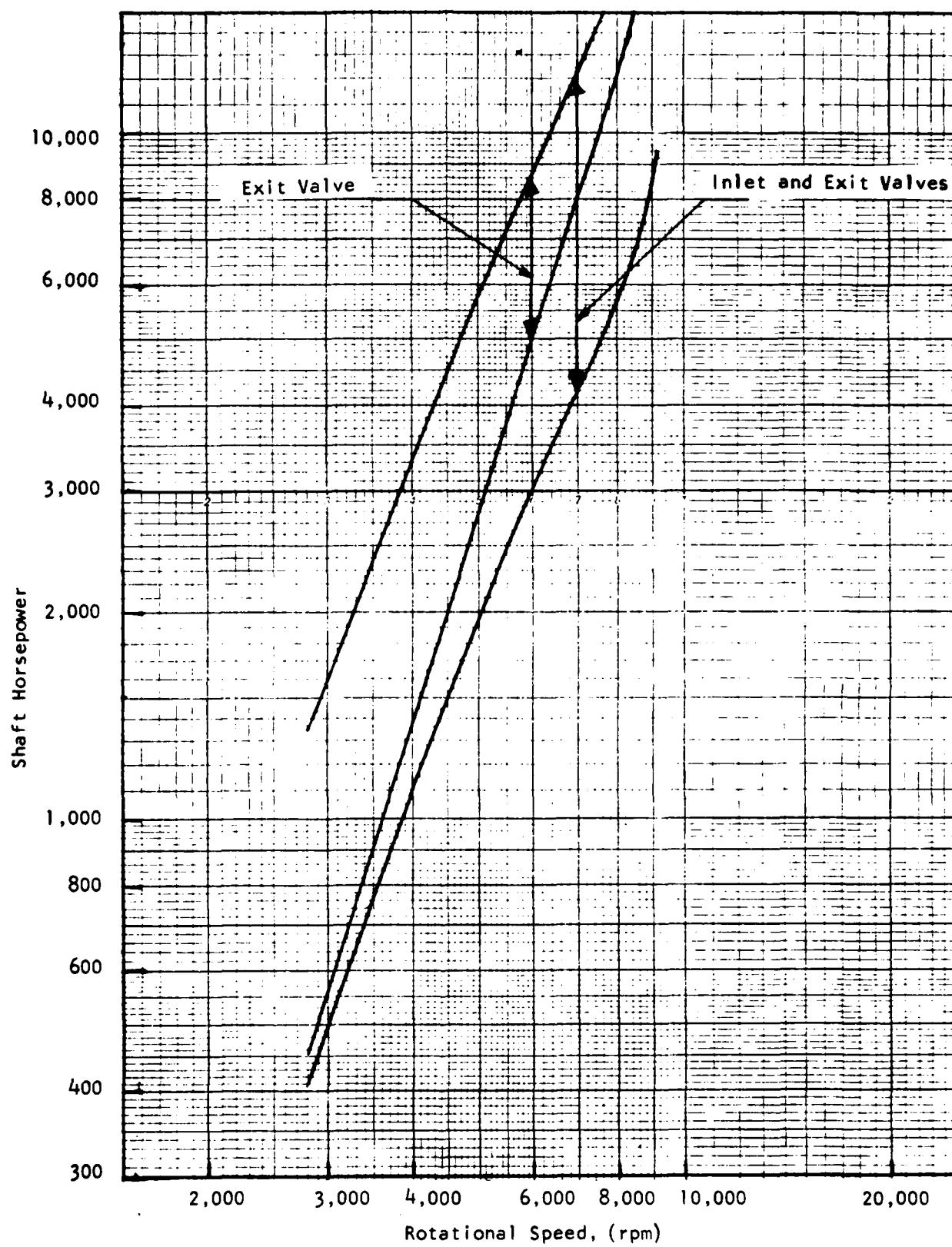


FIGURE 24 - EFFECT OF RPM AND INLET AND EXIT VALVES ON POWER - SINGLE STAGE RADIAL OUTFLOW COMPRESSOR (F1-ROC-S)

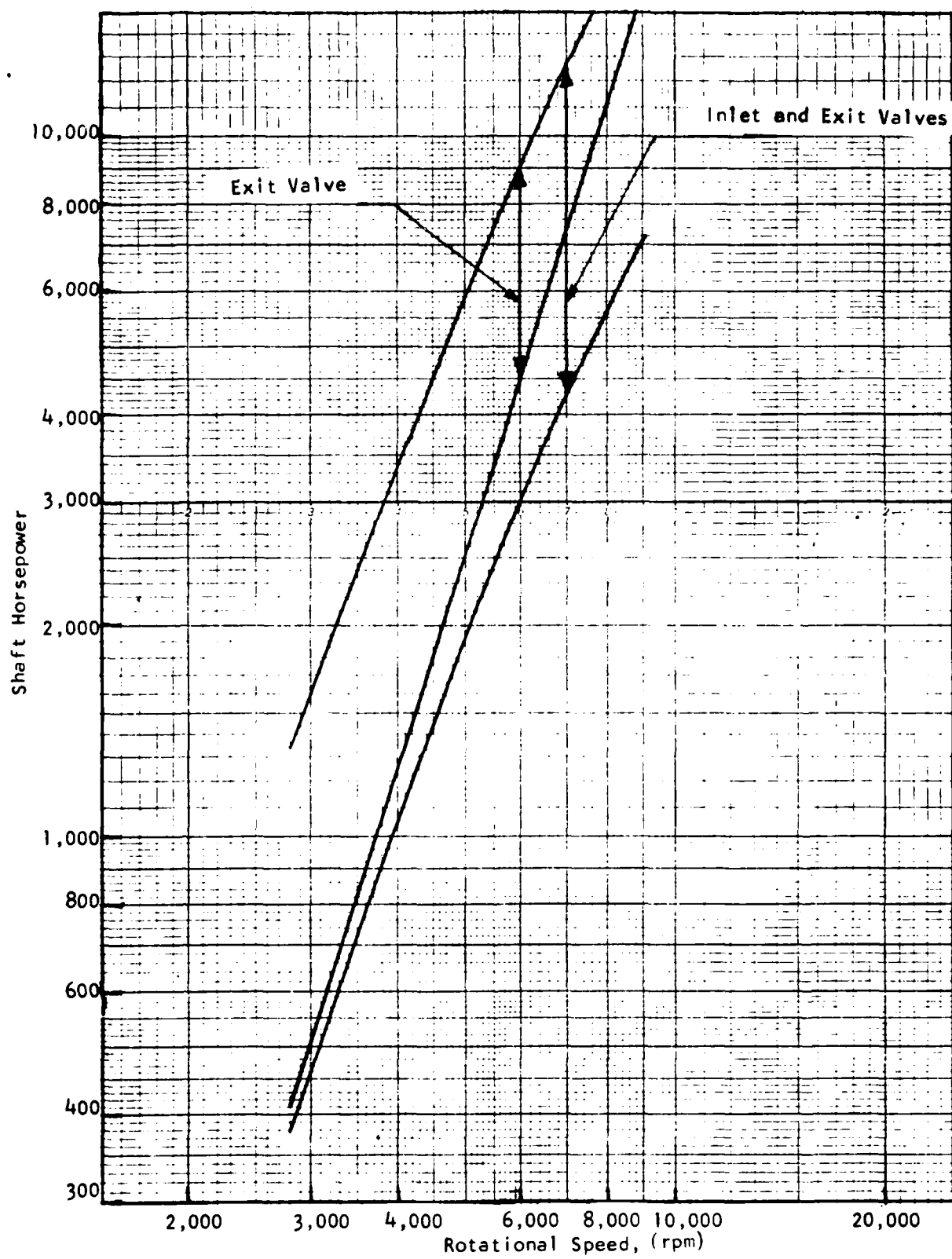


FIGURE 25 - EFFECT OF RPM AND INLET AND EXIT VALVES ON POWER - DOUBLE ENTRY RADIAL OUTFLOW COMPRESSOR (F1-ROC-D)

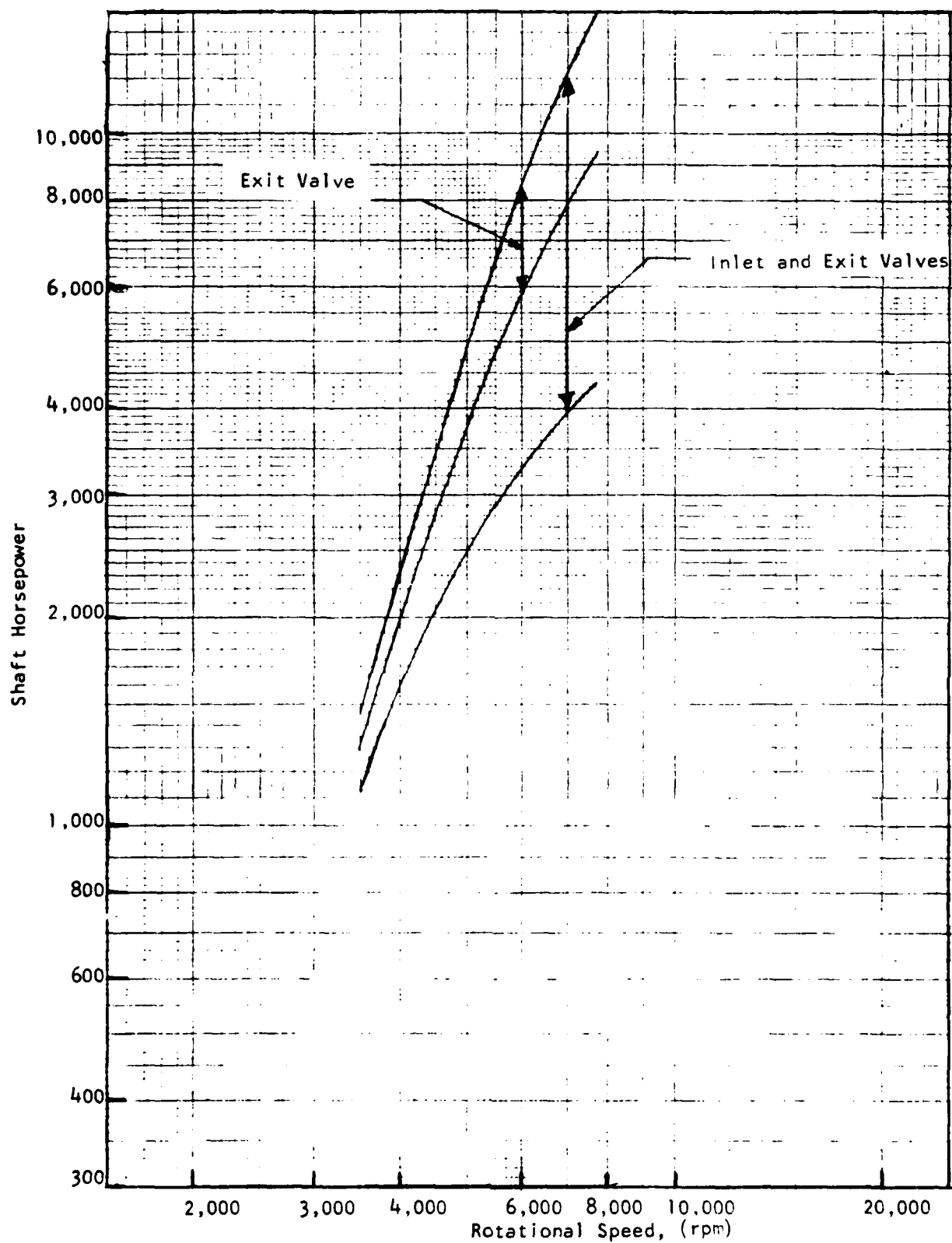


FIGURE 26 - EFFECT OF RPM AND INLET AND EXIT VALVES ON POWER - CONSTA
HUB 5-STAGE AXIAL COMPRESSOR (F1-AC5-H)

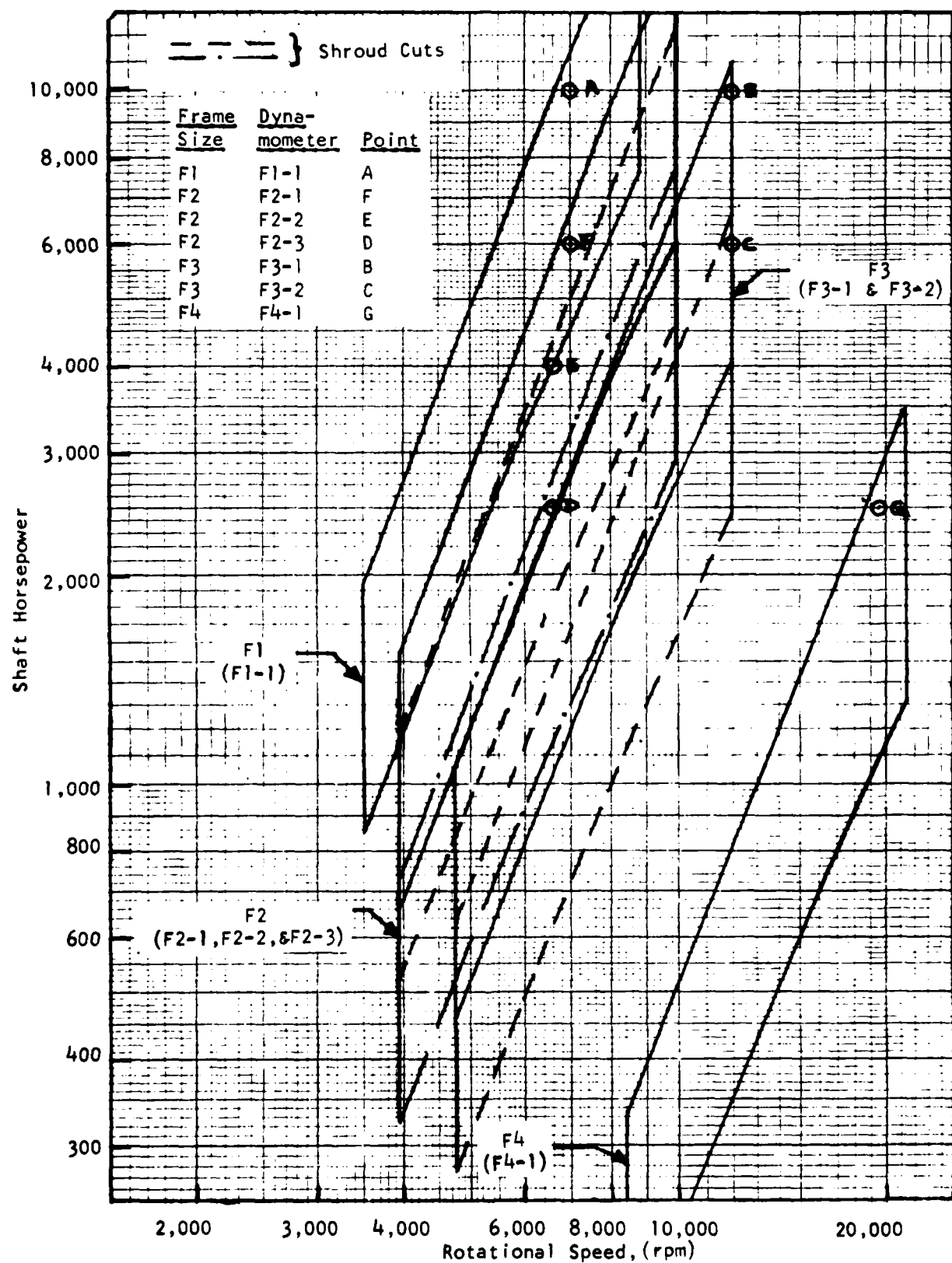


FIGURE 27 - PERFORMANCE ENVELOPES OF DYNAMOMETERS WITH INLET AND EXIT VALVES - SINGLE-STAGE CENTRIFUGAL COMPRESSOR (CC-S)

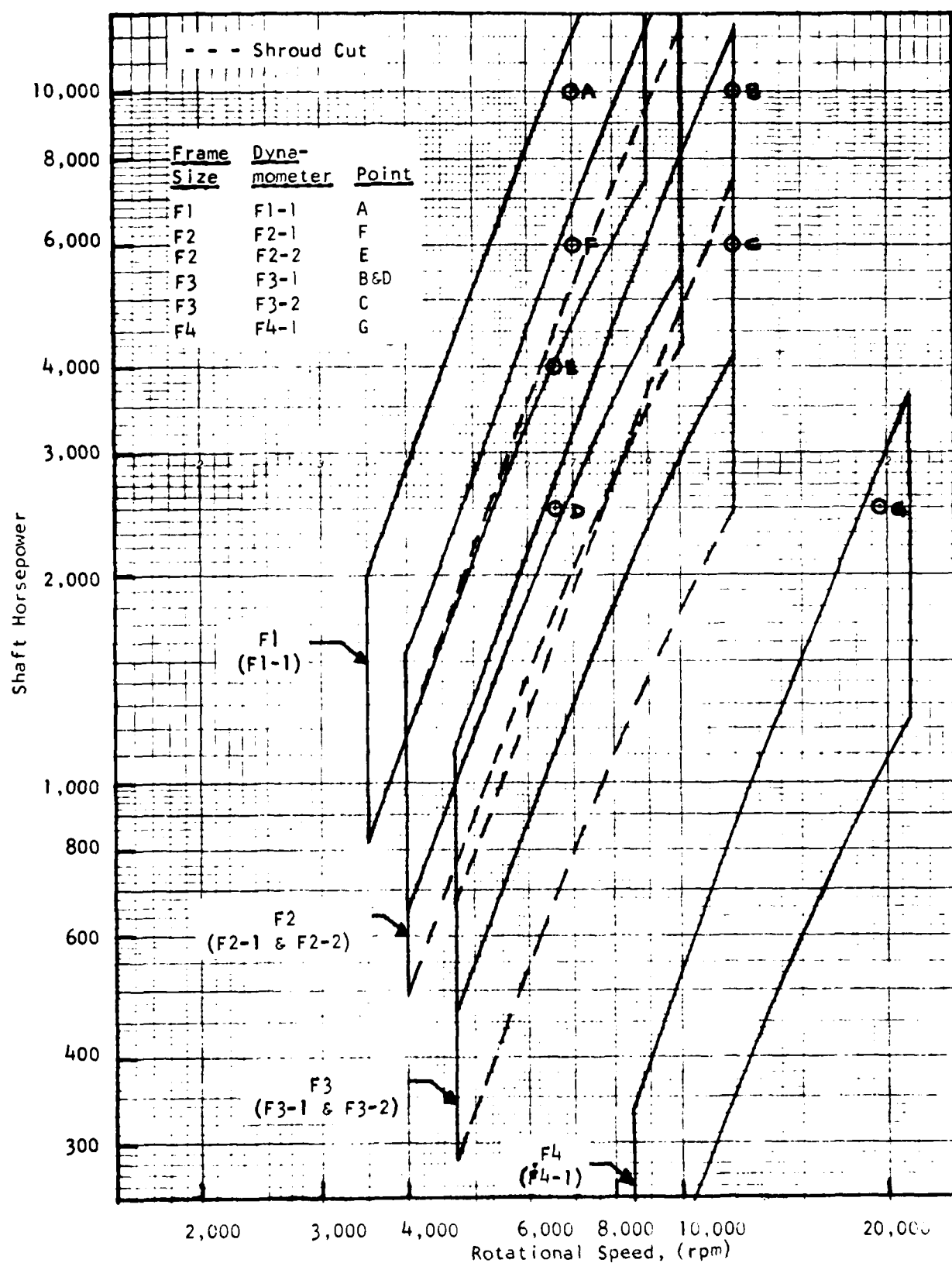


FIGURE 28- PERFORMANCE ENVELOPES OF DYNAMOMETERS WITH INLET AND EXIT VALVES - DOUBLE-ENTRY CENTRIFUGAL COMPRESSOR (CC-D)

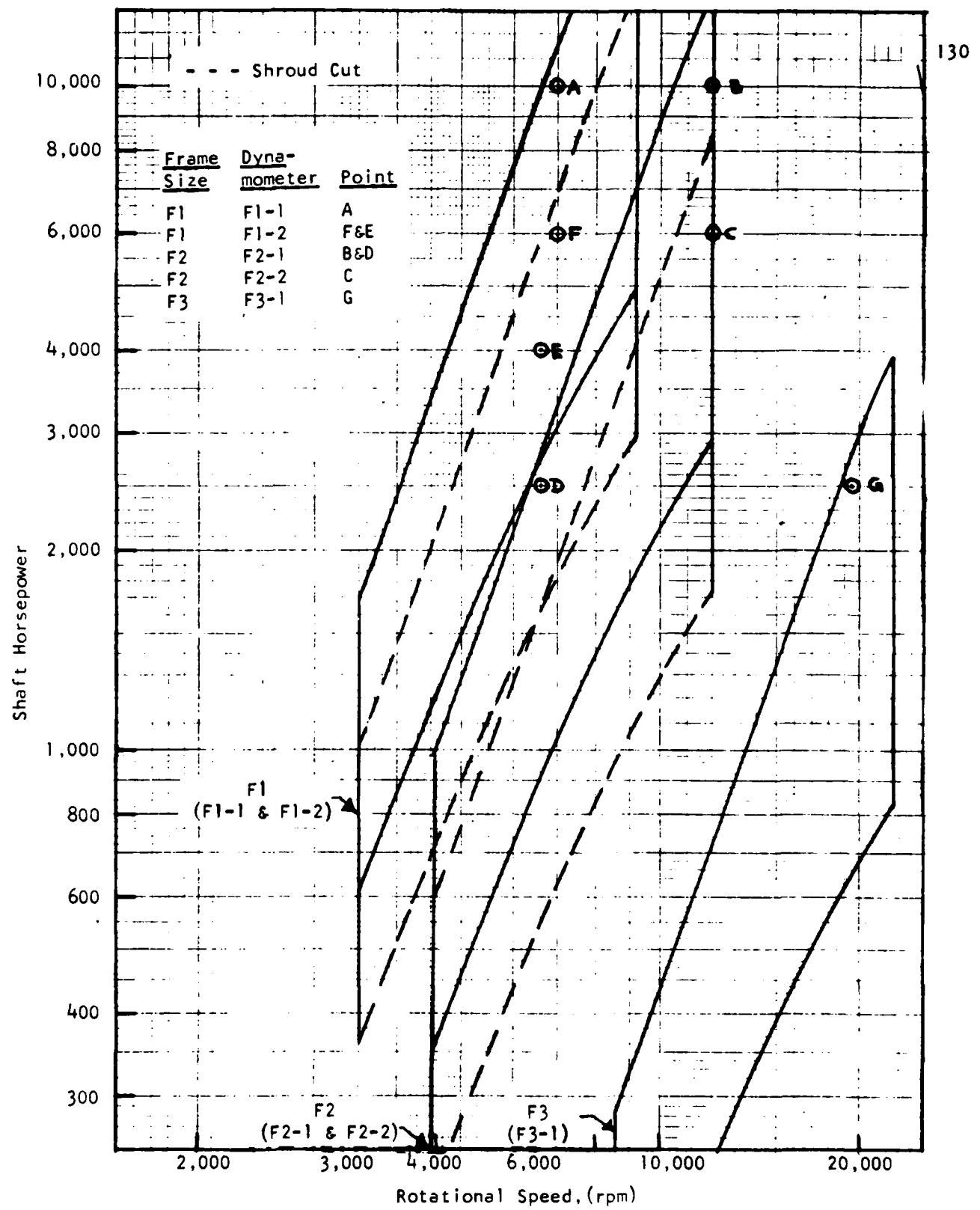


FIGURE 29 - PERFORMANCE ENVELOPES OF DYNAMOMETERS WITH INLET AND EXIT VALVES - TANDEM CENTRIFUGAL COMPRESSOR (CC-T)

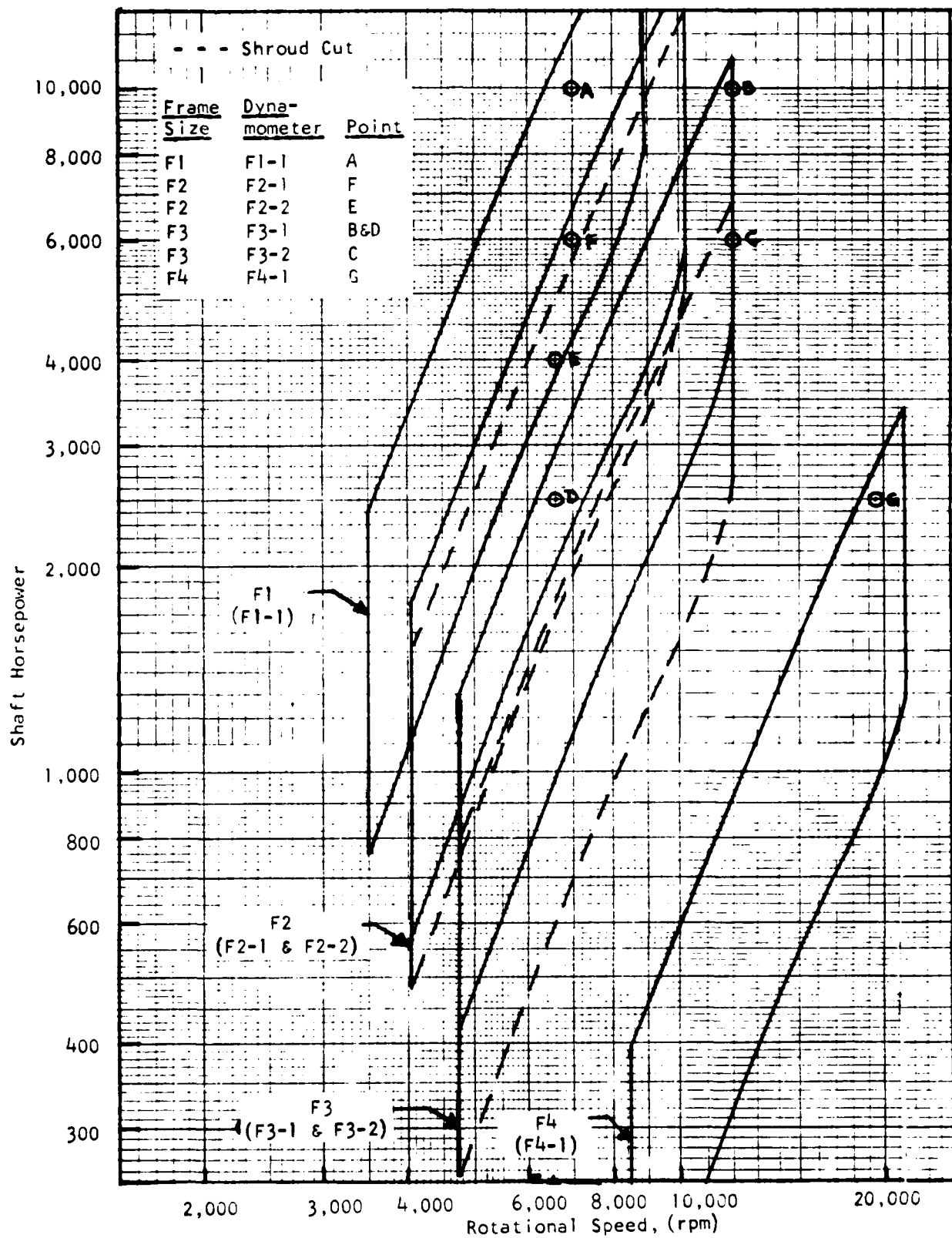


FIGURE 30 - PERFORMANCE ENVELOPES OF DYNAMOMETERS WITH INLET AND EXIT VALVES - SINGLE-STAGE RADIAL-OUTFLOW COMPRESSOR (ROC-S)

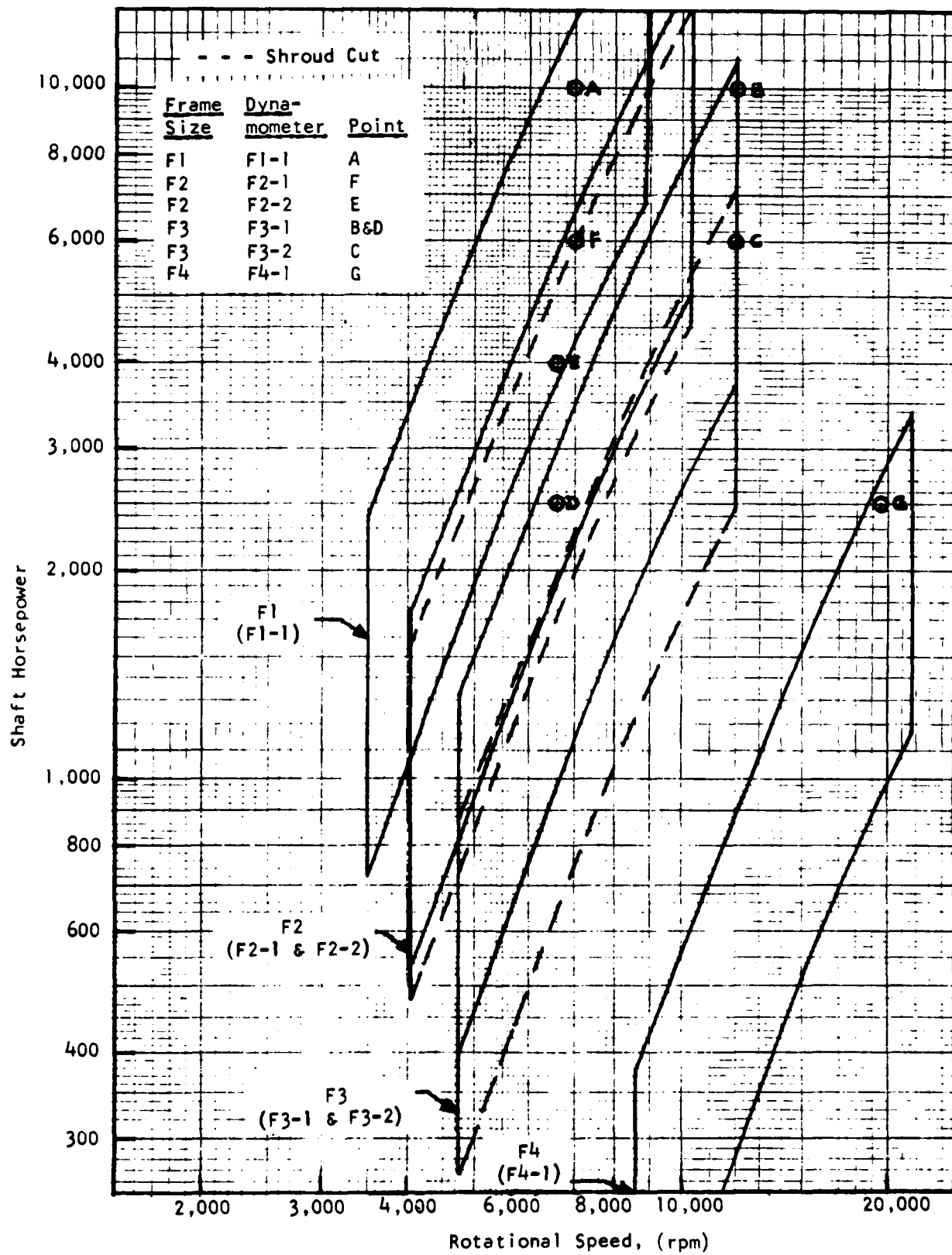


FIGURE 31 - PERFORMANCE ENVELOPES OF DYNAMOMETERS WITH INLET AND EXIT
VALVES - DOUBLE-ENTRY RADIAL OUTFLOW COMPRESSOR (ROC-D)

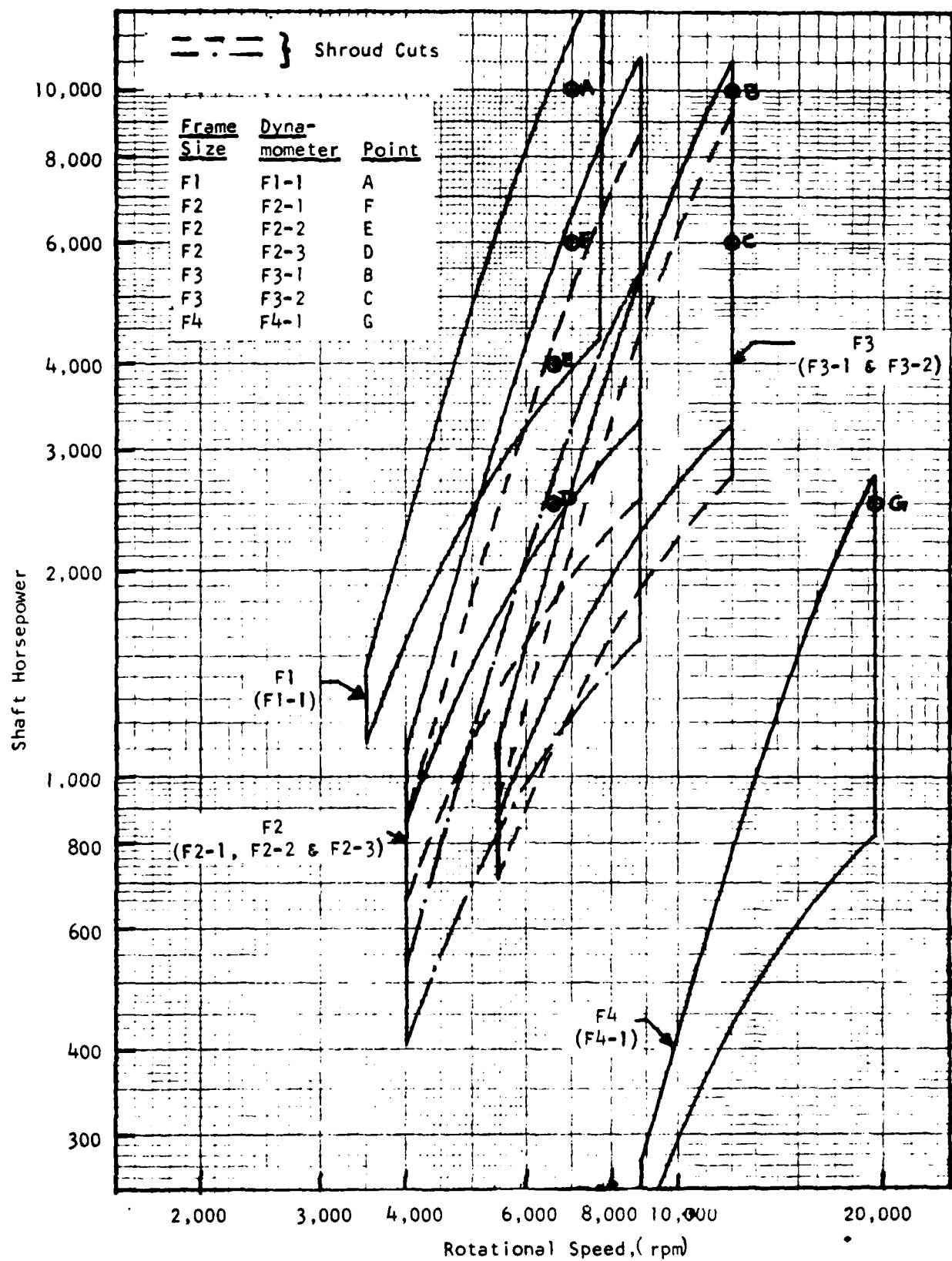


FIGURE 32 - PERFORMANCE ENVELOPES OF DYNAMOMETERS WITH INLET AND EXIT VALVES - 5-STAGE CONSTANT HUB AXIAL COMPRESSOR (AC5-H)

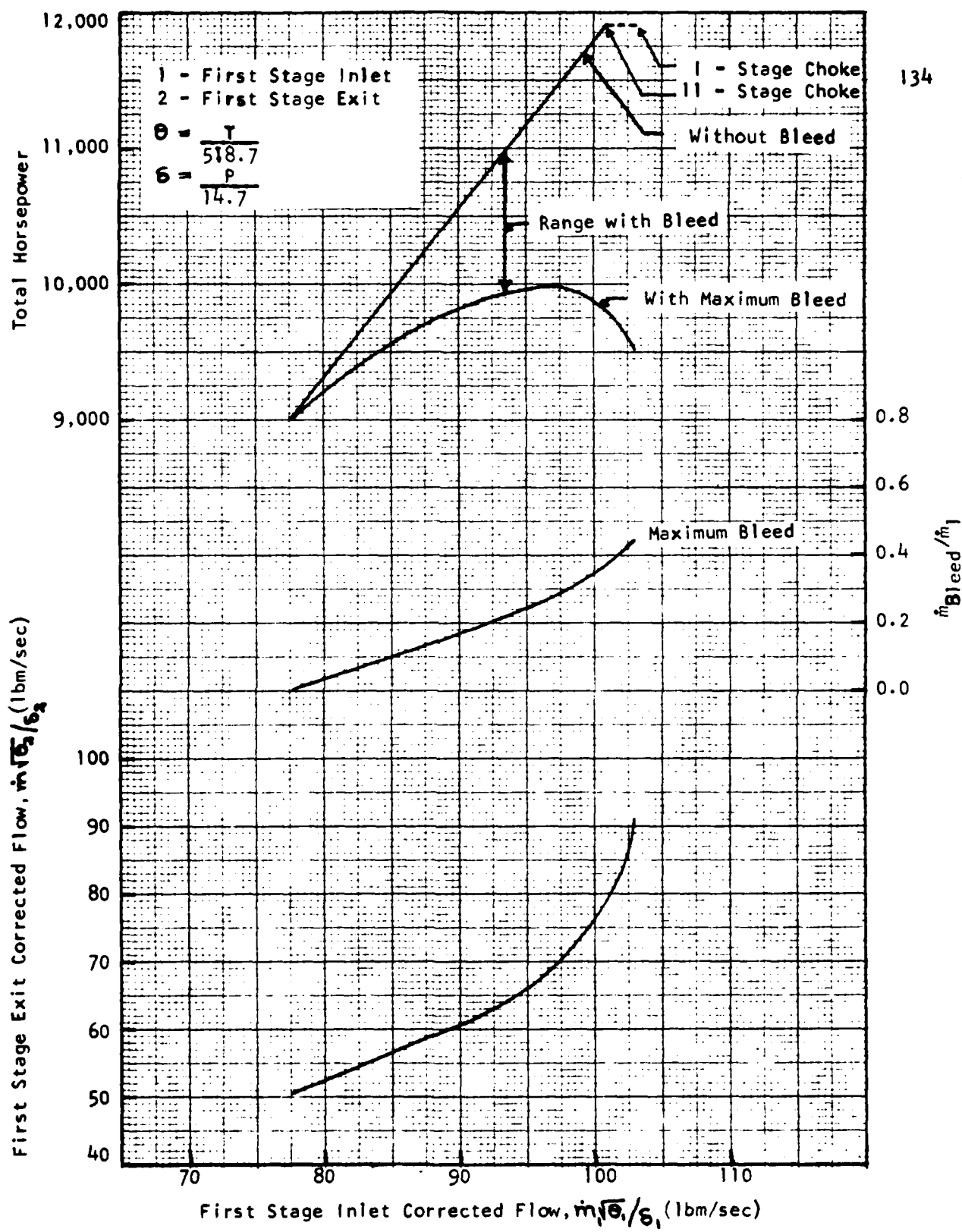


FIGURE 33 - EFFECT OF INTERSTAGE BLEED ON POWER ABSORPTION -
TANDEM CENTRIFUGAL COMPRESSOR

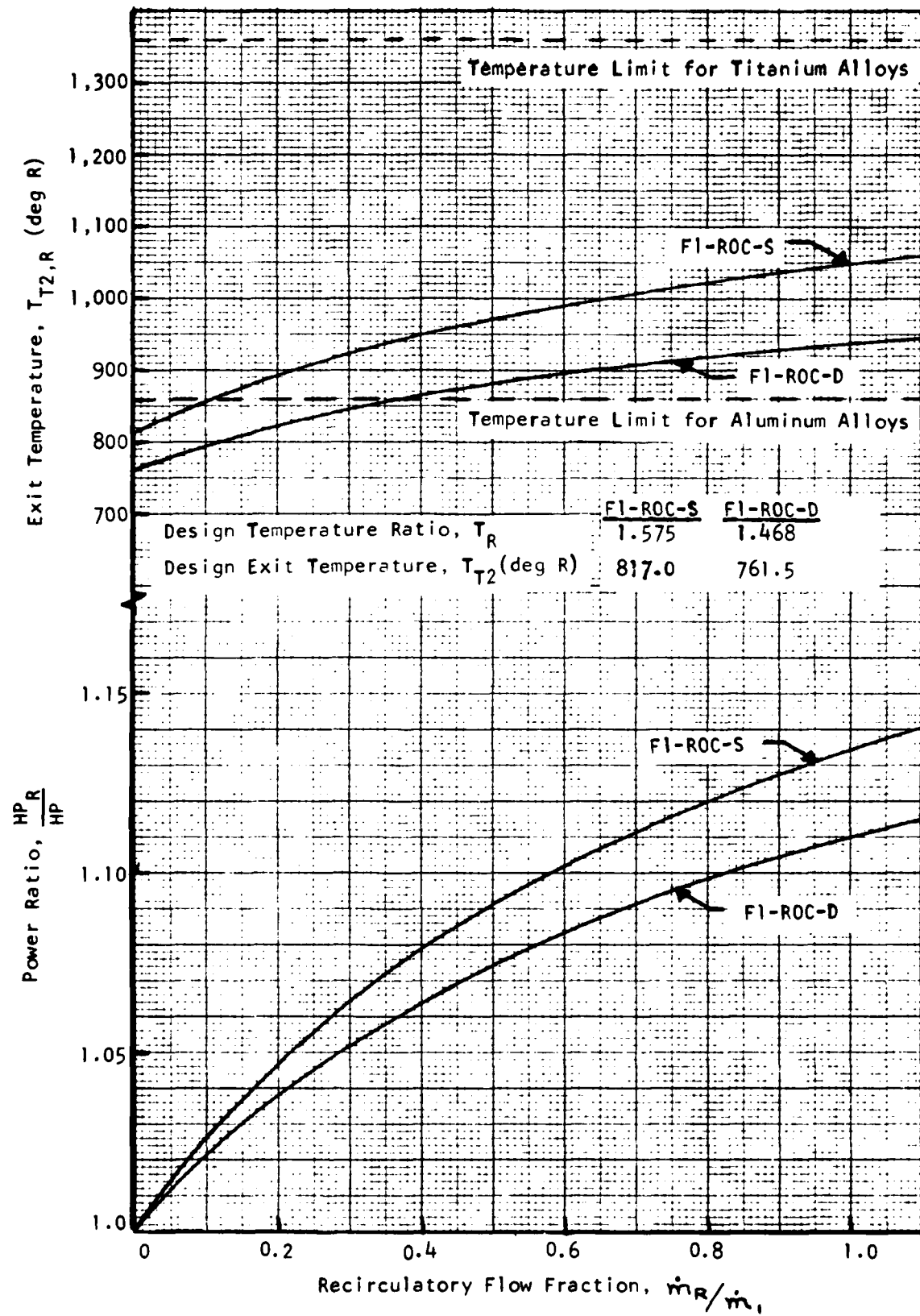


FIGURE 34 - EFFECT OF RECIRCULATION ON POWER AND EXIT TEMPERATURE FOR RADIAL OUTFLOW COMPRESSORS

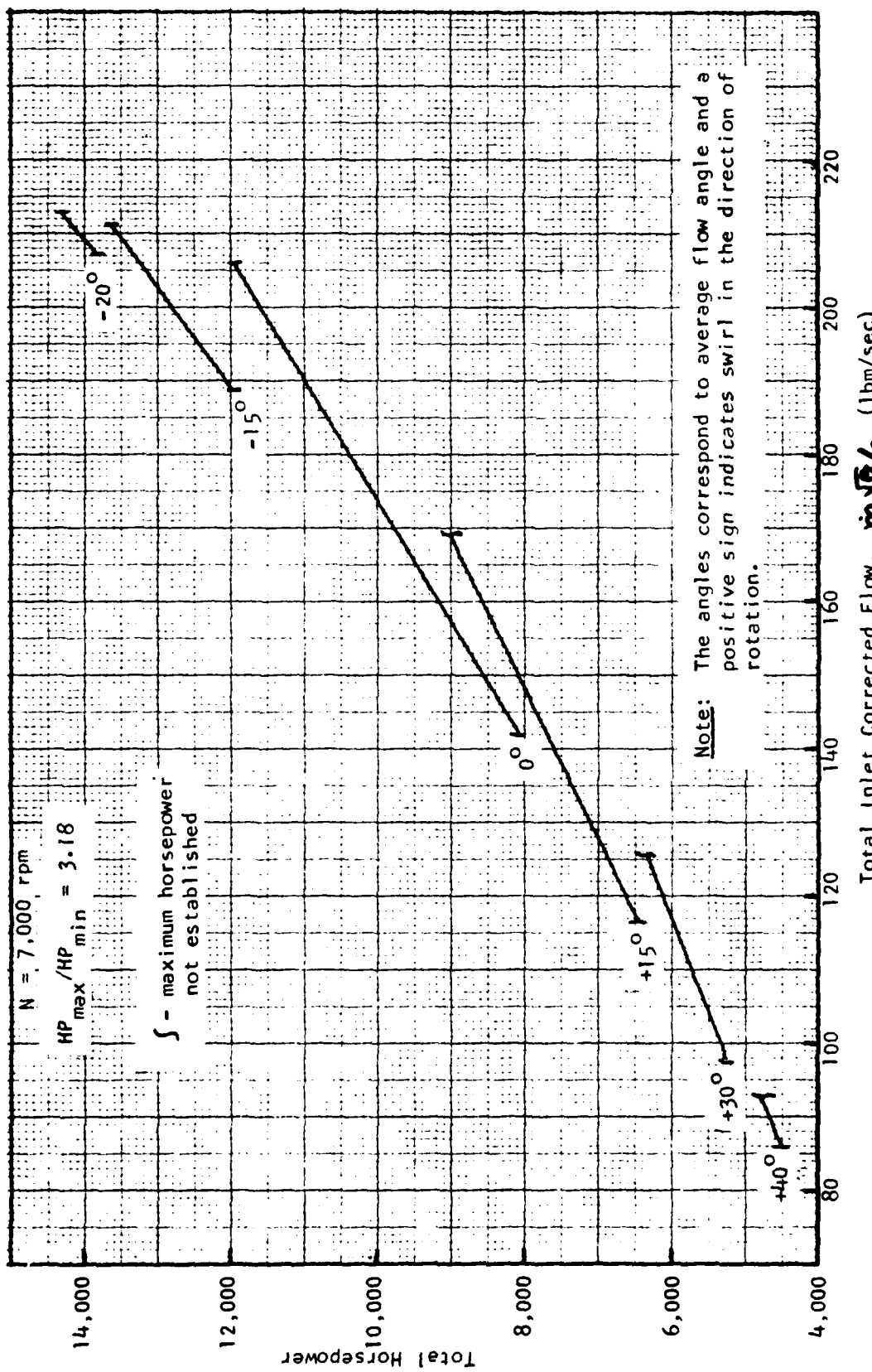


FIGURE 35 - EFFECT OF VARIABLE INLET GUIDE VANES ON FLOW AND POWER - DOUBLE ENTRY CENTRIFUGAL COMPRESSOR (F1-CC-D)

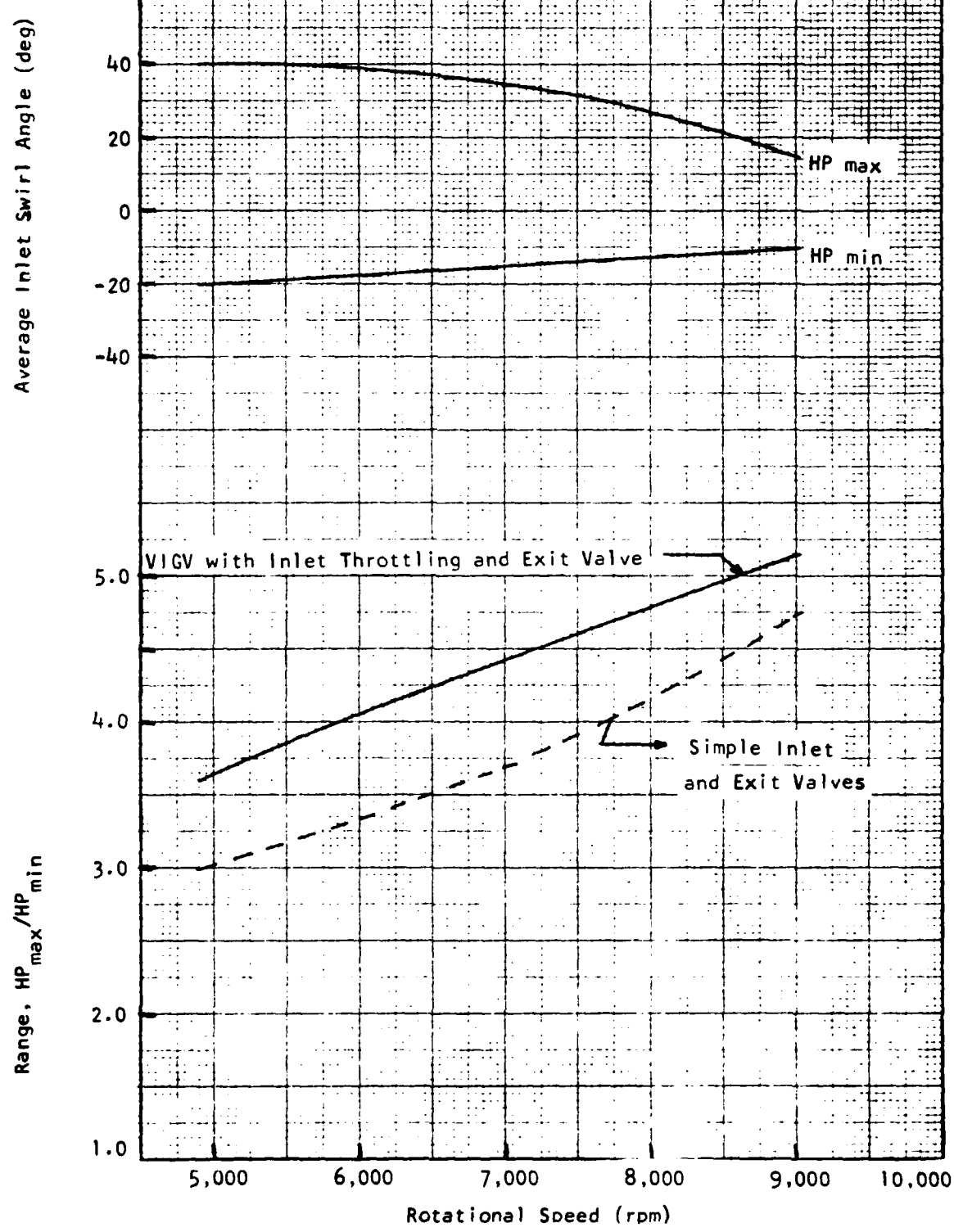


FIGURE 36 - EFFECT ON RANGE OF VARIABLE INLET GUIDE VANES WITH
INLET THROTTLING AND EXIT VALVE - 2-STAGE TANDEM
CENTRIFUGAL COMPRESSOR (F1-CC-T)

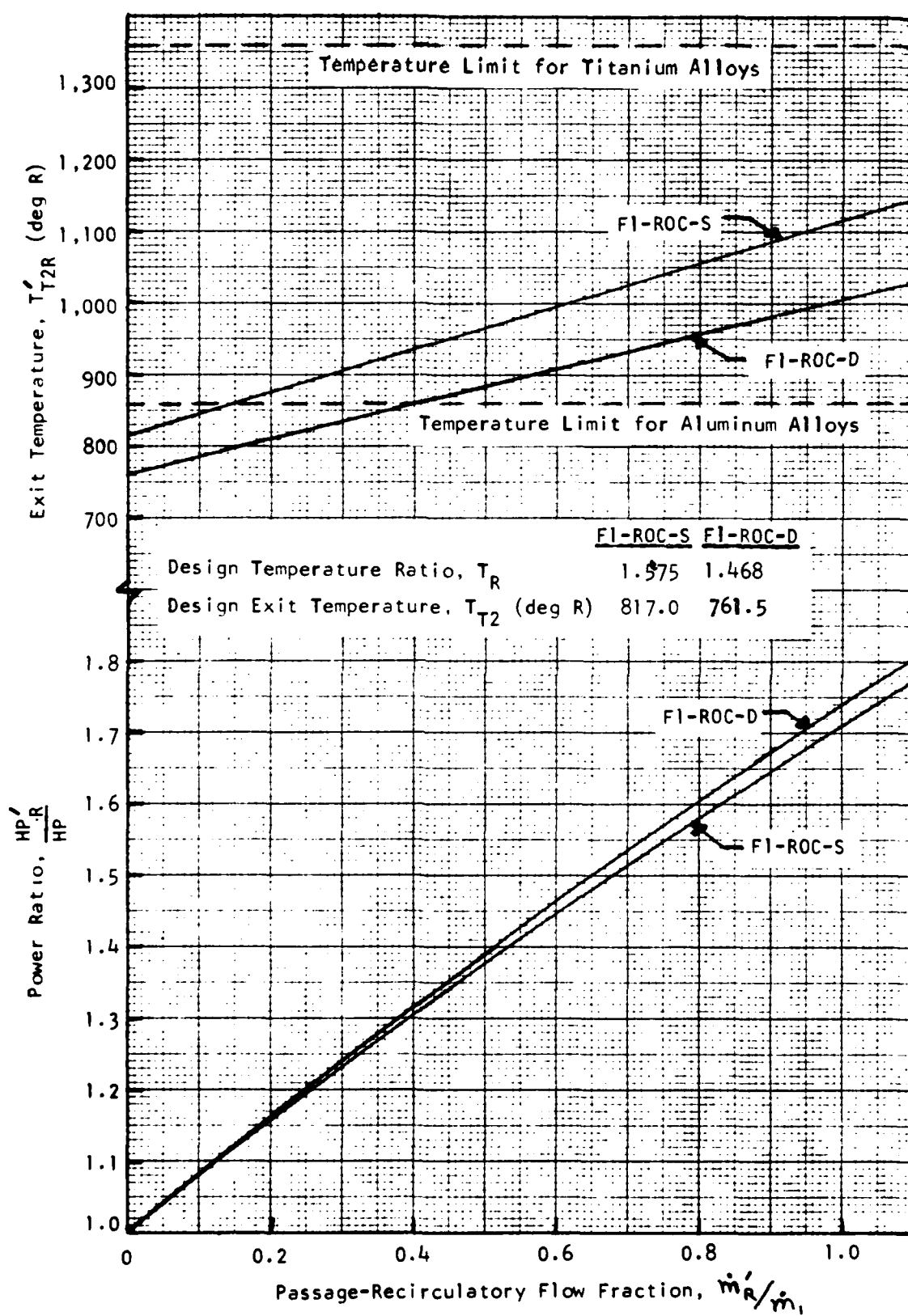


FIGURE 37 - EFFECT OF PASSAGE-RECIRCULATION ON POWER AND EXIT TEMPERATURE FOR RADIAL OUTFLOW COMPRESSORS

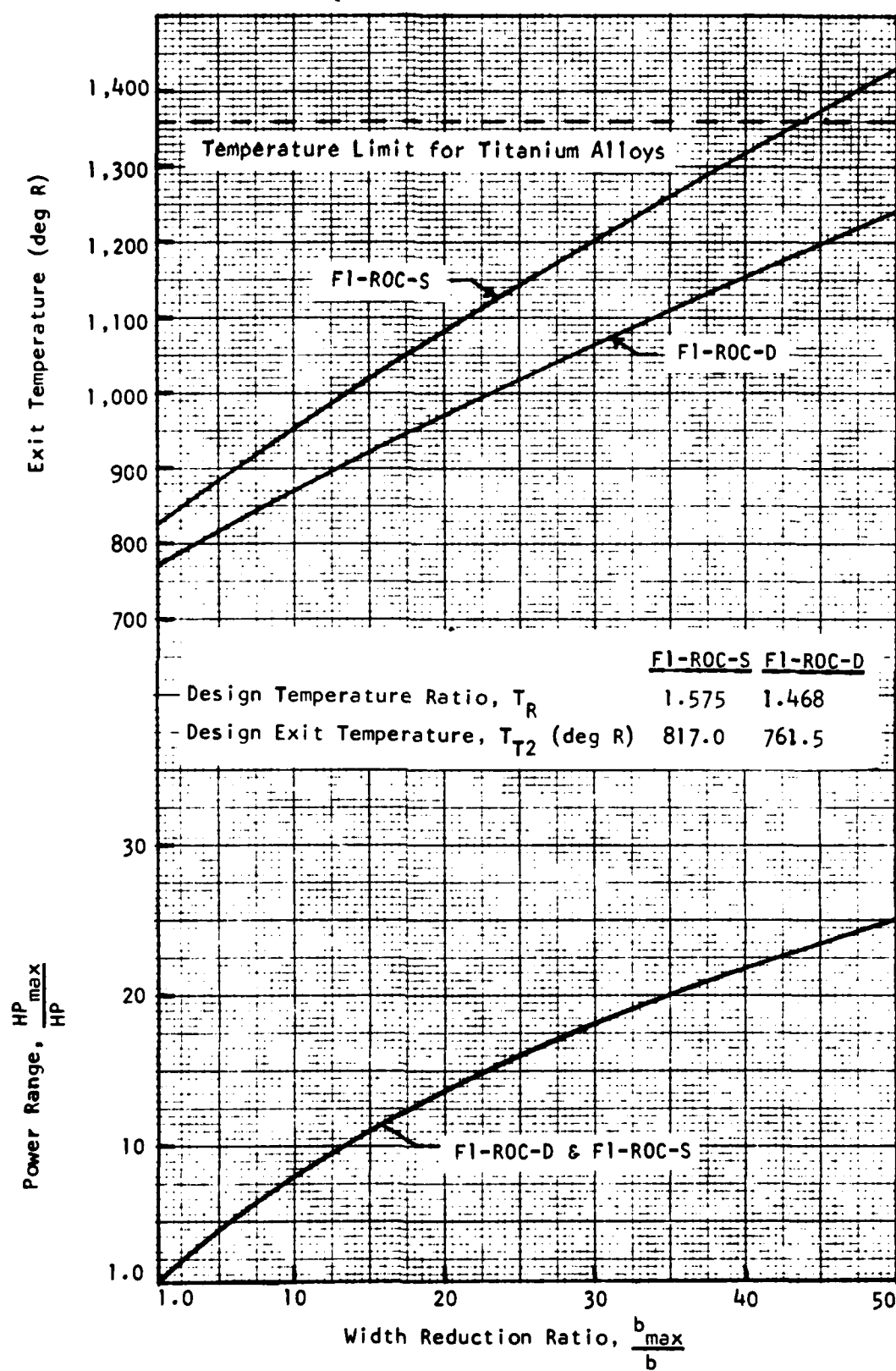


FIGURE 38 - POTENTIAL RANGE AND PROBABLE EXIT TEMPERATURE
FOR VARIABLE-SHROUD RADIAL-OUTFLOW COMPRESSORS

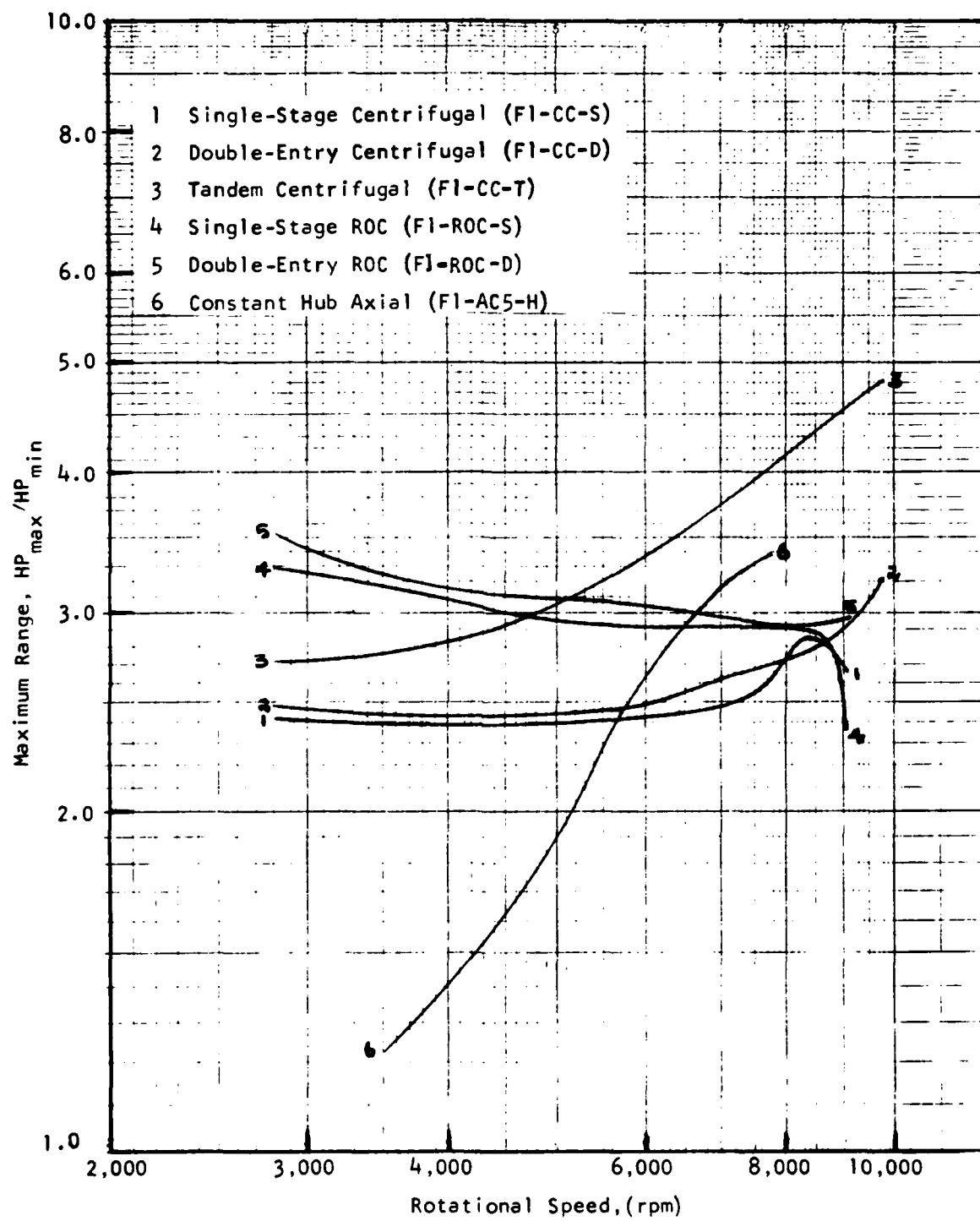


FIGURE 39 - EFFECT OF RPM ON MAXIMUM RANGE FOR VARIOUS COMPRESSOR SYSTEMS WITH INLET AND EXIT VALVES

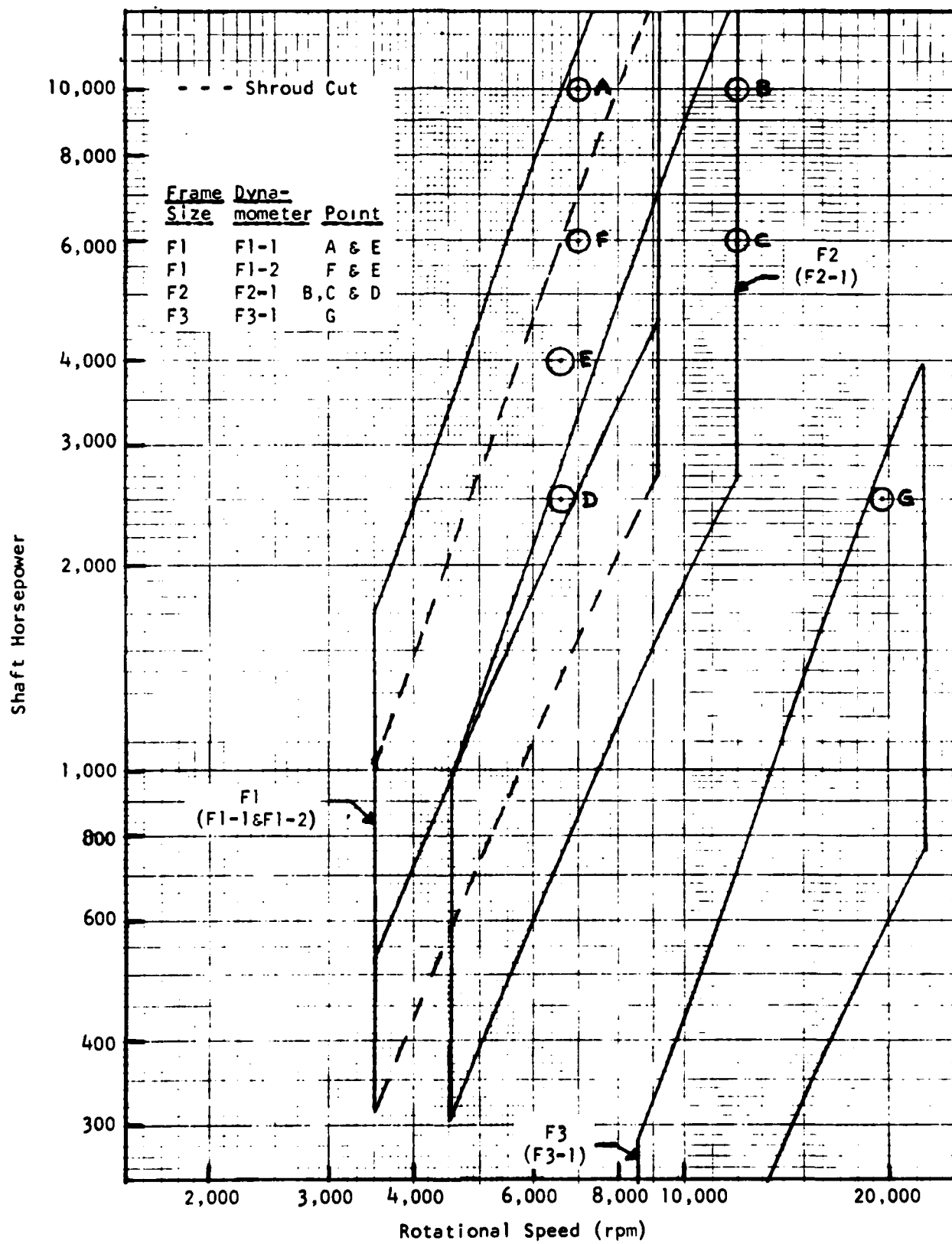


FIGURE 40 - PERFORMANCE ENVELOPES OF TANDEM CENTRIFUGAL DYNAMOMETERS WITH VIGV-THROTTLE AND EXIT VALVE

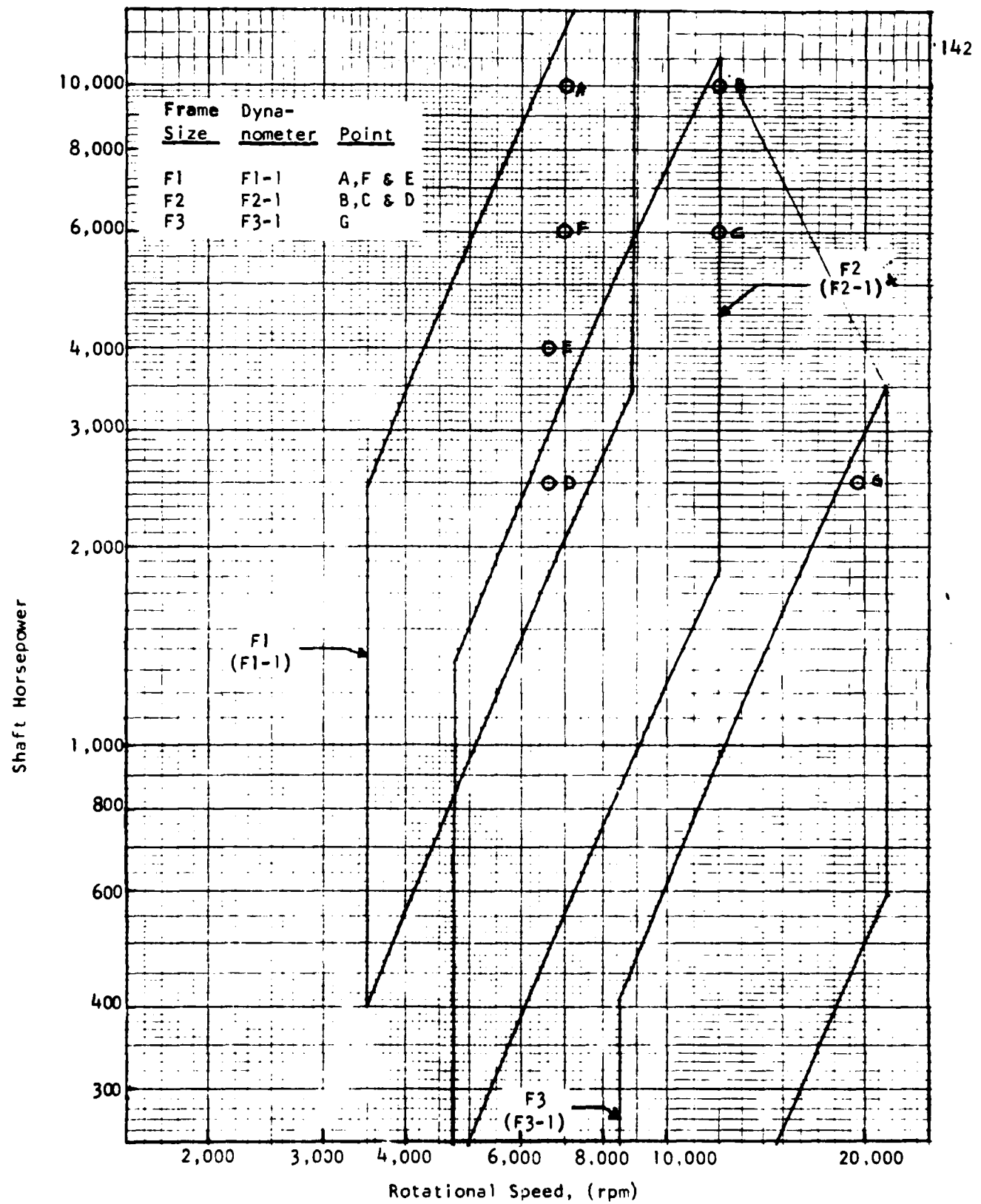


FIGURE 41 - PERFORMANCE ENVELOPES OF RADIAL OUTFLOW DYNAMOMETERS WITH VARIABLE SHROUD

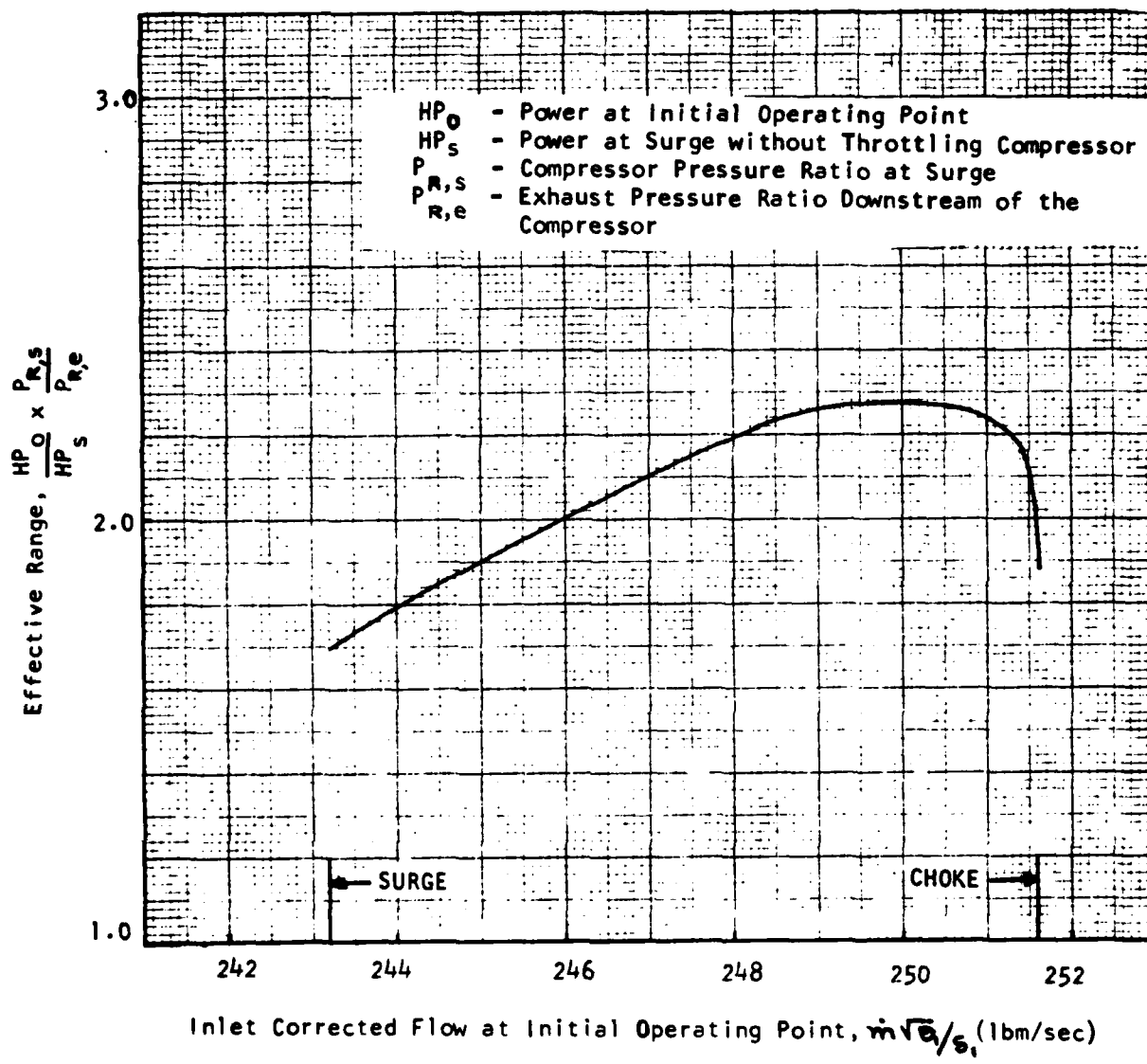


FIGURE 42 - EFFECT OF INITIAL OPERATING POINT ON EFFECTIVE RANGE WITH INLET VALVE FOR 5-STAGE AXIAL COMPRESSOR

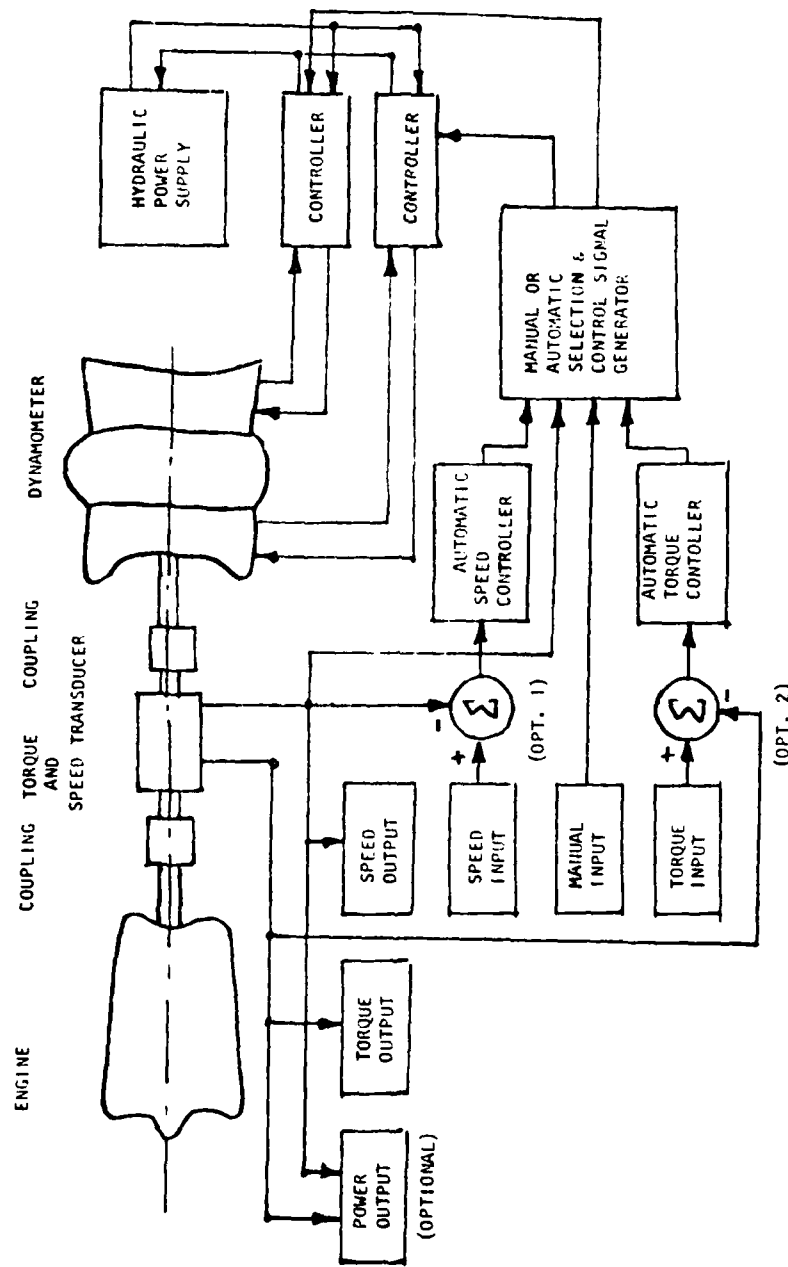


FIGURE 43 - SCHEMATIC OF CONTROL CONFIGURATION FOR DYNAMOMETERS

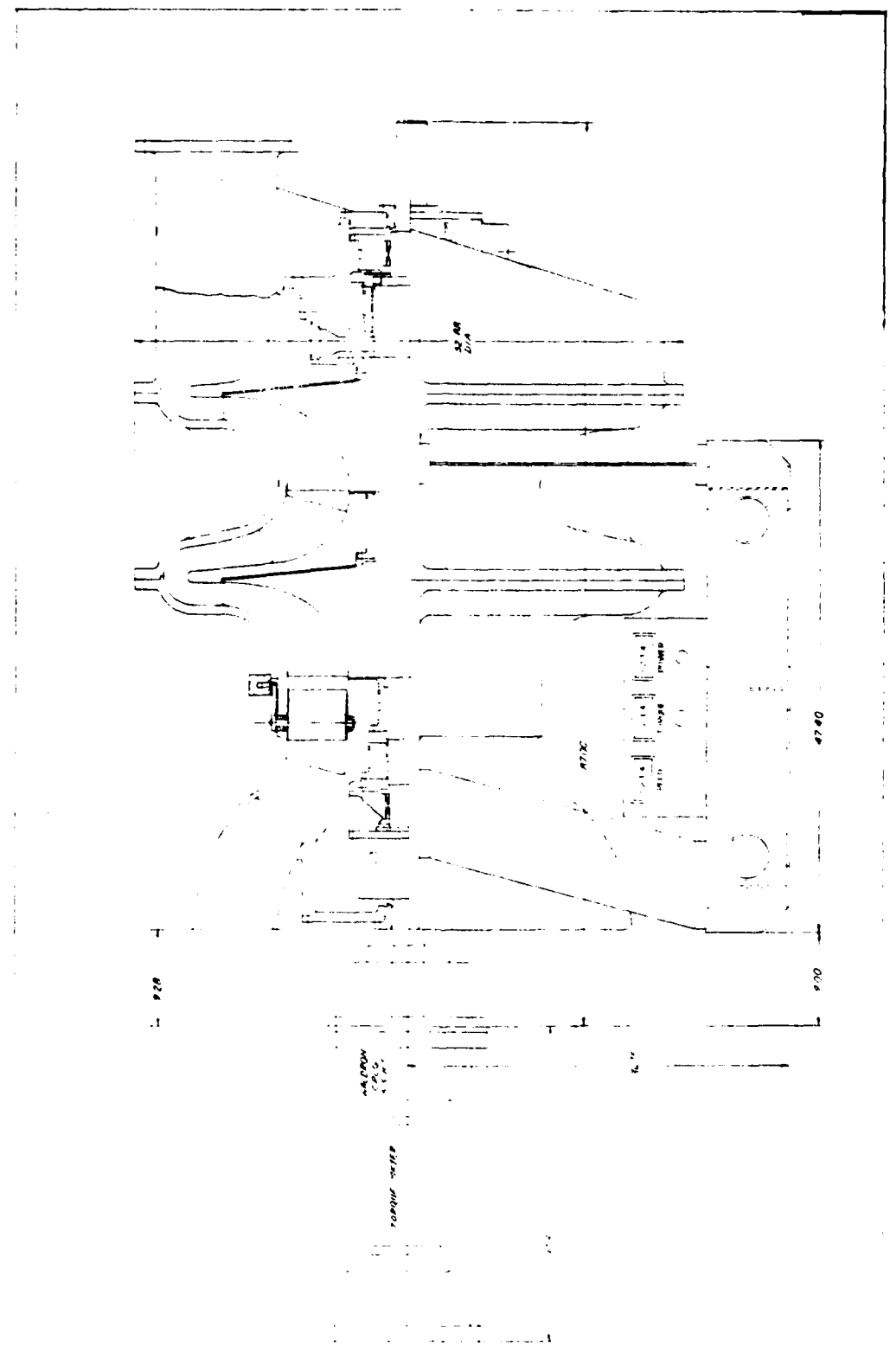


FIGURE 44 - PRELIMINARY DESIGN LAYOUT OF TANDEM CENTRIFUGAL DYNAMOMETER WITH VIGV AND EXIT VALVE-- F1-CC-T

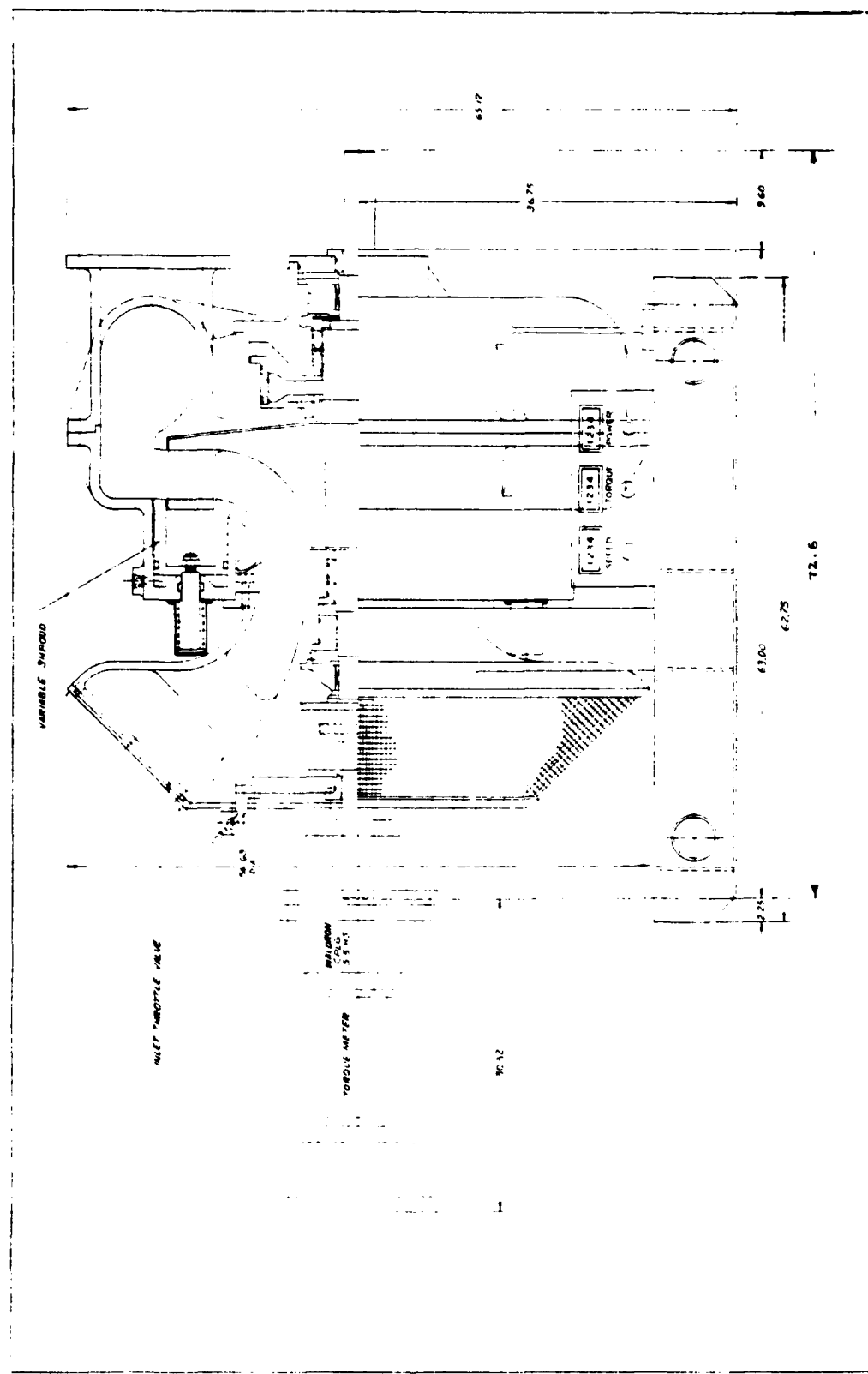


FIGURE 45 - PRELIMINARY DESIGN LAYOUT OF SINGLE-STAGE RADIAL-OUTFLOW DYNAMOMETER WITH VARIABLE SHROUD--FI-ROC-S

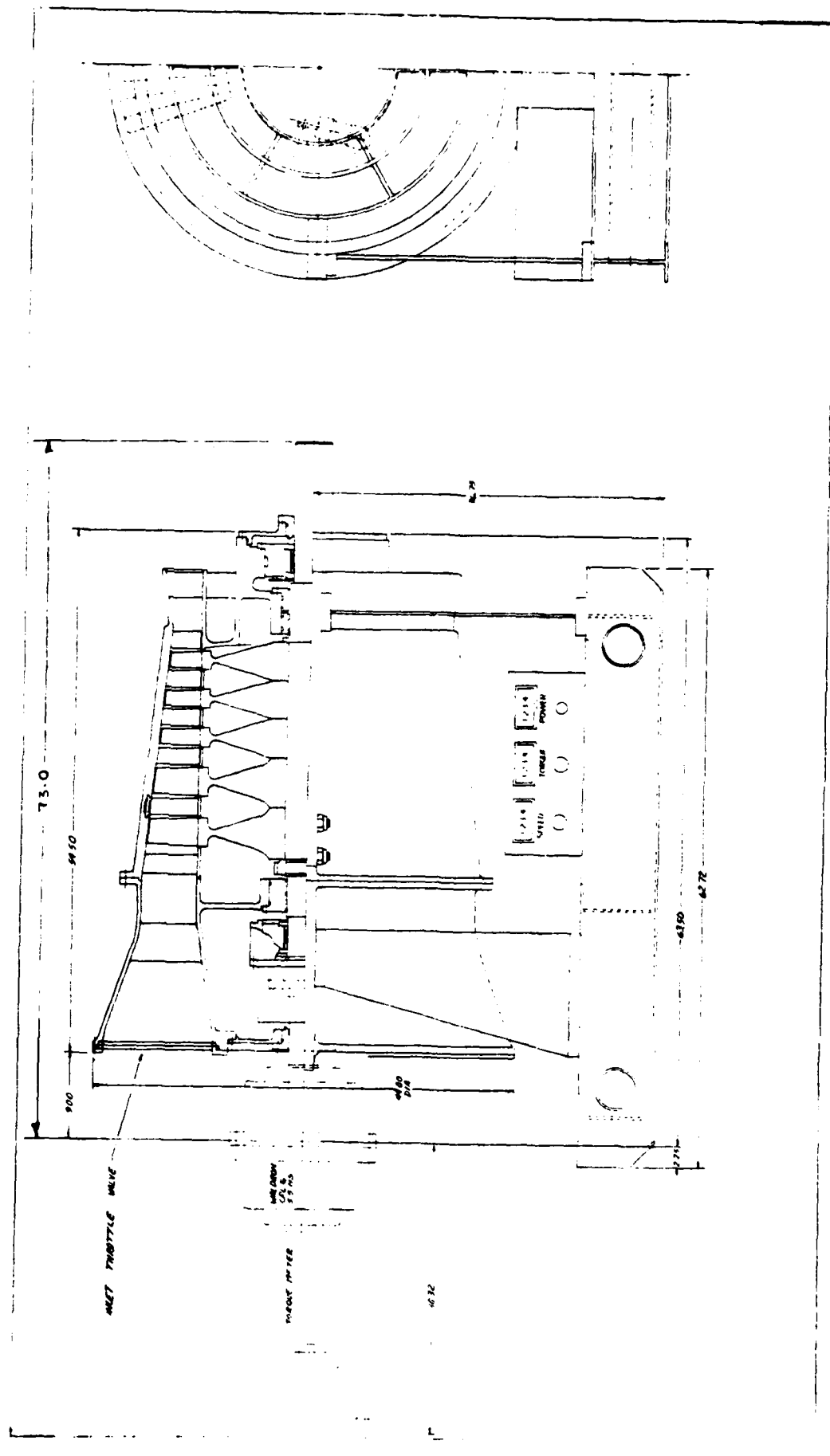


FIGURE 46 - PRELIMINARY DESIGN LAYOUT OF 5-STAGE AXIAL DYNAMOMETER
WITH INLET VALVE -- F1-AC5-H

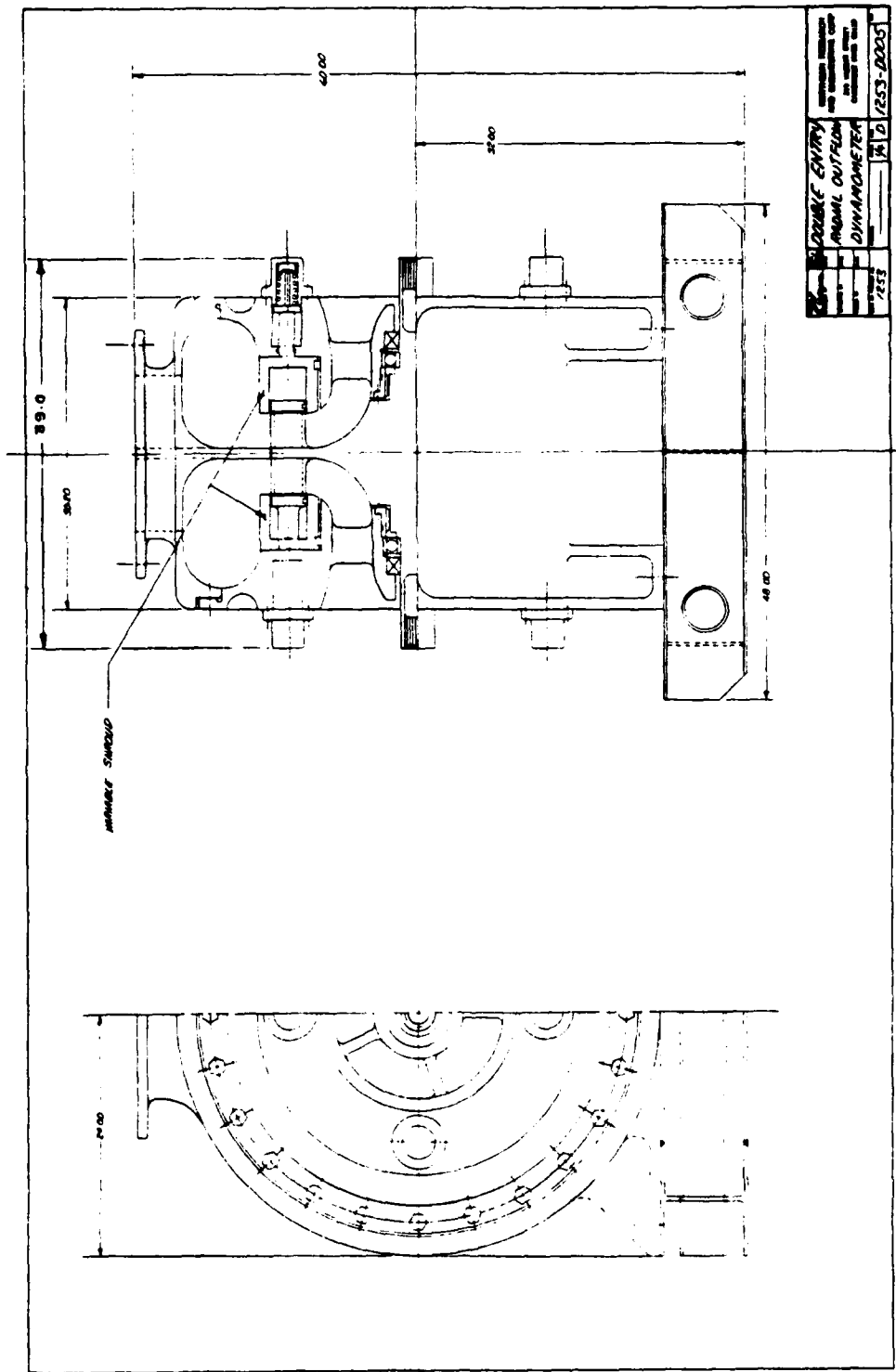


FIGURE 47 - PRELIMINARY DESIGN LAYOUT OF AN OPTIMUM CONFIGURATION FOR DOUBLE-ENTRY RADIAL-OUTFLOW DYNAMOMETER WITH VARIABLE SHROUD-- FI-ROC-D

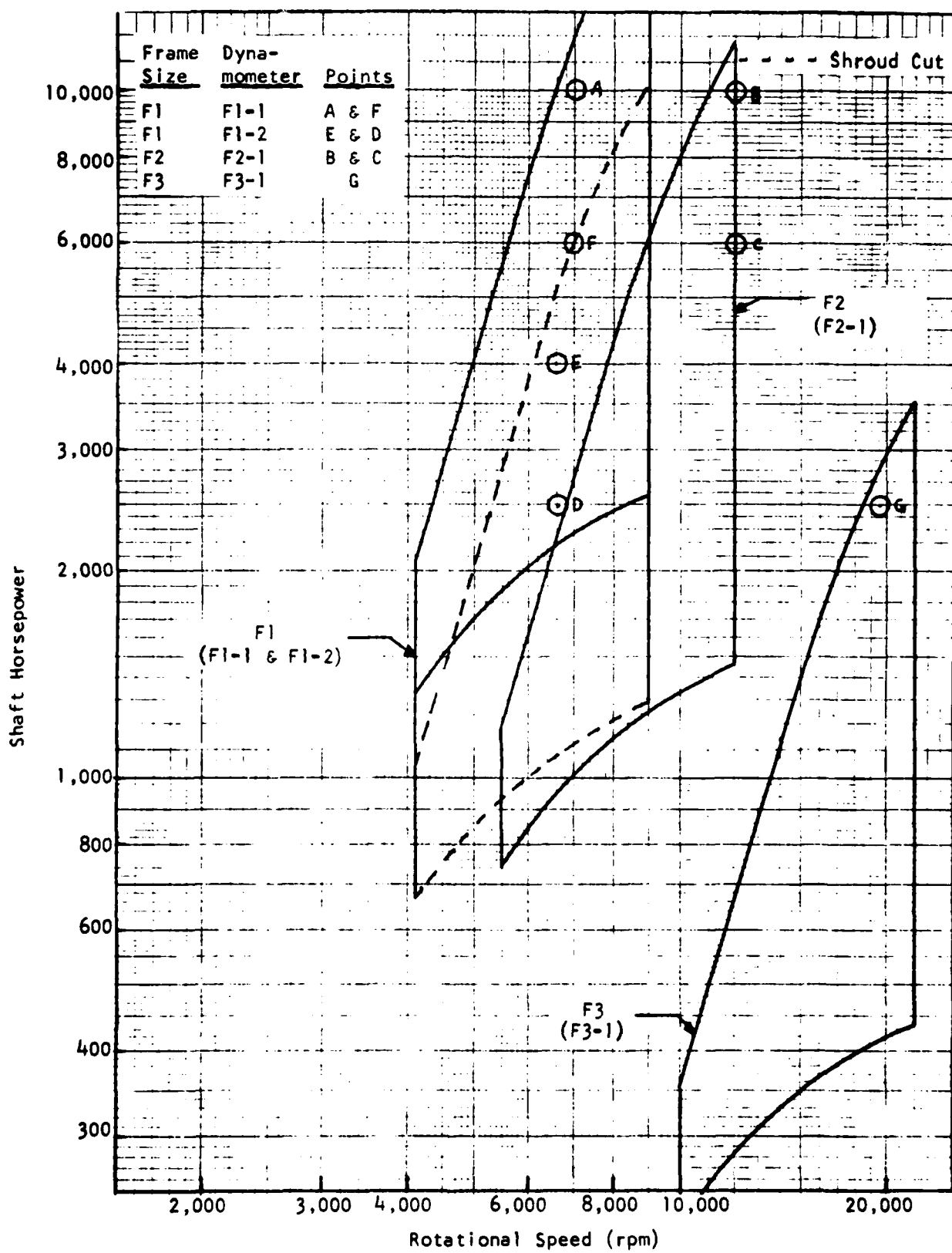


FIGURE 48 - PERFORMANCE ENVELOPES OF DYNAMOMETERS WITH INLET AND EXIT VALVES - 10-STAGE CONSTANT HUB AXIAL COMPRESSOR (AC10-H)

**DATE
FILMED**

8